INFORMATION TO USERS

This manuscript has been reproduced from the microfilm master. UMI films the text directly from the original or copy submitted. Thus, some thesis and dissertation copies are in typewriter face, while others may be from any type of computer printer.

The quality of this reproduction is dependent upon the quality of the copy submitted. Broken or indistinct print, colored or poor quality illustrations and photographs, print bleedthrough, substandard margins, and improper alignment can adversely affect reproduction.

In the unlikely event that the author did not send UMI a complete manuscript and there are missing pages, these will be noted. Also, if unauthorized copyright material had to be removed, a note will indicate the deletion.

Oversize materials (e.g., maps, drawings, charts) are reproduced by sectioning the original, beginning at the upper left-hand corner and continuing from left to right in equal sections with small overlaps. Each original is also photographed in one exposure and is included in reduced form at the back of the book.

Photographs included in the original manuscript have been reproduced xerographically in this copy. Higher quality 6" x 9" black and white photographic prints are available for any photographs or illustrations appearing in this copy for an additional charge. Contact UMI directly to order.

U·M·I

University Microfilms International
A Bell & Howell Information Company
300 North Zeeb Road, Ann Arbor, MI 48106-1346 USA
313/761-4700 800/521-0600

Order Number 9417508

Neurochemical characterization of specific cell populations in the macaque monkey hippocampus

Siegel, Steven J., Ph.D.

City University of New York, 1994

U·M·I
300 N. Zeeb Rd.
Ann Arbor, MI 48106

Neurochemical Characterization Of Specific Cell Populations In The Macaque Monkey Hippocampus

by

Steven J. Siegel

A dissertation submitted to the Graduate Faculty in Biomedical Sciences in partial fulfillment of the requirements for the degree of Doctor of Philosophy, The City University of New York

1994

This manuscript has been read and accepted by the Graduate Faculty in Biomedical Sciences in satisfaction of the dissertation requirement for the degree of Doctor of Philosophy

Date 1/10/94

James L. Roberts, Ph. D.
Examining Committee Chair

Date 1/10/94

Terry Kruiwich, Executive Officer

Patrick R. Hof, M.D.

Bruce S. McEwen, Ph.D.

John H. Morrison, Ph. D.

Klaudiusz Weiss, Ph. D.

Supervisory Committee

The City University of New York

Abstract

Neurochemical Characterization Of Specific Cell Populations In The Macaque Monkey Hippocampus

by

Steven J. Siegel

Adviser: Professor John H. Morrison, Ph. D.

The current study investigates various neurochemical characteristics of identified neuronal populations in the monkey hippocampus with respect to normal distribution patterns, developmental regulation and the effects of environmental perturbations. The hippocampal formation was selected for investigation following initial efforts to identify neuroanatomic correlates of behavioral abnormalities as a result of social deprivation. To this end, chapter 3 describes an increase in the level of immunoreactivity for a nonphosphorylated epitope of neurofilament proteins in the granule cell layer of the dentate gyrus in juvenile monkeys which experienced social deprivation as compared with age matched socially reared animals. Following this observation, studies were designed to determine whether such a pattern represented a delayed developmental progression or the induction of a neuropathologic process. Observations in 15 monkeys ranging from 9 days of age to 9 months of age indicate that the pattern of neurofilament immunoreactivity seen in socially deprived animals does not exist normally in juvenile animals suggesting that such a pattern may represent a neuropathologic alteration reminiscent of the type of cytoskeletal alterations seen following a variety of insults to the nervous system. It has been previously hypothesized that such cytoskeletal changes in discrete neuronal

populations may be mediated by excitotoxic mechanisms. Therefore, in order to further understand the factors which contribute to cell-type specific alterations following particular insults to the nervous system, investigations were initiated to examine the regional, cellular and ultrastructural distribution patterns of several excitatory amino acid receptor subunits. These studies indicate that immunoreactivity for the excitatory amino acid receptor subunits GluR2, GluR5-7 and NMDAR1 are ubiquitously distributed throughout all portions of the hippocampus and furthermore that virtually every neuronal profile in the hippocampus which is immunoreactive for one of these sets of subunits also contains the others. However, ultrastructural data from work described in this thesis as well as in related studies indicate that certain excitatory circuits within the hippocampus are mediated preferentially if not exclusively by a subset of ionotropic excitatory amino acid receptor subtypes. Specifically, synapses between mossy fiber axons of dentate gyrus granule cells and thorny excrescences on dendrites of CA3 pyramidal cells appear to be immunoreactive for GluR2 and GluR5-7 (Good et al., 1993), but lack immunoreactivity for NMDAR1. This pattern was markedly different than the pattern characterizing synapses on more distally located dendritic specializations of CA3 pyramidal cells, which receive associational/commissural excitatory inputs, where all three receptor subtypes were located. Such circuit specific distributions for the various receptor subtypes may contribute to differential vulnerability seen in response to a variety of insults to the nervous system including social deprivation.

Dedication

For all their selfless support and understanding over the years

This work is dedicated to
my parents Norma and Leon Siegel
my sister Michele
and
my wife Ayuko

Acknowledgments

I wish to thank my advisor, Dr. John H. Morrison for his continuing guidance, support and friendship during the course of my thesis training.

I also wish to thank William Janssen for major technical assistance during the preparation and analysis of electron microscopic material; Dr. Victor Freidrich for assistance in statistical design of optical density comparisons; Karen George and Angel Soto for animal care and technical assistance during the social deprivation studies; Stephanie Greene for preparation of GST protein used as a control in chapter 5; Adam Gazzaley for assistance with tissue preparation in chapter 6; Patrick Convery for his efforts on the developmental studies, and Robert. S. Woolley for photographic assistance throughout this work.

I thankfully acknowledge our collaborators Drs. Nils Brose, Stephen Heinemann, Thomas Moran and Scott Rogers for their efforts and support during the excitatory amino acid receptor studies; as well as Drs. Stephen Foote, Stephen D. Ginsberg, Gary Kraemer, and William McKinney for their help with the social deprivation studies. Portions of the studies included within this thesis which were performed by individuals other than the author are included in the appendix.

I wish to extend a special thanks to each of the members of my thesis committee for their time and efforts on my behalf, and to Drs. George W. Huntley, James C. Vickers, my fellow students, and other members of the Fishberg Research Center for Neurobiology for helpful comments and guidance during all phases of my training.

This work was generously funded in part by the John D. and Katherine T. MacArthur Foundation Research Network I.

Table of contents

List of tables

List of illustrations

Abbreviations

BSA	bovine serum albumin
cDNA	complimentary deoxyribonucleic acid
CMV	cytomegalovirus
DAB	3,3-diaminobenzidine tetrahydrochloride
DiI	1,1-dioctadecyl-3,3,3',3'-tetramethyl-iodocarbocyanine perchlorate
DNA	deoxyribonucleic acid
EAA	excitatory amino acid
FITC	fluorescein isothiocyanate
GABA	γ-aminobutyric acid
GluR	glutamate receptor
GST	glutathione-S-transferase
HEK	human embryonic kidney
IACUC	Institutional Animal Care and Use Committee
IgG	γ type immunoglobulin
IgM	μ type immunoglobulin
ir	immunoreactive
KA1	kainate binding protein 1
KA2	kainate binding protein 2
kD	kiloDalton
LTP	long term potentiation
mAb	monoclonal antibody
MAP2	microtubule associated protein 2
mRNA	messenger ribonucleic acid
NF	neurofilament
NF-H	neurofilament-high molecular weight protein
NF-L	neurofilament-low molecular weight protein
NF-M	neurofilament-medium molecular weight protein
NMDA	N-methyl-D-aspartate
PBS	phosphate buffered saline
PSD	post synaptic density
SDS-PAGE	sodium dodecyl sulfate polyacrylamide gel electrophoresis
SPM	synaptic plasma membranes

Chapter 1

Introduction

Overview

Neuronal alterations and damage can result from a wide variety of events including disease processes, traumatic injury and environmental manipulations. However, different neuronal subpopulations are affected by injurious events to variable degrees. Such differential vulnerability to a given pathogen constitutes the underlying theme throughout all studies described in this dissertation. There are two primary components to this thesis. The first seeks to identify neuroanatomic substrates for the behavioral abnormalities observed in monkeys which were raised in social deprivation, while the second describes the distribution patterns for three classes of ionotropic excitatory amino acid (EAA) receptor subunits and correlates such patterns with the differential vulnerability observed in hippocampal neurons.

Biological Approach

Behavioral abnormalities seen following social deprivation in primates are proposed to have a neurobiological basis, which could be manifested in the form of morphologic, physiologic, and/or neurochemical alterations in the brain. Morphologic alterations include changes in the size, shape or number of specific cellular components of the nervous system. Physiologic alterations include abnormal functioning of one or more components of the nervous system, possibly to the extent that the brain's ability to perform its normal tasks is impaired. Finally, neurochemical

alterations include changes in the amount and/or localization of specific molecules within nervous tissue. However, the boundaries separating these three parameters may be defined more by the method of detection than by any real separation of form and function. For example, a change in the number of neurons in one part of the brain may be seen alternatively as a morphologic change on gross or microscopic inspection of the affected area; a physiologic change if one were to measure some aspect of the neuronal activity in the affected region; or a neurochemical change if one were to measure a substance normally produced by the missing subset of neurons. Within this thesis, a variety of techniques have been used to evaluate morphological and neurochemical parameters in the brains of several groups of monkeys. Primarily, immunocytochemistry was used to localize specific proteins within identified neuronal and non-neuronal elements of the nervous system. This technique can also provide information regarding the morphologic characteristics of cells which contain the protein(s) of interest. Therefore, we have chosen to examine the distribution of several functionally important proteins which reveal morphologic and neurochemical information about particular brain regions, neuronal populations and circuits in the brain [1].

The hippocampus is proposed to be one principal locus of deprivation-induced neuropathologic changes due to its proposed role in two affected behaviors; learning (Parkinson et al., 1988; Zola-Morgan and Squire, 1990) and the stress response (Sapolsky et al., 1991). Neuroanatomic changes seen in animals which experience early social deprivation may be due to either a delayed progression of normal developmental processes or alternatively, to

[1] Please see below for description of individual proteins examined within this dissertation.

the induction of neurodegenerative alterations in existing structures. Based on data presented within this dissertation, alterations in hippocampal neurons secondary to early social deprivation in monkeys are proposed to represent a neurodegenerative process. It is further hypothesized that such alterations observed secondary to environmental perturbations such as social deprivation exhibit a pattern of selective distribution such that only specific neuronal populations and circuits will be affected.

Neurodegenerative and other neuronal changes occur in response to a variety of factors including traumatic insults such as ischemia and anoxia; disease processes such as epilepsy, Huntington's disease and Parkinson's disease; and even environmental stressors such as handling condition and restraint stress (Choi, 1988; Meaney et al., 1988; Rothman and Olney, 1987; Uno et al., 1989; Watanabe et al., 1992). Cellular damage in each of these examples has been proposed to be mediated largely by excitotoxic mechanisms from a cascade of events, principally involving increased intracellular Ca^{2+} concentration following excessive glutamatergic neurotransmission at membrane bound receptors (Armanini et al., 1990; Choi, 1988). However, in each of these examples, only specific neuronal populations are adversely affected by the excitotoxic cascade. It is proposed that the differential vulnerability which individual neuronal populations exhibit in response to excitotoxic events is due in part to their EAA receptor subunit profile. This receptor subunit profile includes both the subunit composition within a neuronal population, as well as the subcellular localization of these subunits and by extrapolation the circuits in which they participate.

Social Deprivation

Social deprivation during early postnatal life has profound and long lasting effects on the behavior of primates (Harlow et al., 1971). Although the cellular changes that underlie such alterations in behavior are unknown, environmentally induced psychopathology may involve morphologic or biochemical changes in specific neuronal cell populations.

Behavior Abnormalities in Social Deprivation

The behavior of monkeys which have been raised in social deprivation has been well characterized over the last 30 years. Behavioral abnormalities in socially deprived animals include exaggerated and prolonged responses to stress, appetitive, immune system and motor disturbances, sexual dysfunction, and various learning deficits (Harlow et al., 1971; Kraemer, 1992). Exaggerated responses to stressful or novel stimuli include several forms of self injurious behavior such as biting and banging themselves into the cage walls. These animals can display either hyper- or hypophagic/dipsic ingestive patterns, often accompanied by abnormally small physical stature. Furthermore, animals which have been removed from the deprivation paradigm and housed with other animals of the same or opposite sex fail to integrate normally into the group and do not interact normally in either sexual or non-sexual activities (Kraemer, 1992).

Social Deprivation and Stress

Studies in both rats and monkeys have shown that high levels of circulating glucocorticoids as well as differential handling conditions within the first two weeks of life can lead to changes in glucocorticoid binding

capacity as well as the density and morphology of hippocampal cells (Meaney and Aitken, 1985; Sapolsky et al., 1990; Uno et al., 1989). Furthermore, such changes have been linked to age related hippocampal pathologic changes and decreased negative feedback of the glucocorticoid cascade (Sapolsky et al., 1991). High levels of glucocorticoids have been shown to result in degeneration of CA3 neurons (Sapolsky et al., 1990), while adrenalectomy has been demonstrated to result in degeneration of dentate granule cells (Gould et al., 1990; Sapolsky et al., 1991; Sloviter et al., 1989). Although much of this work on the interaction between glucocorticoids and hippocampal cell development has been done in rats (Gould et al., 1991; Gould et al., 1990; Meaney and Aitken, 1985; Meaney et al., 1985), several reports have described hippocampal pathologic changes in adult primates following exogenous glucocorticoid administration or various stress paradigms (Sapolsky et al., 1990; Uno et al., 1990; Uno et al., 1989). Biochemical analyses of the stress cascade in socially reared and socially deprived monkeys indicate that deprived animals have significantly decreased levels of circulating adrenocorticotropin during some phases of the stress response. (Dr. A. S. Clarke, personal communication). Therefore, it is possible that alterations of glucocorticoid levels in socially deprived monkeys may disrupt normal granule cell maturation. Furthermore, since CA3 is the major target of the mossy fiber system which originates from the dentate granule cells, changes in granule cells might be related to the type of degeneration which has been reported in CA3 of animals which were subjected to other types of stress (Meaney et al., 1988; Sapolsky et al., 1990).

Hippocampus and Social Deprivation

Although behavioral abnormalities in socially deprived animals include a variety of motor and non-motor behaviors, potential neuroanatomic substrates have only been identified for the former [2]. In contrast to these positive findings, changes in structures related to the exaggerated stress response and learning deficits described in these animals have been more elusive. However, since the hippocampus has been linked to both of these behaviors (Parkinson et al., 1988; Sapolsky et al., 1991; Zola-Morgan and Squire, 1990), it has been selected as one potential site of social deprivation induced neurobiological changes.

Hippocampus

The hippocampus has long been used as a model for the study of cortical connectivity and physiology. This is in part, due to the relative simplicity of the extrinsic and intrinsic circuitry in this region. Additionally, this area has proven useful due to the high degree of laminar and regional specificity exhibited by several identified axonal projections (Frotscher, 1991; Frotscher et al., 1988). Together, these two factors have enabled investigators to study the morphologic and physiologic characteristics of a given neuronal population, while knowing the predominant origin of the inputs to each portion of its dendritic tree as well as the destination of its axonal output. This thesis will focus primarily on one intrinsic hippocampal circuit, the mossy fiber projection from dentate granule cells to CA3 pyramidal cells. A short synopsis of the extrinsic and intrinsic components of hippocampal circuitry follows.

---

[2] Please see discussion section of chapter 3 for a more complete review of this point.

Hippocampal Circuitry

The major cortical afferent system to hippocampus is the perforant path, which originates from layer II pyramidal cells in the entorhinal cortex, and synapses primarily on the distal dendritic segments of dentate gyrus granule cells, as well as on pyramidal cell dendrites in the molecular layer of CA1 and CA3. The efferent projection of the granule cells is the mossy fiber system, which synapses *en passant* on hilar mossy cells and terminates in CA3 on pyramidal cell apical dendrites within the stratum lucidum and basal dendrites in stratum oriens. CA3 pyramidal cells send Schaffer collateral axons which terminate in the stratum radiatum on pyramidal cells in CA1; a commissural/associational input to the contralateral and ipsilateral stratum radiatum of CA3; and contribute to the fimbria/fornix, which projects subcortically to the hypothalamus, thalamus, septum and midbrain. Axons from CA1 pyramidal cells contribute to the fimbria/fornix system, as well as projecting to the subiculum which in turn provides the major hippocampal output to the neocortex (Frotscher, 1991; Frotscher et al., 1988; Rosene and Van Hoesen, 1987; Seress, 1992; Seress and Mrzljak, 1992) (fig. 1.1).

Hippocampal Function

Learning deficits in socially deprived monkeys include poor performance on oddity tasks, reduced adaptation to reinforcing stimuli, and decreased response inhibition (Beauchamp and Gluck, 1988; Beauchamp et al., 1990). The hippocampal formation has been proposed to play a critical role in certain aspects of learning and memory (Parkinson et al., 1988; Zola-Morgan and Squire, 1990), and physiologic studies have demonstrated that within the hippocampal formation, dentate granule cells as well as pyramidal

cells in both CA1 and CA3 exhibit long term potentiation (LTP), which has been viewed as a model for learning and synaptic plasticity (Bliss and Lømo, 1973; Cooper et al., 1991). However, recent studies suggest that several regions of temporal neocortex including perirhinal and entorhinal cortices are also strongly involved in the performance of various learning and memory tasks (Meunier et al., 1993). Additionally, the hippocampus is thought to participate in negative feedback of the hypothalamic-pituitary-adrenal stress response (Sapolsky et al., 1991). Therefore, changes in this region might underlie learning deficits as well as the prolonged and exaggerated stress responses that socially deprived animals display. Such exaggerated stress responses are maintained years after socially deprived monkeys are apparently rehabilitated by resocialization with younger monkeys (Anderson and Mason, 1978), suggesting a long lasting effect of an initial perturbation.

Hippocampal Development

Sensitive periods for the anatomic and physiologic maturation of sensory functions such as vision have been demonstrated during postnatal development (Hubel and Wiesel, 1970). Similarly, sensitive periods have been demonstrated for behavioral measures in socially deprived animals (Kraemer, 1992). Therefore, it is possible that the neuroanatomic substrates of perturbed behaviors display vulnerability to environmental manipulations only within a sensitive period of postnatal development. The hippocampal formation may be particularly vulnerable to aberrant rearing conditions during early postnatal life due to its postnatal developmental pattern. Although many primate dentate granule cells are postmitotic at birth, there is a significant level of neurogenesis lasting through 6 months of age

(Eckenhoff and Rakic, 1988; Seress, 1992; Stanfield and Cowan, 1988). Additionally, many granule cells continue to undergo changes in connectivity and morphology throughout the first year of life (Eckenhoff and Rakic, 1988; Seress, 1992; Stanfield and Cowan, 1988). This postnatal developmental pattern is consistent with previous work by Gould and coworkers (Gould et al., 1991) which suggests that administration of glucocorticoids during the first postnatal week in rats interferes with normal granule cell death and development.

The developmental pattern of axonal outgrowth from the granule cells has been described in rats (Gaarskjaer, 1986). Data from a variety of studies suggest that mossy fibers begin to grow very soon after a granule cell's final mitotic event. Mossy fibers have been demonstrated to be sparsely present in proximal CA3 at birth with additional growth continuing until postnatal day 24 (Gaarskjaer, 1981). Since the majority of granule cells are born prenatally in monkeys (Eckenhoff and Rakic, 1988), it was postulated that the mossy fiber projection in primates would be present at birth. To test this hypothesis, studies were initiated to determine whether or not mossy fiber axons were present at their target cells in CA3 at birth, and furthermore to examine the developmental distributions of several proteins within this projection to yield more precise information and insight as to the maturity of this system throughout prepubertal development.

Proteins of Interest

The proteins examined in this thesis are contained within specific neuronal subsets, and display particular patterns of subcellular distribution. Antibodies to neurofilament (NF) proteins were used to examine the

structural integrity of a group of neurons, since these proteins are thought to exhibit altered expression and/or modification in degenerating neurons, as well as other forms of neuronal alterations (Vickers and Morrison, 1992). Two of the remaining proteins of interest were chosen based on their localization to individual components of particular excitatory circuits within the hippocampus which appear to be altered within the brains of socially deprived animals [3]. Immunoreactivity for calbindin was used to examine the mossy fiber axons of dentate gyrus granule cells, while antibodies directed against the microtubule associated protein MAP2 were used to visualize pyramidal cell dendrites in the CA3 hippocampal region. Finally, antibodies directed against ionotropic EAA receptor subunits were used to examine their distribution relative to excitatory pathways in the hippocampus, as well as their possible role in establishing differential vulnerability to a variety of harmful circumstances, including social deprivation.

Neurofilaments

Neurofilament proteins are among a class of largely tissue-type specific cytoskeletal proteins called intermediate filament proteins and are present in a functionally diverse subset of central and peripheral neurons which include both the granule cells and CA3 pyramidal cells of the hippocampal formation (Vickers and Costa, 1992; Vickers et al., 1991). The NF triplet class of intermediate filament proteins consist of three structurally related proteins of 70 kD, 140-160 kD, and 200 kD, respectively (Nixon and Sihag, 1991). These subunits, termed the neurofilament low (NF-L), medium (NF-M) and high (NF-H) molecular weight proteins, assemble into filamentous structures with a diameter of approximately 10 nm. The core of

[3] Please see chapters 3 and 4 for details regarding the effects of social deprivation.

the filament is composed of repeating rod units from all three proteins, with side arms comprised of the C-terminal end of the NF-M and NF-H subunits (Lee et al., 1988). Multiple phosphorylation sites are present on each of the three subunits and the phosphorylation state of certain sites plays a role in subcellular localization (Nixon and Sihag, 1991). Studies with phosphorylation-dependent antibodies have shown that particular forms of phosphorylated NF proteins are localized primarily in axons while the corresponding nonphosphorylated form of NF proteins are largely in the somatodendritic compartment (Lee et al., 1988; Sternberger and Sternberger, 1983). All three subunits can be phosphorylated at multiple sites with a possible ratio of 50 moles of phosphate per mole of protein. (Lee et al., 1988; Nixon and Sihag, 1991).

Although the functions of NF proteins have not been definitively determined, maintenance of axonal caliber (Hoffman et al., 1984), neuronal shape and dendritic arbor (Campbell et al., 1991) have been proposed. It has been further hypothesized that NF proteins play a key role in neuronal vulnerability in various neurodegenerative conditions. Initially, this hypothesis was based on correlative data linking the distribution of NF proteins with the distribution of vulnerable neurons in Alzheimer's disease (Morrison et al., 1987). Similarly, reduction of neurons containing NF proteins has been shown in the brains of patients with both Alzheimer's disease (Hof and Morrison, 1990) and Huntington's disease (Cudkowicz and Kowall, 1990). Recently, it has been shown that certain neuronal populations which are lost in Alzheimer's disease, such as CA1 pyramidal cells, show dramatic increases of nonphosphorylated NF protein in their soma and dendrites during early stages of the disease prior to their eventual

loss (Vickers and Morrison, 1992). This strongly supports the notion that not only is NF protein content an important marker for vulnerable cells, but that the expression or modification of NF proteins is an important component of the degenerative process.

Furthermore, several neuronal types have been demonstrated to display developmentally regulated expression or phosphorylation of NF proteins. For example, cerebellar granule cells display increased immunoreactivity for both phosphorylated and nonphosphorylated epitopes during early postnatal life, while Purkinje cells do so in the fetal period (Bignami et al., 1985; Cambray and Burgoyne, 1986). Thus, it is possible that developmentally-linked alterations, as well as degenerative events in the hippocampus may be mediated by or manifested in shifts in NF protein distribution or regulation.

MAP2

Microtubule-associated protein 2 (MAP2) is composed of three proteins MAP2a, MAP2b and MAP2c of roughly 280 kD, 260 kD and 65-70 kD respectively (Riederer, 1990). These proteins are highly conserved throughout evolution with strong homology from Xenopus to rat (Tucker, 1990). Like many other cytoskeletal elements, MAP2 is proposed to stabilize cell shape by crosslinking other proteins such as microtubules and neurofilaments (Riederer, 1990; Tucker, 1990). The three forms of MAP2 display somewhat different developmental patterns with MAP2c peak expression earlier than that of MAP2a and MAP2b, the latter of which is highly correlated with dendritic branching (Riederer, 1990; Tucker, 1990). MAP2 is expressed early in neuronal differentiation and is present in all

neurites (Tucker, 1990). However, as a cell becomes polarized, MAP2 is localized to the somatodendritic compartment and therefore serves as a useful marker for dendrites in the adult brain (Dotti et al., 1988). In this thesis, antibodies to MAP2 will be used to visualize dendritic organization and morphology in particular neuronal populations.

Calcium-Binding Proteins

Calbindin is one of a class of small acidic proteins which have been shown to buffer intracellular calcium and may also act as transducers and modulators of calcium's action on other proteins within neurons (Celio, 1989). Calbindin is colocalized with γ-aminobutyric acid (GABA) in a subset of neocortical interneurons (Celio, 1989; Hendry et al., 1989) and is present in a small subset of cortical pyramidal cells (DeFelipe and Jones, 1992) as well as a group of large layer I neurons called Cajal-Retzius cells (Huntley and Jones, 1990). The granule cells of the dentate gyrus, and CA1 pyramidal cells are also among the neuronal populations which are labeled with antibodies to calbindin. In dentate granule cells, both the somatodendritic and axonal compartments are strongly labeled in the adult rat and primate brain (Celio, 1990; Seress et al., 1992).

Previous studies regarding the ontogeny of calbindin immunoreactivity in the rat nervous system have determined that calbindin-immunoreactive neurons are present on E14 in a variety of brain structures (Enderlin et al., 1987). Calbindin immunoreactivity in a set of hippocampal cells does not appear until E15 and dentate granule cells appeared postnatally with faint immunoreactivity of the mossy fibers at P12. Furthermore, these studies concluded that calbindin is expressed shortly after

a cell's final mitosis, during its migration and differentiation. Other studies confirm this result and draw the additional conclusion that calbindin expression in the rat granule cells does not occur until the elaboration of axonal and dendritic processes in the early postnatal period and is coincident with synaptogenesis (Rami et al., 1987). Developmental studies of calbindin expression in primate striate cortex found expression to be highest during the prenatal period of thalamocortical ingrowth, and declined following birth (Hendrickson et al., 1991). In this thesis, immunoreactivity for calbindin will be used primarily to visualize hippocampal mossy fiber axons during development, as well as in animals which were socially reared or socially deprived.

Excitatory amino acid receptors

There are two main classes of EAA receptors, termed the metabotropic and ionotropic classes (Bettler et al., 1990). The former class of receptors are G protein-linked membrane bound proteins with seven transmembrane domains (Houamed et al., 1991). The latter class are ligand gated ion channels, which can be further divided pharmacologically and functionally into two main groups. N-methyl-D-aspartate (NMDA) receptors are voltage-sensitive Ca^{2+}, K^+ and Na^+ channels (Moriyoshi et al., 1991; Nakanishi, 1992; Seeburg, 1993; Sommer and Seeburg, 1992). Although there are at least five NMDA receptor subunits termed NMDAR1 and NMDAR2A-D, NMDA receptor complexes *in vivo* are thought to be composed of hetero-oligomer complexes containing at least one subunit of NMDAR1 (Nakanishi, 1992). Non-NMDA receptors are ion channels which are thought to be composed of five subunits, each with four transmembrane domains (Barnes and Henley, 1992; Hollman et al., 1991;

Keinänen et al., 1990) and are primarily permeable to K^+ and Na^+ but may also allow the passage of Ca^{2+} depending upon subunit composition (Seeburg, 1993). Non-NMDA receptor subunit proteins are currently designated GluR1 through GluR7 (Sommer and Seeburg, 1992), with GluR1 through GluR4 (GluR1-4) binding with high affinity to α-amino-3-hydroxy-5-methyl-4-isoxazole propionate (AMPA) and less so to kainate, while GluR5 through GluR7 (GluR5-7) bind primarily to kainate (Bettler et al., 1992; Sommer and Seeburg, 1992). Two additional kainate-binding proteins termed KA-1 and KA-2 have been shown to bind kainate with high affinity, but are thought to be incapable of forming functional homomeric channels in vivo (Herb et al., 1992; Werner et al., 1991) Although non-NMDA receptors are probably heteromeric *in vivo* (Sommer and Seeburg, 1992), their exact stochiometric combination is not known. Immunoprecipitations of receptor subunits expressed in oligodendrocyte precursor cells (Puchalski et al., Submitted) and rat brain synaptic plasma membranes (Brose et al., 1993) suggest that both AMPA/kainate (GluR1-4) and kainate (GluR5-7 and KA-1,2) subunits assemble into functional channels only with members of their own subgroup and neither group assemble with NMDA receptor subunit proteins.

Several studies have been recently published on the localization of EAA receptor subunits. Each of the EAA receptor subtypes are represented in a wide distribution of brain areas and on a variety of neuronal and non-neuronal cell types (Bettler et al., 1990; Good et al., 1993; Huntley et al., 1993; Martin et al., 1993; Pellegrini-Giampietro et al., 1991; Petralia and Wenthold, 1992; Vickers et al., 1993; Siegel et al., 1994). Electron microscopic studies have characterized hippocampal ionotropic EAA

receptor subunits as primarily present on neuronal postsynaptic densities as well as in the dendritic and somatic cytoplasm (Good et al., 1993; Petralia and Wenthold, 1992; Siegel et al., 1994).

Within the adult hippocampal formation, ligand binding studies have described regional and developmental patterns for each of the EAA receptor subtypes. In the adult rat, high affinity kainate binding is primarily located in CA3 and dentate granule cells (Miller et al., 1990), while AMPA and NMDA binding is primarily localized to CA1 and dentate granule cells (Insel et al., 1990). Developmentally, ligand binding studies have described initially low levels of NMDA and non-NMDA EAA receptors in rat hippocampus at birth as compared to adult number (Insel et al., 1990; Miller et al., 1990). For example, kainate binding in the stratum lucidum of CA3 is highest in the adult rat, but remains relatively low in the juvenile (Miller et al., 1990). Periods of peak increases in the degree of binding have been proposed to relate to the development of LTP (McDonald and Johnston, 1990) and have been linked both temporally and spatially to the ingrowth of afferent fibers within the hippocampal formation (McDonald and Johnston, 1990).

Specific Aims and Hypotheses

This thesis will examine the neurochemical characteristics of particular neuronal populations within the monkey hippocampus. Special emphasis will be placed on the role of specific structural and neurotransmitter related proteins in determining the potential physiologic characteristics and differential vulnerability exhibited by individual neuronal classes.

Specific Aim 1

To determine the morphological correlates of perturbed behaviors in monkeys which experienced social deprivation.

Specific regions of the monkey brain will be selected for examination based on the proposed localization of behaviors which are affected by rearing condition. Particular neuronal populations will be studied using immunohistochemistry for a set of structural proteins which allow for the visualization of cellular morphology, and are thought to be altered during various states of neuronal modification and/or degeneration.

Specific Aim 2

To determine if alterations in the brains of monkeys which experience early social deprivation represent delay of a normal developmental progression, or a neuropathologic alteration in existing structures.

Several proteins are known to display distinct cellular and subcellular immunocytochemical distribution patterns. Such patterns will be utilized to visualize particular portions of specific cell populations in monkeys which

were either socially reared or socially deprived during early life. These patterns will then be compared to normal immunocytochemical patterns at several time points during early postnatal development to compare the state of specific neuronal circuits in differentially reared monkeys to those seen during normal development.

Specific Aim 3

To determine the regional, cellular and subcellular distribution patterns of the EAA receptor subunits GluR2 and NMDAR1 in monkey hippocampus, and further to determine the degree of colocalization of each of these subunits with GluR5-7.

Immunocytochemistry using subunit specific antibodies directed at members of the AMPA/kainate, kainate and NMDA receptor subtypes will be used to describe the degree of cellular colocalization of the different receptor categories. Furthermore, the correlation between the subcellular segregation of individual subunits and laminarly specific inputs to particular neuronal populations will be investigated.

Figure 1.1

The perforant path (PP) is comprised of axons from layer II pyramidal cell in the entorhinal cortex (EC). These axons cross the hippocampal fissure (HF) and synapse within the dentate molecular layer (DML). This projection forms a major afferent to the dentate granule cells, whose cell bodies lie within the granule cell layer (GCL). The major efferent of the granule cells is the mossy fiber projection (MF) to CA3, where it synapse on pyramidal cell apical dendrites within the stratum lucidum (SL) and basal dendrites in stratum oriens. CA3 pyramidal cells send Schaffer collateral axons (SC) in turn to pyramidal cells in CA1, as well as a commissural/associational input (C/A) to the contralateral and ipsilateral CA3, and contributing to the fimbria/fornix (F/F), which projects to the hypothalamus, thalamus, septum and midbrain. Axons from the CA1 pyramidal cells also contribute to the fimbria/fornix system, as well as projecting to the subiculum (SUB) which provides the major hippocampal output to the neocortex.

Figure 1.1:

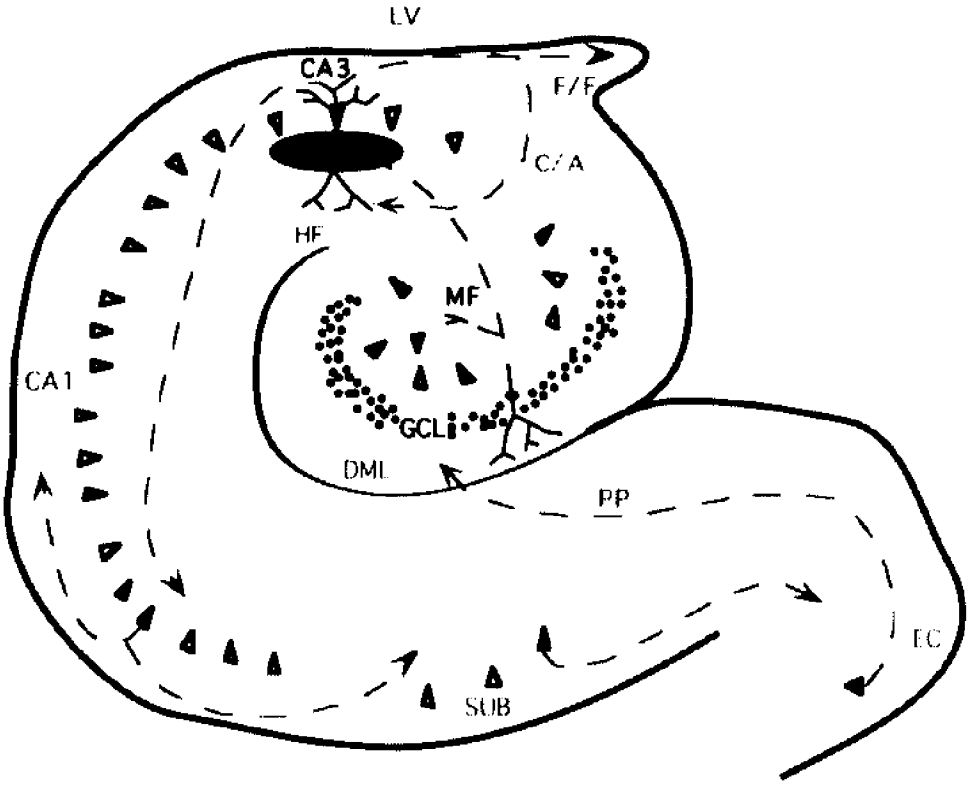

Chapter 2

General Methods and Materials

Animals

These and related studies within the laboratory of J. H. Morrison included the brains of 24 monkeys from the Wisconsin Regional Primate Center. Social deprivation studies included eight monkeys which were sacrificed between 1.5 and 2.5 years of age, while developmental studies included a total of 16 animals sacrificed at either one week, one month, three months, six months and nine months of life, respectively. Brain tissue from an additional six adult monkeys from the Mount Sinai School of Medicine was included in the EAA receptor studies. All protocols were conducted within NIH guidelines for animal research and were approved by the Institutional Animal Care and Use Committee (IACUC)

Tissue Preparation

Animals were deeply anesthetized with ketamine hydrochloride (15-25 mg/kg i.m.) and pentobarbital sodium (10-20 mg/kg i.p.) and perfused transcardially with cold 1% paraformaldehyde in 0.01 M phosphate buffered saline (PBS) for approximately 1 minute and then with cold 4% paraformaldehyde in PBS for an additional 8-9 minutes. The brains were removed, cut into approximately 5 mm tissue-blocks and placed in cold 4% paraformaldehyde in PBS for 6 hours. Additional material was prepared with fixation that included 0.25-1% glutaraldehyde as well as 4% paraformaldehyde.

Some tissue blocks were then prepared for frozen sectioning. These blocks were taken through graded sucrose solutions of 12, 16 and 18%, frozen on dry ice, and cut coronally at 40 µm on either a cryostat (Reichert) or a sliding microtome (Reichert). Other tissue blocks were processed for vibratome sectioning. Following fixation, these tissue blocks were placed directly into cold PBS and sectioned in a plane perpendicular to the superior temporal sulcus at 50-80 µm using a vibratome (Ted Pella Inc., Irvine, CA).

Immunocytochemistry

Tissue sections were processed for either single or double labeling immunohistochemistry as described below. For single label immunohistochemistry, tissue sections were incubated for 24-48 hours with primary antibody in diluent (PBS, 0.05% bovine serum albumin). Following three washes in PBS, sections were processed for visualization with either conventional light or fluorescence microscopy. Sections for conventional light microscopic analysis were processed by avidin-biotin-peroxidase method using Vectastain ABC kit (Vector Laboratories, Burlingame, CA) followed by treatment with 0.05% 3,3-diaminobenzidine tetrahydrochloride (DAB), and 0.003% hydrogen peroxide. Additional sections were further processed for electron microscopy. Following DAB, these sections were treated with 0.5% osmium tetroxide in 7% sucrose, embedded in resin (Araldite, Electron Microscopy Sciences, Fort Washington, PA), and sectioned at 3 µm on an ultramicrotome (Ultracut E, Reichert-Jung, Germany). These sections were then re-imbedded and thin sectioned for electron microscopy. Tissue sections which were processed for fluorescence microscopic analysis were incubated with FITC-conjugated goat anti-mouse IgG, heavy and light chain specific antisera (Vector Laboratories,

Burlingame, CA) or biotinylated horse anti-mouse IgG, heavy and light chain specific antisera (Vector Laboratories, Burlingame, CA), followed by Texas Red-conjugated avidin (Vector Laboratories, Burlingame, CA). Sections received three 10 minute washes between all antibody steps.

Double label immunohistochemistry was performed by incubating tissue sections with a combination of an IgG type and an IgM type primary antibody for 24-48 hours. Following three washes in PBS, sections were incubated for 2 hours in FITC-conjugated goat anti-mouse IgM μ chain specific antisera (Vector Laboratories, Burlingame, CA) and biotinylated horse anti-mouse IgG γ chain specific antisera (Vector Laboratories, Burlingame, CA). Following three additional washes in PBS, sections were incubated with Texas Red-conjugated avidin (Vector Laboratories, Burlingame, CA). As an immunohistochemical control for this procedure, additional sections were incubated with an IgG type antibody followed by FITC-conjugated goat anti-mouse IgM μ chain specific antisera or an IgM type antibody followed by biotinylated horse anti-mouse IgG γ chain specific antisera and Texas Red-conjugated avidin. Neither of these conditions resulted in the visualization of the appropriate primary antibody by an inappropriate secondary antibody.

Tract Tracing

Crystals of the lipophilic fluorescent dye 1,1-dioctadecyl-3,3,3',3'-tetramethyl-iodocarbocyanine perchlorate (DiI) (Molecular Probes, Eugene, OR) were used to trace the mossy fiber axonal projections from dentate granule cells. Following six hour fixation with 4% paraformaldehyde, crystals of DiI dissolved in methanol were placed around the entire extent of

the dentate gyrus within the granule cell layer under microscopic visualization. These blocks were then be stored in the dark in PBS with 0.1% sodium azide at 37° C for a period of five weeks. Blocks were then sectioned at 50 μm on a vibratome (Ted Pella, Irvine CA) and either examined directly under florescence microscopy or treated for fluorescence immunocytochemistry as described above.

Analysis

Microscopic analyses

Both DAB- and Texas Red/FITC-labeled tissue sections were examined on an Axiophot microscope (Zeiss, Germany) for conventional bright field and fluorescence light microscopic analyses. Double labeled fluorescence material was also analyzed on a confocal laser scanning microscope (Zeiss, Germany). Ultrastructural analyses were performed on a Hitachi 7000 electron microscope (Hitachi, Japan).

Optical density

Optical density is calculated from the amount of light which passes through a tissue section, and as such is a direct measure of local light transmission. High immunoreactivity, resulting in low light transmission will yield a high optical density number. Optical density values range from zero to 165, thus a value of zero corresponds to no obstruction in the light path relative to a glass slide, while a value of 165 indicates the absence of light at the detector. All optical density readings were taken using an Axiophot light microscope (Zeiss, Germany) equipped with a MSP-65 motorized stage unit (Zeiss, Germany) and a DEC 3100 workstation-based

morphometry and measurement analysis system. Individual fields (800 μm X 620 μm) were digitized by the computer and optical density measurements were taken within each of the specified regions on each tissue section analyzed.

Table 2.1

Antibody	Source	Antigen	Reference
SMI32 - monoclonal 1/10,000	Sternberger Monoclonals Inc., Jarrettsville, MD	nonphosphorylated epitope of NF-H and NF-M proteins	(Campbell and Morrison, 1989; Lee et al., 1988; Sternberger and Sternberger, 1983)
SMI31 - monoclonal 1/5000	Sternberger Monoclonals Inc., Jarrettsville, MD	phosphorylated epitope of NF-H and NF-M proteins	(Sternberger and Sternberger, 1983)
MAP2 - monoclonal 1/1000	Sigma Immuno Chemicals, St. Louis, MO	microtubule-associated proteins (2a, 2b 2c)	(Riederer, 1990)
Calbindin - monoclonal 1/2500	M. R. Celio	28 kD calcium-binding protein	(Enderlin et al., 1987)
3A11 - monoclonal 1/100	S. H. Heinemann, T. Moran, J. H. Morrison, & S. W. Rogers	GluR2, putative N-terminal region	(Puchalski et al., Submitted; Siegel et al., in preparation)
54.1 monoclonal 1/250	N. Brose, S. H. Heinemann, R. Jahn, & J. H. Morrison	NMDAR1, intracellular loop between transmembrane domains 3 and 4	(Siegel et al., 1994)
4F5 monoclonal 1/500	S. H. Heinemann, T. Moran, J. H. Morrison, & S. W. Rogers	GluR5-7, putative N-terminal region	(Huntley et al., 1993)

Chapter 3

Effects of Social Deprivation in Prepubescent Rhesus Monkeys: Immunohistochemical Analysis of the Neurofilament Protein Triplet in the Hippocampal Formation [4]

Abstract

Social deprivation during early postnatal life has profound and long lasting effects on the behavior of primates, including prolonged and exaggerated responses to stress as well as impaired performance on a variety of learning tasks. Although the cellular changes that underlie such alterations in behavior are unknown, environmentally induced psychopathology may involve morphologic or biochemical changes in select neuronal populations. The hippocampal formation of both socially deprived and socially reared prepubescent rhesus monkeys was selected for immunocytochemical investigation because of its association with the behavioral stress response and learning. Immunocytochemical analysis using antibodies specific for the NF protein triplet was performed since these proteins are modified within degenerating neurons in a variety of neurodegenerative disorders. Results from optical density measurements indicate an increase in the intensity of nonphosphorylated NF protein immunoreactivity in the dentate gyrus granule cell layer of socially deprived monkeys in comparison with that of socially reared animals, suggesting that early social deprivation may result in an increase in the amount of nonphosphorylated NF protein in these cells. This phenotypic difference in

[4] This chapter appears in *Brain Research* (1993) **619** pp 299-305, and is reprinted here with the express permission of Elsevier Science Publishers.

dentate granule cells between differentially reared monkeys supports the notion that specific subpopulations of neurons in brain regions that subserve complex behaviors may undergo long term modifications induced by environmental conditions. Furthermore, the data suggest that constitutive chemical components related to structural integrity may be as susceptible to early environmental manipulations as the more traditionally viewed measures of cellular perturbations, such as neurotransmitter dynamics, cell density and the establishment of connectivity. The observed modifications may serve as an anatomical substrate for behavioral abnormalities that persist in later life.

Introduction

Behavioral abnormalities in socially deprived monkeys include exaggerated and prolonged responses to stress, appetitive disturbances, sexual dysfunction, and various learning deficits (Harlow et al., 1971). Previous reports have correlated motor disturbances with abnormalities in certain brain structures in monkeys that experienced early social deprivation. For example, reduced Purkinje cell soma size, reduction of dendritic branching in motor cortex, and alterations of basal ganglia chemoarchitecture have all been reported in monkeys with varying degrees of social deprivation (Floeter and Greenough, 1979; Martin et al., 1991; Struble and Riesen, 1978). However, many of these studies have focused on adult monkeys and have therefore had to contend with the possible confounding effects of aging (Araujo et al., 1990; Brizzee et al., 1980; Walker et al., 1988) and varied post-deprivation conditions superimposed on the cascade of events initiated by early social deprivation. By looking at the brains of prepubescent monkeys that are still within the deprivation paradigm, the present study seeks to identify early morphologic or phenotypic changes which may precede later neuropathologic alterations.

Studies in a variety of species have shown that differential handling conditions (Meaney et al., 1988) as well as several forms of psychological stress (Uno et al., 1991; Uno et al., 1989; Watanabe et al., 1992) can lead to changes in the density and morphology of specific hippocampal cell types. Restraint stress in rats (Watanabe et al., 1992) as well as social subordination in tree shrews and monkeys (Uno et al., 1991; Uno et al., 1989) have been correlated with alterations of CA3 neurons. Furthermore, such changes have

been linked to decreased negative feedback of the glucocorticoid cascade (Sapolsky et al., 1991). Based on this correlation between pathologic changes within the hippocampus and various stress paradigms (Meaney et al., 1988; Uno et al., 1991; Uno et al., 1989; Watanabe et al., 1992), the hippocampus was selected for cytochemical analysis within the context of social deprivation. It was further hypothesized that changes in cell morphology would be preceded by cytoskeletal changes. Therefore, in the present study, analyses were directed at a cytoskeletal constituent, the NF protein triplet, which has been previously demonstrated to be useful in visualizing vulnerable neuronal populations in a variety of neurodegenerative disorders (Cudkowicz and Kowall, 1990; Goldman et al., 1983; Hof and Morrison, 1990; Manetto et al., 1989; Morrison et al., 1987; Vickers et al., 1992; Vickers et al., 1992).

Methods and Materials

Animals

The brains of eight 1.5-2.5 year-old monkeys reared in social deprivation (n = 4) or group cages (n = 4) were examined in this and other related studies (Ginsberg et al., 1993; Ginsberg et al., 1991; Ginsberg et al., 1993; Ginsberg et al., 1992; Morrison et al., 1990). Each socially reared animal was housed in an individual cage with its mother until 5 months of age. They were then placed in group cages of approximately ten animals. Socially deprived animals were taken from their mothers at three days of age and placed in a nursery where they received nourishment from human caregivers with minimal physical contact. At 30 days of age they were moved to individual cages where they were unable to have physical contact

with other monkeys or human handlers. Socially deprived animals were sacrificed at 19, 19, 27, and 27 months of age, while socially reared animals were sacrificed at 18, 18, 19, and 20 months of age.

Additionally, the brains of 16 macaque monkeys from the Wisconsin Regional Primate Center were utilized within a developmental study. Animals were sacrificed at one week, one month, three months, six months and nine months of life respectively. All protocols were conducted within NIH guidelines for animal research and were approved by the Institutional Animal Care and Use Committee (IACUC) at the University of Wisconsin at Madison.

Tissue Preparation

Animals were deeply anesthetized with ketamine hydrochloride (15-25 mg/kg i.m.) and pentobarbital sodium (10-20 mg/kg i.p.) and perfused transcardially with cold 1% paraformaldehyde in phosphate buffered saline (PBS) for approximately 1 minute and then with cold 4% paraformaldehyde in PBS for an additional 8-9 minutes. The brains were removed, cut into 5 mm tissue-blocks, placed in cold 4% paraformaldehyde in PBS for 6 hours, and taken through graded sucrose solutions of 12, 16 and 18% in preparation for cryostat sectioning. Frozen coronal sections were cut at 40 μm. A one in twenty series was taken from a portion of the mid body of the hippocampus, as defined by presence of the lateral geniculate nucleus (Rosene and Van Hoesen, 1987). Following 24 hour incubation with primary antibody, all tissues were processed by avidin-biotin-peroxidase method using Vectastain ABC kit (Vector Laboratories, Burlingame, CA) followed by treatment with

0.05% DAB, 0.003% hydrogen peroxide and intensified with 0.025% nickel ammonium sulfate and 0.025% cobalt chloride.

Immunocytochemistry

Immunocytochemistry was performed using monoclonal antibody SMI32 (Sternberger Monoclonals Inc., Jarrettsville, MD), which has been shown previously in biochemical and immunohistochemical studies to recognize a nonphosphorylated epitope of the high and medium molecular weight subunits of the NF protein triplet (table 2.1) (Campbell and Morrison, 1989; Lee et al., 1988; Sternberger and Sternberger, 1983). To evaluate the distribution of phosphorylated NF proteins, several tissue sections which were not used in the quantitative analysis were labeled with monoclonal antibody SMI31 (table 2.1) (Sternberger Monoclonals Inc., Jarrettsville, MD) which recognizes a phosphorylated epitope of NF protein or with monoclonal antibody SMI32 for nonphosphorylated NF protein following incubation with 400 µg/ml bovine intestinal mucosa alkaline phosphatase in 0.1 M Tris HCl pH 8.0 at 37° C for 4 hours, a modification of the method of Sternberger and Sternberger (1983).

Analysis

All analyses within this study were performed blind with respect to rearing condition. Both qualitative and quantitative analyses of SMI32 immunoreactivity in the hippocampal formation were performed. The intensity of SMI32 immunoreactivity in hippocampi from both groups of animals was evaluated via optical density measurement. The following regions were evaluated; the granule cell layer, which contains the perikarya and proximal dendrites of the dentate granule cells (Rosene and Van Hoesen,

1987), the dentate molecular layer, which contains distal dendrites of granule cells and axons of the perforant path (Rosene and Van Hoesen, 1987), as well as the pyramidal cell layer and molecular layer of CA3. Additionally, the fimbria was chosen as an internal standard for each tissue section since it was not immunolabeled with SMI32 in any monkey. A more complete discussion of the optical density technique used in this analysis has been previously described (Campbell and Morrison, 1989). Briefly, optical density is calculated from the amount of light which passes through a tissue section, and as such is a direct measure of local light transmission. High immunoreactivity, resulting in low light transmission will yield a high optical density number. Optical density values range from zero to 165, thus a value of zero corresponds to no obstruction in the light path relative to a glass slide, while a value of 165 indicates the absence of light at the detector. In addition to a raw optical density value within each of the specified regions for each rearing condition, optical density ratios were calculated relative to the unlabeled fimbria for each of the remaining areas to control for individual variation in staining intensity between sections. All optical density readings were taken using an Axiophot light microscope (Zeiss, Germany) equipped with a MSP-65 motorized stage unit (Zeiss, Germany) and a DEC 3100 workstation-based morphometry and measurement analysis system. Individual fields (800 μm X 620 μm) were digitized by the computer and 15 optical density measurements were taken within each of the specified regions on each tissue section analyzed. Layers were defined by adjacent Nissl- and acetylcholinesterase-stained sections. Each optical density sample was measured within a computer generated standardized square which fit within the thickness of each of the evaluated regions and

measured 464 μm2. Four tissue sections were evaluated for each of eight monkeys.

Results

For all animals examined, SMI32 immunoreactivity in the hippocampal formation consisted of dark somatodendritic staining in CA2, CA3 and CA4 pyramidal cells as well as the polymorphic cells of stratum oriens and the dentate hilus. Pyramidal cells in both CA1 and the parasubiculum were faintly stained. Cells in the subiculum, presubiculum, prosubiculum and some of the layer II cells of the entorhinal cortex also displayed intense immunoreactivity. All monkeys contained some SMI32 positive cells within the granule cell layer of the dentate gyrus. However, increased intensity of SMI32 labeling was found within the dentate granule cells of the socially deprived group (fig. 3.1). The stronger SMI32 labeling within the granule cell layer of the four deprived animals was comprised of both darker and more numerous labeled cell bodies as well as darker proximal dendritic processes and neuropil (fig. 3.2). Quantitatively, socially deprived animals had a raw optical density value and optical density ratio which was significantly higher than that of the socially reared animals, signifying greater SMI32 immunoreactivity within the granule cell layer ($p < 0.05$, $n = 8$, Student's two-tailed t-test) (fig. 3.3). None of the other zones which were evaluated differed between rearing condition in either their raw optical density value or ratios. (fig. 3.3) Sections treated with alkaline phosphatase displayed increased immunoreactivity throughout the hippocampus, including increased labeling intensity of the perforant path axons. However, no change was observed within in the granule cell layer. In contrast to the somatodendritic localization of SMI32 immunoreactivity,

SMI31 labeled axons of the mossy fiber projection and perforant path in both socially reared and socially deprived animals. Finally, no gross differences were noted in any region of the hippocampal formation among any animals on Nissl-stained tissue sections.

Discussion

The pattern of SMI32 immunoreactivity present in various neuronal subpopulations of the hippocampus in both socially reared and socially deprived animals was consistent with published reports of NF triplet immunoreactivity in the guinea-pig and human (Vickers and Costa, 1992; Vickers and Morrison, 1992). In socially reared animals, this pattern included intense staining in CA2, CA3, CA4, subiculum, presubiculum, prosubiculum, layer II cells of the entorhinal cortex, and polymorphic cells of both the stratum oriens and dentate hilus, with lighter immunoreactivity in CA1, parasubiculum, and granule cell layer of the dentate gyrus. A similar pattern was found in socially deprived animals, with the exception of increased intensity of SMI32 immunoreactivity within the dentate granule cell layer. This consistency of SMI32 immunolabeling across rearing conditions in other regions of the hippocampal formation indicates that the increase in intensity of NF protein immunoreactivity in the socially deprived monkeys may be specific for certain neuronal populations such as the dentate granule cells.

Differences in SMI32 immunoreactivity may represent differential NF protein accumulation or changes in the expression and/or phosphorylation of NF proteins. Pretreatment with alkaline phosphatase, which removes phosphate groups, failed to yield increased immunoreactivity with SMI32

within the granule cell layer. Although it is possible that the alkaline phosphatase treatment did not completely dephosphorylate all NF protein epitopes, the additional lack of immunoreactivity within the granule cell layer of either group of animals with SMI31, which labels phosphorylated NF proteins, indicates that the granule cells of socially reared animals do not have a phosphorylated form of this protein in their soma and dendrites. It is therefore likely that the increased intensity of SMI32 immunoreactivity within the granule cell perikarya represents a higher content of the NF protein triplet. This may in turn be due to a variety of factors including increased expression and/or stability of NF proteins or decreased transport of these proteins to other parts of the cell.

Increased SMI32 immunoreactivity in the dentate granule cells may represent delayed development, as various neuronal types have been demonstrated to display developmentally regulated expression or phosphorylation of NF proteins. For example, cerebellar granule cells display increased immunoreactivity for both phosphorylated and nonphosphorylated epitopes during early postnatal life while cerebellar Purkinje cells do so in the fetal period (Bignami et al., 1985; Cambray and Burgoyne, 1986). However, preliminary data in macaque monkeys suggest that dentate granule cells do not have increased SMI32 immunoreactivity at several time points examined during the initial nine months of postnatal life (Siegel et al., 1992). Immunoreactivity for nonphosphorylated NF proteins is present only at extremely low levels in the nine day old monkey hippocampus. At approximately 3 months of age both CA2 and subicular neurons develop a pattern of immunoreactivity for nonphosphorylated NF proteins which resemble the adult pattern, while CA3 neurons and hilar

neurons appear to do so only at six to nine months of age. At no point in the analysis thus far, has a pattern of immunoreactivity been observed in the dentate granule cells which suggest that the pattern seen in socially deprived animals represents a normal developmental stage. Therefore, preliminary data suggest that increased immunoreactivity for NF proteins seen in dentate granule cells following social deprivation may represent a neuropathologic process. Similar alterations in cytoskeletal proteins have been observed in a variety of neurodegenerative conditions including normal aging, Alzheimer's Disease, Parkinson's disease and Huntington's disease (Cudkowicz and Kowall, 1990; Goldman et al., 1983; Hof and Morrison, 1990; Morrison et al., 1987; Vickers and Costa, 1992; Vickers et al., 1992). Additionally, deafferentation (Shaw et al., 1988), diabetes (Burnstock et al., 1988), thyroid deficiency (Marc et al., 1986), as well as morphine and cocaine (Beitner-Johnson et al., 1992) can cause alterations in NF proteins which indicates that these may be dynamic proteins whose level and/or modification respond to a combination of intrinsic and extrinsic factors. These types of regulated alterations in the cytoskeletal profile of discrete neuronal populations may be expected to have significant effects on the normal functioning of cells.

Although the precise role of NF proteins have not been definitively determined, maintenance of axonal caliber (Hoffman et al., 1984), neuronal shape, dendritic arbor (Campbell et al., 1991) and neuronal stability (Vickers et al., 1992) have been proposed. It has been further hypothesized that NF proteins are linked to neuronal vulnerability in various neurodegenerative conditions. This hypothesis is based on correlative data linking the distribution of the NF protein triplet with the distribution of vulnerable neurons in Alzheimer's disease (Hof and Morrison, 1990; Morrison et al.,

1987; Vickers et al., 1992), Huntington's disease (Cudkowicz and Kowall, 1990), Parkinson's disease and amyotrophic lateral sclerosis (Goldman et al., 1983; Manetto et al., 1989; Vickers and Costa, 1992). Furthermore, it has been shown that certain neuronal populations which are lost in Alzheimer's disease, such as CA1 pyramidal cells, show dramatic increases of nonphosphorylated NF protein in their soma and dendrites during aging, which is potentiated during the early stages of the disease and is coincident with neurofibrillary tangle formation and possibly increased neuronal sprouting (Vickers and Morrison, 1992). Such changes in the cytoskeletal profile of these hippocampal neurons may be linked to deficits in learning and memory that occur in normal aging and Alzheimer's disease, and supports the proposal that not only is NF protein content an important marker for vulnerable cells, but that the expression or modification of NF proteins is an important component of many degenerative processes. Similarly, alterations in the cytoskeletal conformation of dentate gyrus granule cells as observed in this study may reflect the early stages of a degenerative process, which would be expected to impinge on normal hippocampal function later in life. Such a hypothesis is consistent with previous investigations which have shown that early differential handling conditions in rats resulted in alterations of CA3 neurons only in aged rats, suggesting that early events may initiate long-term modifications which affect neuronal survival (Meaney et al., 1988).

The hippocampal formation has been shown to play a critical role in certain aspects of learning and memory (Parkinson et al., 1988; Zola-Morgan and Squire, 1990), in addition to participating in negative feedback of the hypothalamic-pituitary-adrenal stress response (Sapolsky et al., 1991).

Learning deficits in socially deprived monkeys consist of poor performance on oddity tasks, reduced adaptation to reinforcing stimuli, and decreased response inhibition (Beauchamp and Gluck, 1988; Beauchamp et al., 1990). Therefore, changes in this region might underlie learning deficits as well as the prolonged and exaggerated behavioral stress response that socially deprived animals display. Such behavioral and cognitive abnormalities in socially deprived animals are maintained years after they are apparently rehabilitated by resocialization with younger monkeys (Anderson and Mason, 1978), suggesting a long lasting effect of an initial perturbation.

Although behavioral abnormalities in socially deprived animals include a variety of motor and non-motor behaviors, neuroanatomic substrates have only been previously identified for the former. Socially deprived animals exhibit altered motor behavior such as stereotypies in comparison with their socially reared cohorts even years after being placed in similar housing conditions (Lewis et al., 1990). Therefore, previous investigations have focused on permanent perturbations in motor systems of aged monkeys which experienced early total social isolation. Socially isolated animals in these studies had reduced immunoreactivity for calbindin, leu-enkephalin, substance P, and tyrosine hydroxylase within the striatum as well as tyrosine hydroxylase-positive cells in the substantia nigra (Martin et al., 1991). Yet other studies have identified specific neuronal changes in motor cortex and Purkinje cells of young socially deprived animals (Floeter and Greenough, 1979; Struble and Riesen, 1978). In contrast to these positive findings, changes in structures related to the exaggerated behavioral stress response and cognitive deficits described in these animals have been more elusive.

Studies of other brain regions which are thought to be related to affected behaviors are currently under investigation in our laboratory using a variety of markers in these and similarly reared monkeys. However, these studies have so far failed to show any difference between groups. Tyrosine hydroxylase- and corticotropin releasing factor-immunoreactive cell perikarya and dopamine-ß-hydroxylase-immunoreactive varicosities in the hypothalamus as well as neocortical pyramidal cells immunolabeled with SMI32 and non-pyramidal, presumably GABAergic, interneurons which were labeled with antisera to calcium-binding proteins, are consistent across rearing conditions (Ginsberg et al., 1993; Ginsberg et al., 1991; Morrison et al., 1990). These data suggest that although several measures in a variety of brain structures are not affected by social deprivation, there are striking differences in the NF protein immunolabeling of dentate gyrus granule cells between rearing conditions.

Previous reports have correlated alterations in CA3 pyramidal cell cytoarchitecture with social conditions in the wild (Uno et al., 1991; Uno et al., 1989). In the laboratory, restraint stress (Watanabe et al., 1992) as well as differential handling conditions (Meaney et al., 1988) have been linked to alterations in CA3 pyramidal cells in rodents. Similarly, social deprivation serves as a controlled experimental paradigm to assess the interaction between the environment and primate brain development. Alterations in dentate granule cell morphology and density have been described following decreased levels of circulating glucocorticoids secondary to adrenalectomy in rats (Gould et al., 1990; Sapolsky et al., 1991; Sloviter et al., 1989). Although no data exist as to the level of circulating glucocorticoids in socially deprived monkeys, biochemical analyses of blood plasma in socially

reared and socially deprived monkeys indicate that socially deprived monkeys have decreased levels of circulating adrenocorticotropin at one time point during the stress response. (Dr. A. S. Clarke, personal communication). Furthermore, CA3 is the major target of the mossy fiber system which originates from the dentate granule cells. Therefore, alterations in granule cell phenotype might be related to the types of changes which have been reported in CA3 of animals which were subjected to either restraint stress (Watanabe et al., 1992) or social subordination (Uno et al., 1991; Uno et al., 1989).

Additionally, sensitive periods for the anatomic and physiologic maturation of sensory functions such as vision have been demonstrated during postnatal development (Hubel and Wiesel, 1970). It is possible that the neuroanatomic substrates of perturbed behaviors display vulnerability to environmental manipulations only within a sensitive period of postnatal development. For example, sensitive periods have been demonstrated for behavioral measures in socially deprived animals, with deprivation during the first six months of life resulting in qualitatively different effects than similar deprivation for longer periods later in life (Griffin and Harlow, 1966; Kraemer, 1992). Dentate gyrus granule cells may be particularly vulnerable to aberrant rearing conditions during early postnatal life due to their postnatal developmental pattern. Although many primate dentate granule cells are postmitotic at birth, there is a significant level of neurogenesis lasting through six months of age (Eckenhoff and Rakic, 1988; Stanfield and Cowan, 1988). Moreover, many granule cells continue to undergo changes in connectivity and morphology throughout the first year of life (Eckenhoff and Rakic, 1988; Seress, 1992; Stanfield and Cowan, 1988).

The immunocytochemically identified change described in this study is the first demonstration of a social deprivation induced alteration within a primate brain region, the hippocampus, which is potentially related to both negative feedback of the stress response and learning deficits. Such an immunohistochemically identified change in a specific protein, which is not evident with Nissl staining or other strictly morphologic techniques, underscores the importance of looking for subtle changes which result from environmental manipulations yet may permanently affect the cellular processes and structural integrity of particular neurons.

Figure 3.1

SMI32 staining patterns in the dentate gyrus of socially deprived and socially reared monkeys. A,B) Low power photomicrographs of hippocampal formation of a socially deprived (A) and socially reared (B) monkey. C) Dense immunoreactivity of the granule cell layer in a deprived monkey. D) Socially reared monkeys displayed lower immunoreactivity in the granule cell layer, although some immunopositive cells are present. Abbreviations and symbols: (DG) dentate gyrus, (H) hilus of the dentate gyrus, (SUB) subiculum, (arrow) granule cell layer of the dentate gyrus, (asterisk) dentate gyrus molecular layer. Scale bar = 1000 μm (A,B), 50 μm (C, D).

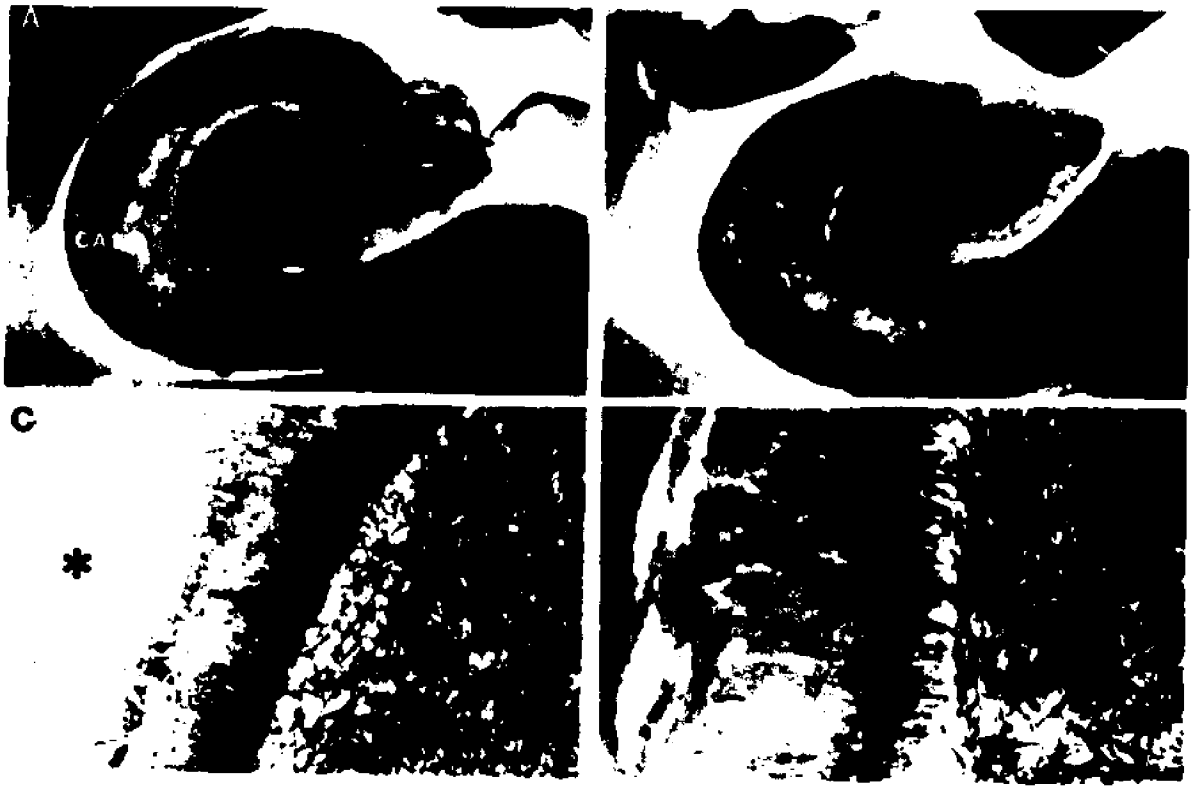
A
CA
C
*

Figure 3.2

High power photomicrograph of SMI32 labeling in the granule cell layer from a socially deprived (A) and a socially reared (B) animal. Note the increased intensity of SMI32 immunoreactivity in (A). Tissue sections are counterstained with cresyl violet. Abbreviations: (GCL) granule cell layer. Scale bar = 25 μm.

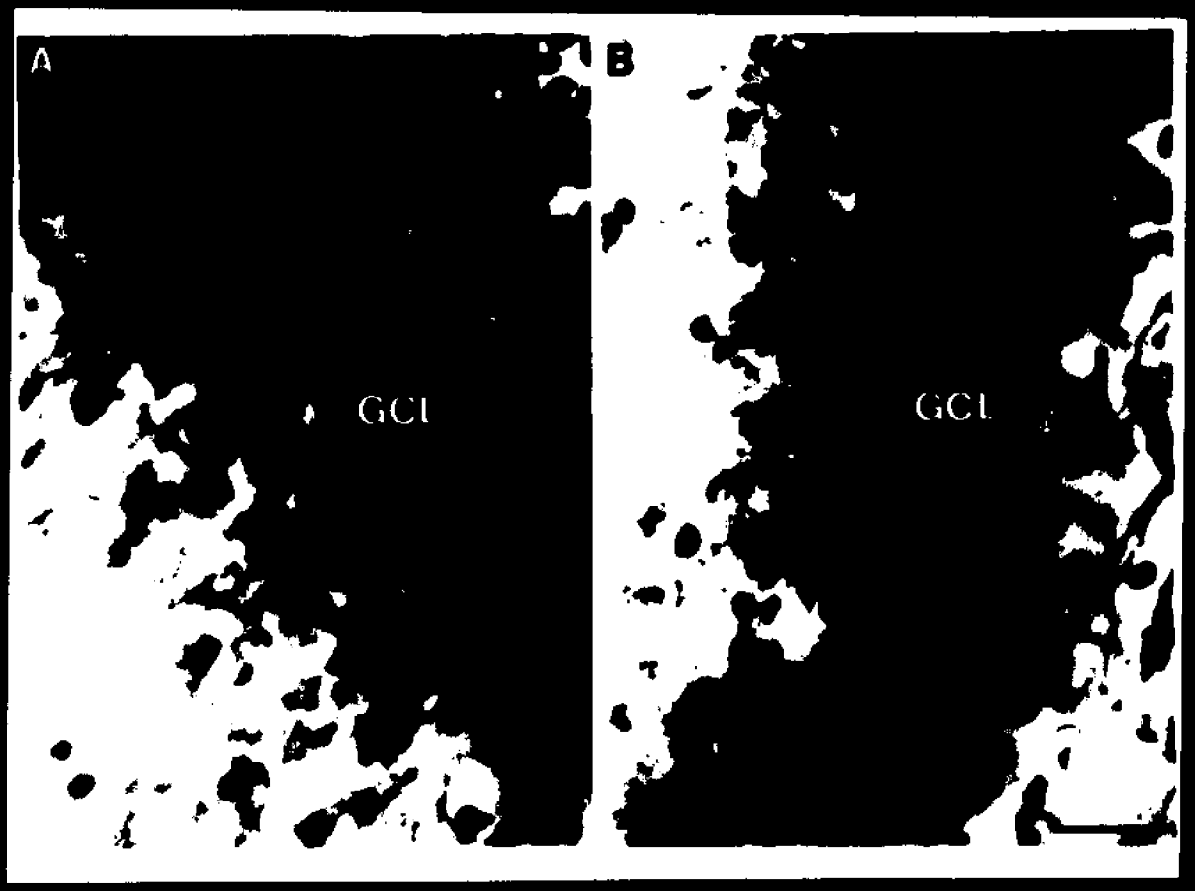
A
GCL
B
GCL

Figure 3.3

Optical density measurements for SMI32 immunoreactivity in socially reared (SR) and socially deprived (SD) monkeys within five regions of the hippocampus. A) Raw optical density values generated on a scale of 0.0 (no obstruction in the light path) to 165 (no light reaches the detector). The difference in the optical density within the granule cell layer is statistically significant at $p = 0.04$. B) Optical density ratios for the CA3 pyramidal cell layer and molecular layer as well as the dentate gyrus granule cell layer and molecular layer to the unstained fimbria. The difference in optical density ratio within the granule cell layer is statistically significant at $p = 0.02$. Abbreviations: DG - dentate gyrus, gcl - granule cell layer, ml - molecular layer, pcl - pyramidal cell layer. * indicates $p < 0.05$.

Figure 3.3

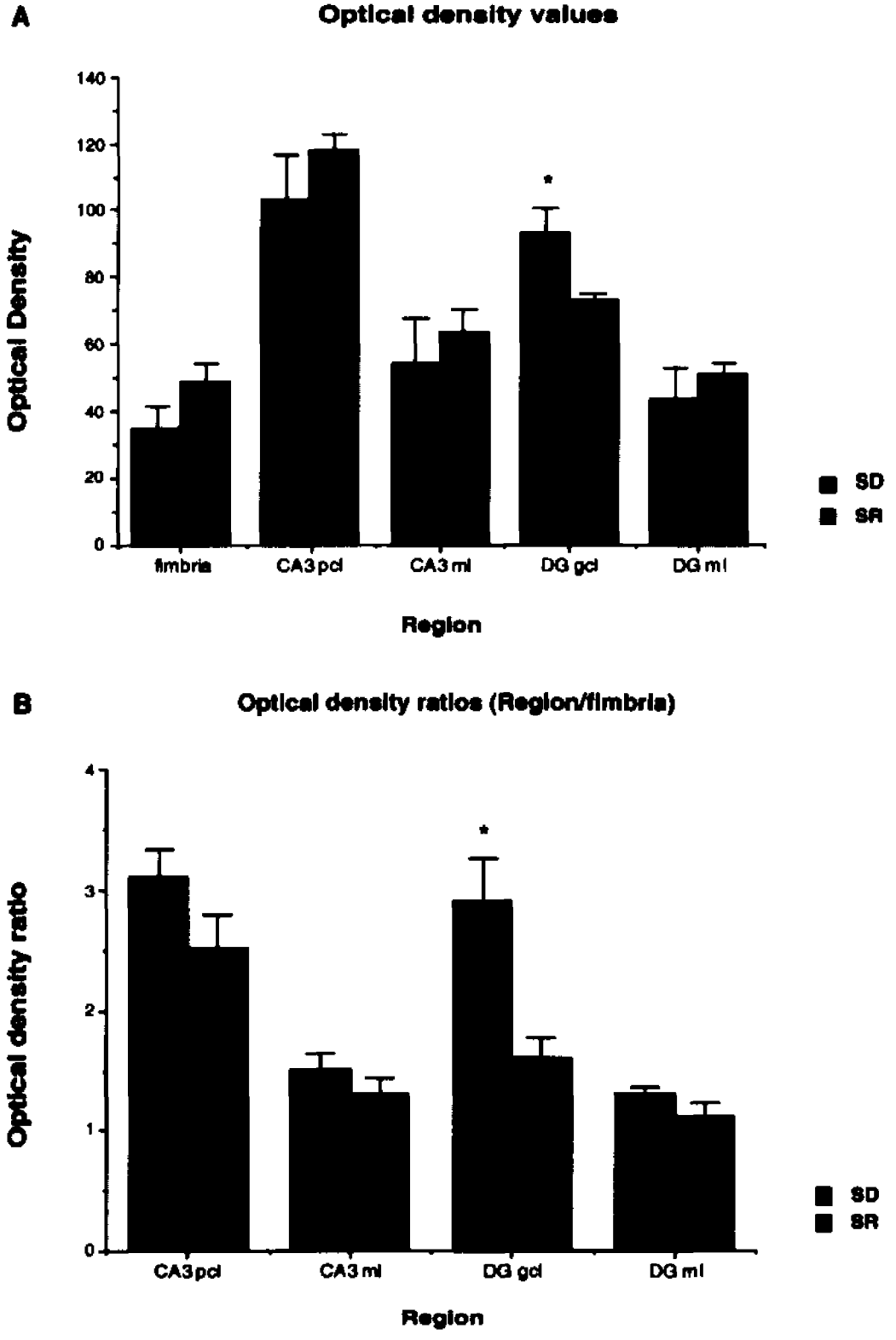
A
Optical density values
Optical Density
140
120
100
80
60
40
20
0
*
fimbria
CA3 pcl
CA3 ml
DG gcl
DG ml
Region
SD
SR
B
Optical density ratios (Region/fimbria)
Optical density ratio
4
3
2
1
0
*
CA3 pcl
CA3 ml
DG gcl
DG ml
Region
SD
SR

Chapter 4

Effects of Social Deprivation in Prepubescent Rhesus Monkeys: Immunohistochemical Analysis of the Mossy Fiber Projection and CA3 Pyramidal Cells

Abstract

Following the observation of alterations in immunoreactivity for nonphosphorylated NF proteins in the dentate granule cells of socially deprived monkeys (Chapter 3), studies were designed to examine the effects of social deprivation on the axonal projection of these cells. As axonal projections are thought to affect the dendritic organization of recipient cell populations, the current study also examines patterns of dendritic organization of CA3 pyramidal cells, which are the primary target of granule cell axons. Immunocytochemistry using antibodies to MAP2 was used to visualize CA3 pyramidal cells, while antibodies to calbindin and phosphorylated NF proteins labeled mossy fiber axons. Results from these experiments indicate that a subset of the socially deprived animals differed from the remaining animals with markers for both the mossy fiber axons, and dendritic organization in CA3. A second series of experiments was then performed to examine the patterns of immunoreactivity for each of the markers described above in a group of nine day old animals, as well as immunoreactivity for phosphorylated NF proteins at four additional time points during the first nine months of life. Data from these experiments indicate that patterns of immunoreactivity within mossy fiber axons and CA3 pyramidal cell dendrites in nine day old monkeys are similar to those seen in socially reared juvenile animals. Such data suggest that patterns of

immunoreactivity seen within the brains of socially deprived animals may represent a change from a previously existing condition, rather than a failure to develop.

Introduction

Environmental perturbations such as social deprivation are proposed to affect the maturation of the primate brain in such a way as to retard or disrupt the normal development of specific neuronal populations at both the cellular and intercellular levels. Chapter 3 reviews previous work regarding both the behavioral and anatomic effects of social deprivation in monkeys. Additionally, the previous chapter documents the observation of increased levels of immunoreactivity for the nonphosphorylated (somatodendritic) form of NF proteins in the dentate gyrus granule cells of monkeys which were raised in social deprivation. The current study extends this work by examining the effects of social deprivation on the axonal projection of the dentate gyrus granule cells. Furthermore, as axonal ingrowth has been suggested to have profound organizational effects on the morphology of recipient neuronal populations (Hendry and Jones, 1983), the current study also examines the neuronal population on which dentate granule cell axons terminate. Previous studies have suggested that dentate granule cell axons may influence the dendritic architecture of CA3 pyramidal cells during normal maturation. For example, studies in rats have shown that characteristic synapses called thorny excrescences on CA3 pyramidal cells only develop in the presence of mossy fibers (Gaiarsa et al., 1992; Represa et al., 1991). Therefore, the current study will focus on this intrinsic hippocampal circuit between dentate granule cells and CA3 pyramidal cells in the context of social deprivation induced alterations in specific neuronal populations.

Rearing condition-dependent differences in the presence, relative amount, molecular form or subcellular distribution of specific proteins may represent either the induction of abnormal intracellular processes or alternatively, the disruption of normal developmental events. Thus the current study seeks to determine whether changes in immunoreactivity within specific cell populations secondary to social deprivation represent a delayed developmental phenomenon or alternatively, the induction of a neuropathologic response to an environmental condition. In order to provide a developmental context in which to interpret observed differences related to rearing condition, the current study examines immunoreactivity for several proteins which are localized to either the mossy fiber projection or CA3 pyramidal cell dendrites. Specifically, patterns of immunoreactivity for phosphorylated NF and calbindin which are localized to mossy fiber axons, and MAP2 which labels pyramidal cell dendrites, were examined within the hippocampal formations of 1.5-2.5 year old animals which were either socially reared or socially deprived, as well as during early postnatal life in a series of animals which were sacrificed between 9 days and 9 months of life. Furthermore, the normal maturation of granule cell axons within the monkey hippocampus was also examined using of tract tracing techniques.

Methods and Materials

Animals

The current study utilized brain tissue from the two groups of animals described within chapter 3. Briefly, this included eight juvenile animals which were either socially reared (n=4) or socially deprived (n=4), as well as 15 monkeys which were sacrificed in groups of three at nine days, one month, three months, six months or nine months of life respectively.

Tissue Preparation

Tissue preparation for frozen sections was performed as described above. However, no intensification technique was used following DAB treatment. Tissue preparation for vibratome material is described below within the DiI portion of the methods.

Immunocytochemistry

Immunocytochemistry was performed using monoclonal antibodies SMI32 (Sternberger Monoclonals Inc., Jarrettsville, MD) and SMI31 (Sternberger Monoclonals Inc., Jarrettsville, MD) which are described in chapter 3, as well as a monoclonal antibodies to the calcium binding protein calbindin (table 2.1) (kindly provided by Dr. M Celio), and the microtubule associated protein MAP2 (table 2.1) (Sigma Immuno Chemicals, St. Louis, MO).

DiI

Crystals of the lipophilic fluorescent dye DiI were placed in the granule cell layer on a block of tissue which was approximately 1 mm in diameter to evaluate the presence of the mossy fiber axons at 9 days of age. Following six hour fixation with 4% paraformaldehyde, crystals of DiI dissolved in methanol were placed around the entire extent of the dentate gyrus within the granule cell layer under microscopic visualization. These blocks were then stored in the dark in PBS with 0.1% sodium azide at 37° C for a period of five weeks. Tissue blocks were then sectioned at 50 µm on a vibratome (Ted Pella, Irvine CA) and either examined directly under fluorescence microscopy or treated for immunocytochemistry to examine the distribution of phosphorylated NF proteins within DiI-labeled mossy fiber axons. Fluorescence labeled immunocytochemistry with mAb SMI31 was performed as described above with the following modifications. Tissue sections were incubated with mAb SMI31 for 24 hours, followed by three washes in PBS. Sections were then incubated for 2 hours in FITC-conjugated goat anti-mouse IgG heavy and light chain specific antisera (Vector Laboratories, Burlingame, CA), followed by three washes in PBS.

Analysis

All tissue sections were analyzed on an Axiophot microscope (Zeiss, Germany). Tissue sections which were processed for DAB-labeled immunocytochemistry were viewed by conventional bright field microscopy, while DiI-treated and FITC-labeled sections were viewed under fluorescence illumination.

Results

Social Deprivation Studies

In all eight animals included in the rearing condition studies, the mossy fiber projection was immunolabeled with mAb SMI31, which recognizes phosphorylated NF proteins, as well as a monoclonal antibody to the calcium-binding protein calbindin. Although each of these markers labeled the mossy fibers with a pattern which resembled previously reported Timm's stain labeling (Seress, 1992), there were subtle differences between them. Immunoreactivity for phosphorylated NF proteins labeled mossy fibers within the dentate hilus and approximately the proximal two-thirds of the stratum lucidum (fig 4.1). However, immunoreactivity for calbindin was visible within the hilus and throughout the entire extent of the stratum lucidum (fig. 4.2). Furthermore, the intensity and pattern of immunolabeling with both of these markers varied among the eight animals examined.

Phosphorylated Neurofilaments

Among the eight animals examined, there were subtle variations in the pattern of immunoreactivity for phosphorylated NF proteins (fig. 4.1). Although the pattern of immunoreactivity was consistent within the dentate hilus, where the mossy fiber projection was immunolabeled in all animals, the pattern of immunolabeling in the stratum lucidum had two predominant patterns. In two of the animals, diffuse immunolabeling within the proximal 2/3 of the stratum lucidum was of approximately equal intensity to that in the hilus (fig. 4.1 A, B). However, in the remaining six animals, immunolabeling within the stratum lucidum displayed a pattern of intensely

labeled areas interspersed with unlabeled regions (fig. 4.1 C, D). Unlabeled regions were presumed to contain CA3 pyramidal cell dendrites based on data presented below for MAP2 immunoreactivity.

Calbindin

There were two discernible patterns of immunoreactivity for the calcium-binding protein calbindin present within the group (fig. 4.2). Two animals exhibited a pattern of diffuse immunolabeling in the stratum lucidum of CA3, as well as faint labeling of the mossy fibers within the central portion of the dentate hilus (fig. 4.2 A, B). However, the remaining six animals displayed a pattern of immunolabeling which included intense immunoreactivity within the stratum lucidum, fainter labeling within stratum oriens, and labeling of mossy fibers throughout the entire portion of the dentate hilus (fig. 4.2 C, D). Additionally, non-immunolabeled areas interspersed between intensely immunoreactive areas were apparent within the stratum lucidum of the latter six animals with a pattern similar to that described above for phosphorylated NF proteins.

The two animals which displayed faint, diffuse labeling of the mossy fibers within the stratum lucidum and dentate hilus with antibodies for phosphorylated NF proteins and/or calbindin were the youngest animals in this series, as well as both being socially deprived. These animals were also the two subjects among the group of socially deprived animals in which the isolation induced psychopathology was most severe. The group of animals which displayed more intense patterns of immunoreactivity for both antibodies consisted of two socially deprived and four socially reared animals.

MAP2

Immunohistochemistry was also performed for the microtubule associated protein MAP2, which labels the somatodendritic compartment of pyramidal cell bodies throughout Ammon's horn, including those in CA3. Pyramidal cell apical dendrites could be seen within the stratum lucidum of CA3 in all animals examined (fig. 4.3). In six of the eight animals, unlabeled areas were apparent between bundles of labeled apical dendrites (fig. 4.3 C, D). These unlabeled areas were presumed to contain mossy fiber axons as they appeared to correspond to areas which were labeled with calbindin and phosphorylated NF proteins. Such areas of mossy fiber axons and terminals occupying spaces between CA3 pyramidal cell dendrites were also apparent in DiI labeling of the mossy fiber projection (below) and at the electron microscopic level (chapter 5). However, in two of the animals examined, CA3 apical dendrites did not have a bundled appearance, and no unlabeled areas were visible within the stratum lucidum (fig. 4.3 A, B). The two animals which lacked the appearance of dendritic bundling, as well as lacking MAP2 non-immunoreactive areas within the stratum lucidum, were the same two animals which differed from the remaining six animals in immunolabeling of the mossy fiber projection. As noted above, these two animals were the youngest animals within the series as well as both being socially deprived.

Developmental studies

Immunocytochemistry for calbindin, phosphorylated NF proteins and MAP2 was performed within the hippocampal formations of three nine day old animals. Additionally, immunoreactivity for phosphorylated NF proteins

was performed within the hippocampal formations of three animals at one month, three months, six months and nine months of age respectively.

Phosphorylated Neurofilament Proteins

In all animals between nine days and nine months of age, the mossy fiber projection was immunolabeled for phosphorylated NF proteins with a pattern of immunoreactivity which was similar to that seen in socially reared juvenile animals. Within the stratum lucidum, intensely labeled areas were interspersed with non-immunoreactive areas as described above for socially reared juvenile monkeys (fig. 4.1 E, F). Similarly, mossy fibers were immunolabeled within the dentate hilus of all animals at each time point within this study. Immunoreactivity for phosphorylated NF proteins was also localized to the perforant path projection as well as in scattered axonal profiles throughout the hippocampus at all time points examined.

Calbindin

In nine day old animals, immunoreactivity for calbindin exhibited a pattern which was similar to socially reared juvenile monkeys (fig. 4.2 E, F). Immunolabeled mossy fiber axons were visible throughout the dentate hilus, as well as in both the stratum lucidum and oriens of CA3. As in juvenile socially reared monkeys, calbindin immunoreactivity within the stratum lucidum was relatively intense as compared with mossy fiber labeling with in the hilus or stratum oriens. Calbindin also labeled granule cell bodies and the dentate molecular layer, as well as CA1 pyramidal cells.

MAP2

Immunoreactivity for MAP2 was present within pyramidal cell bodies and dendrites in all fields of Ammon's horn in nine day old monkeys. In CA3, apical dendrites within stratum lucidum were immunolabeled, although the bundled appearance seen in juvenile socially reared animals was less pronounced (fig. 4.3 E, F). However, non-immunoreactive areas between dendritic profiles were present within stratum lucidum, as well as in the molecular layer of CA1. In both of these cases, the clearings coincided spatially with the mossy fiber axons and perforant path projection, seen in adjacent nonphosphorylated NF protein and/or calbindin labeled sections, respectively.

DiI

Additionally, ingrowth of the mossy fiber pathway was studied with the use of the lipophilic fluorescent dye DiI to determine when this projection is present within the stratum lucidum of CA3, independent of protein expression. As demonstrated in figure 4.4, the mossy fiber projection can be seen projecting through the dentate hilus into CA3 as early as nine days of age. Mossy fiber axons could be seen within stratum lucidum as well as in the strata pyramidale and oriens. A diffuse pattern of DiI labeling could be seen at regularly spaced intervals within stratum lucidum, approximately one centimeter caudal to the placement of the dye crystals. This pattern was not apparent at the same rostro-caudal plane as the dye placement, where the fine caliber DiI-filled axons were seen within the hilus, as well as above and below the stratum lucidum.

Several of the DiI-treated sections were processed for immunohistochemistry to visualize phosphorylated NF proteins within identified axons (fig. 4.4), or MAP2 to demonstrate the spatial relationship between mossy fiber axons and CA3 pyramidal cell dendrites. Sections labeled for phosphorylated NF proteins showed two predominant patterns. In sections which were taken from approximately the same rostro-caudal level as the placement of DiI crystals, DiI-labeled axons and NF proteins were not strictly colocalized. While DiI was seen within fine axonal profiles above and below stratum lucidum, diffuse NF protein immunoreactivity was most pronounced within stratum lucidum (fig. 4.4 A, B). However, approximately one centimeter caudal to the placement of DiI crystals, DiI and NF protein immunoreactivity was colocalized within stratum lucidum (fig. 4.4 C, D), suggesting that mossy fiber axons course caudally through the hilus and terminate within the stratum lucidum at a level caudal to their origination. Sections which were treated with antibodies to MAP2 also exhibited two main patterns of distribution for DiI. While MAP2-immunolabeled pyramidal cell dendrites were visible within the stratum lucidum in both cases, the pattern of interdigitation of DiI-labeled axons between bundles of MAP2 labeled dendrites was only visible in the more caudal sections.

Discussion

The first portion of the current report describes patterns of immunoreactivity for phosphorylated NF proteins and calbindin within the mossy fiber projection, and MAP2 within CA3 pyramidal cells in eight juvenile monkeys which were either socially reared or socially deprived. The second portion of this study examines the same three

immunocytochemical markers, as well as DiI labeling within the mossy fiber projection and CA3 pyramidal cells of three nine day old monkeys. Patterns of immunoreactivity for phosphorylated NF proteins were examined at four additional time points during the first nine months of life.

Social deprivation

The current report describes alterations in the patterns of immunoreactivity for two axonal markers within the mossy fiber projection and one somatodendritic marker within CA3 pyramidal cells in two of eight juvenile monkeys. Specifically, immunoreactivity for phosphorylated NF proteins and calbindin within mossy fiber axons was less intense in two socially deprived animals than in the remaining animals. Furthermore, CA3 pyramidal cell apical dendrites in stratum lucidum appeared to be homogeneously spaced rather than the bundled appearance exhibited by the remaining six animals. The two animals which differed from the remainder of the group were both the youngest animals in the study and socially deprived, thereby confounding a possible correlation between either age or rearing condition with these perturbations.

Dendritic bundling may represent a developmental pattern (Hirst et al., 1991; Serfling and Schuster, 1983). It may also be possible that there is an organizing effect of the mossy fiber system on CA3 dendrites within stratum lucidum during a sensitive period. Axonal ingrowth has been suggested to have profound organizational effects on the morphology of recipient neuronal populations (Hendry and Jones, 1983). One way in which this relationship has been investigated has been with the use of several genetic mutations in mice. In both weaver and reeler mutant mice, there is a

lack of normal cerebellar development characterized by abnormal granule cell survival and/or migration, which in turn is thought to have profound effects on the morphologic development of other cerebellar cell populations. For example, although Purkinje cells survive in both strains, they fail to develop their normal dendritic branching pattern, presumably due to the absence of parallel fibers from the cerebellar granule cells (Shepherd, 1983). Such an interaction may exist between dentate granule cell axons and the cells which they innervate, CA3 pyramidal neurons. Golgi studies in rat have shown that characteristic synapses called thorny excrescences on CA3 pyramidal cells develop postnatally (Amaral and Dent, 1981), and only in the presence of mossy fibers (Gaiarsa et al., 1992; Represa et al., 1991).

Developmental Study

Due to the interaction between age and rearing condition seen among differentially reared animals, experiments involving a developmental series of animals were initiated to determine the normal developmental pattern of the mossy fiber axons with respect to NF proteins and the calcium-binding protein calbindin. The patterns of immunoreactivity observed in these animals, may provide a context in which to interpret alterations seen in differentially reared animals.

Immunoreactivity for phosphorylated NF proteins as well as calbindin was present within the mossy fiber axons in a group of three nine day old animals. Similarly, the lipophilic dye DiI-labeled mossy fiber axons both within the dentate hilus and stratum lucidum of CA3 in these new born animals. Additionally, immunoreactivity for the somatodendritic marker MAP2 was localized to CA3 pyramidal cells, where a pattern of dendritic

bundling was already apparent at nine days of age. Results from these analyses indicate that the mossy fiber axons are present at their target cells by nine days of age, and furthermore, that patterns of immunoreactivity for phosphorylated NF proteins and calbindin at this time point are similar to those in juvenile animals.

Conclusions

Previous studies have indicated that although mossy fiber axons are present within the dentate gyrus of the primate hippocampus at birth, there is prolonged development of the structural connections between granule cells and their postsynaptic targets through a long postnatal period (Seress, 1992) Therefore, it is possible that alterations seen within the circuit between dentate granule cells and CA3 pyramidal cells secondary to environmental manipulations may result from interference in the normal progression of developmental events. However, immunoreactive patterns within the mossy fiber axons and CA3 pyramidal cells of three nine day old animals were similar to those seen in socially reared juvenile monkeys, suggesting that such patterns are already present perinatally. It is therefore unlikely that the patterns of immunoreactivity seen in two juvenile socially deprived animals represent the failure to develop into a mature pattern. Observations within the current study suggest that alterations seen in mossy fiber axons and CA3 pyramidal cell dendrites, as visualized by immunoreactivity for phosphorylated NF proteins, calbindin, and MAP2 following social deprivation may represent the induction of an aberrant, possibly harmful change in existing structures, rather than a delayed developmental stage.

Figure 4.1

Phosphorylated NF protein immunohistochemistry within the mossy fiber projection from the dentate granule cells labeled with monoclonal antibody SMI31 (Sternberger Monoclonals Inc. Jarrettsville, MD). The intensity and pattern of immunolabeling with phosphorylated NF (SMI31) seems to change with both age and rearing condition. In an 18 month old socially reared monkey (C, D), the pattern consists of intense staining of the mossy fibers within the stratum lucidum, which contains CA3 pyramidal cell apical dendrites. A similar pattern is already present in the 9 day old animal (C, F). However, two of the deprived monkeys (A, B) have a greatly decreased intensity of immunolabeling of the mossy fibers within the SL as compared with both the socially reared and 9 day old monkeys. Abbreviations; arrow - granule cell layer, asterisk - molecular layer of the dentate gyrus, h - hilus of the dentate gyrus, arrow head -stratum lucidum. Scale bars = 500 μm

Phosphorylated Neurofilament

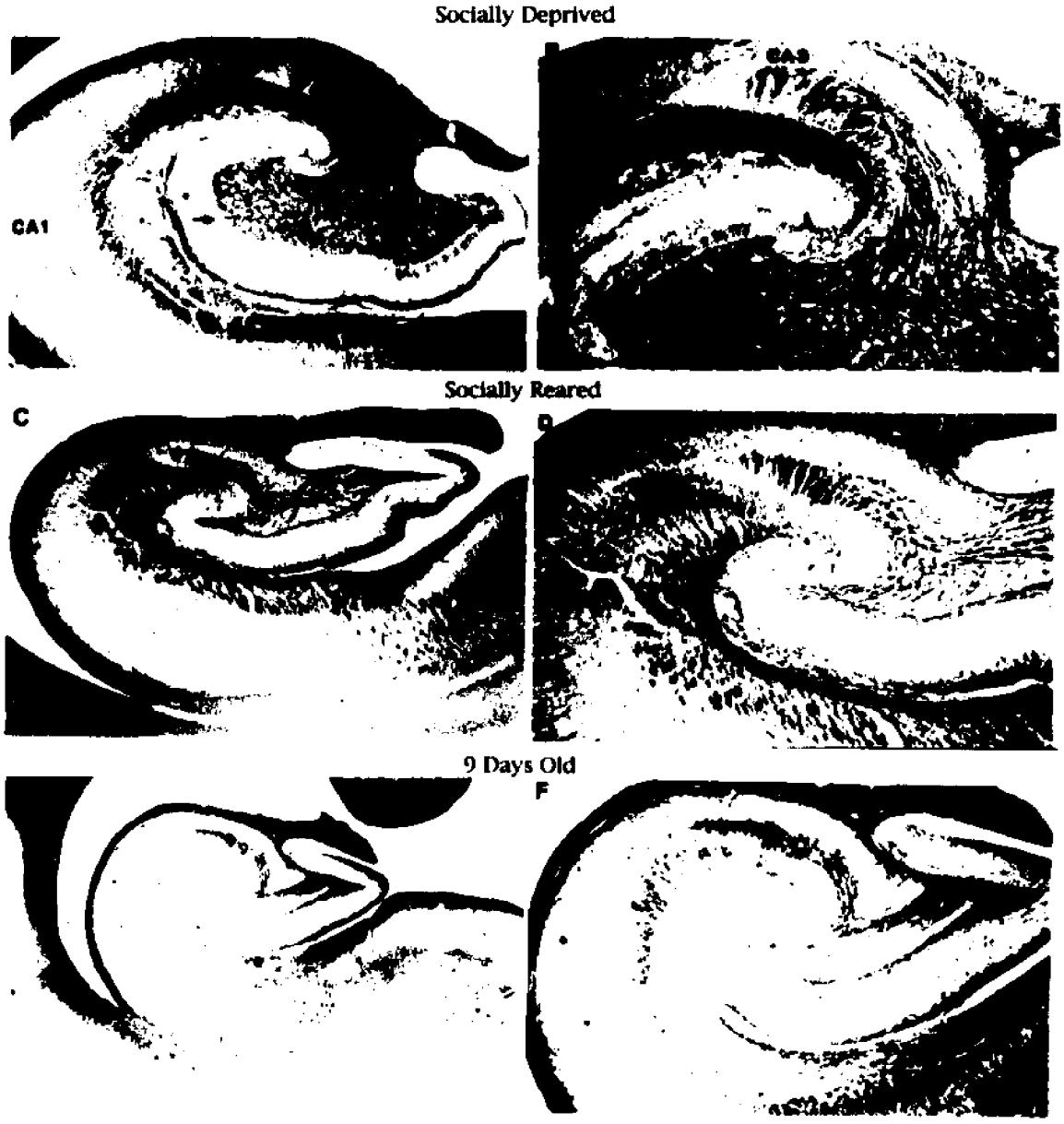

Figure 4.2

Immunohistochemistry directed against the calcium-binding protein calbindin within the mossy fibers. The intensity and pattern of immunolabeling with calbindin seems to change with both age and rearing condition. In an 18 month old socially reared monkey (C, D), the pattern consists of intense staining of the mossy fibers within the stratum lucidum, which contains CA3 pyramidal cell apical dendrites. Less intense staining was present with in the stratum oriens, which contains the basal dendrites of CA3 pyramidal cells. Additionally, there are clear zones present within the stratum lucidum which represent the unstained bundles of CA3 apical dendrites. A similar pattern is already present in the 9 day old animal (E, F). However, two of the deprived monkeys (A, B) have a greatly decreased intensity of immunolabeling of the mossy fibers within the SL as compared with both the socially reared and 9 day old monkeys. Additionally, there is no calbindin immunoreactivity within the stratum oriens of these monkeys. Abbreviations; arrow - granule cell layer, asterisk - molecular layer of the dentate gyrus, h - hilus of the dentate gyrus, arrow head -stratum lucidum. Scale bars = 500 μm

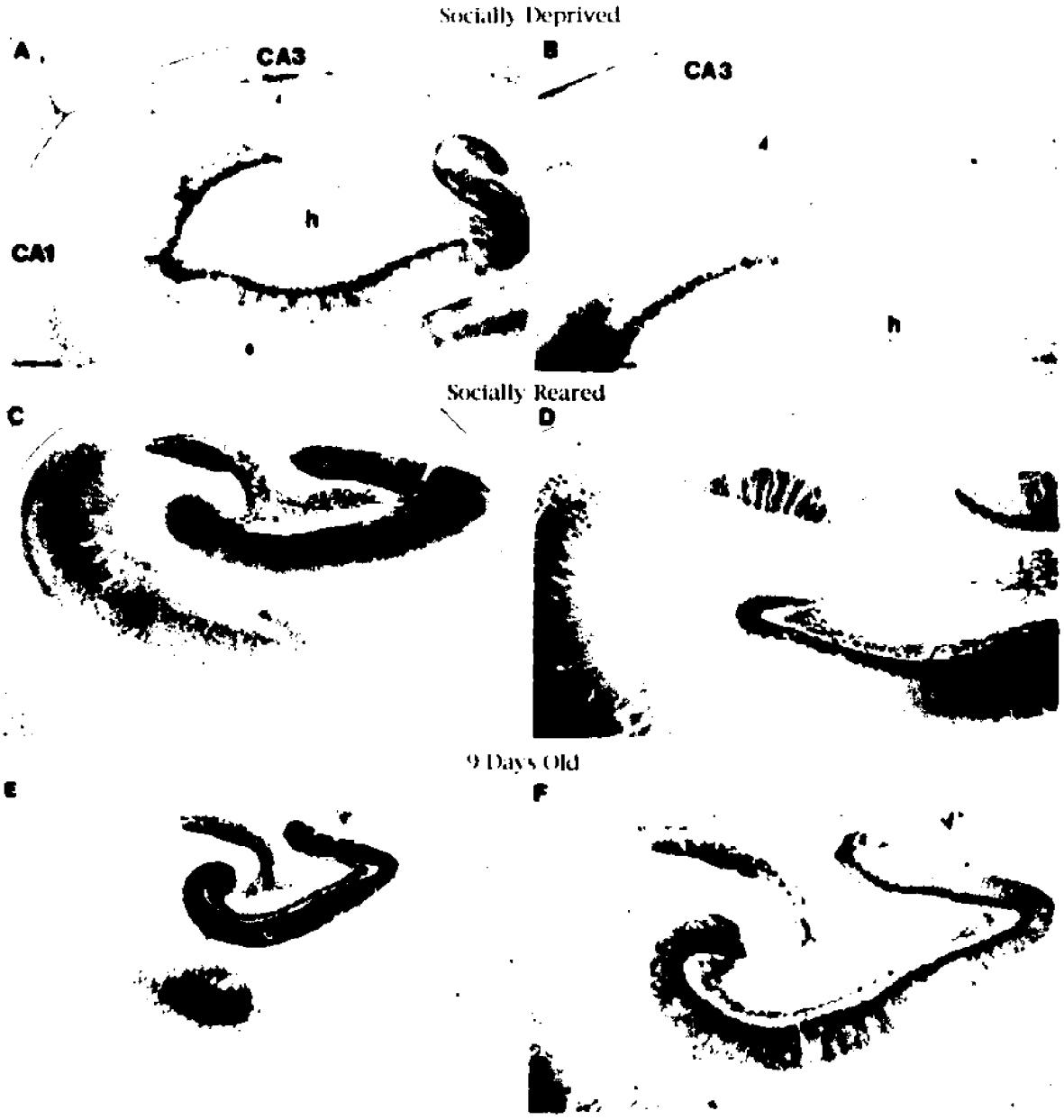
Calbindin
Socially Deprived
A
CA3
CA1
h
B
CA3
h
Socially Reared
C
D
9 Days Old
E
F

Figure 4.3

MAP2 immunohistochemistry using a monoclonal antibody (Sigma Immunochemicals, St. Louis, MO) in the hippocampal formation of socially deprived (SD), Socially Reared (SR), and 9 day old rhesus monkeys. Apical dendrites of CA3 pyramidal cells within the stratum lucidum of displayed decreased bundling and inter-dendritic space in two socially deprived monkeys (A) with respect to both socially reared (B) and 9 day old monkeys (C). Abbreviations; arrow - granule cell layer, asterisk - molecular layer of the dentate gyrus, h - hilus of the dentate gyrus, arrow head -stratum lucidum. Scale bars = 500 μm - A, C, E; 100 μm - B, D, F.

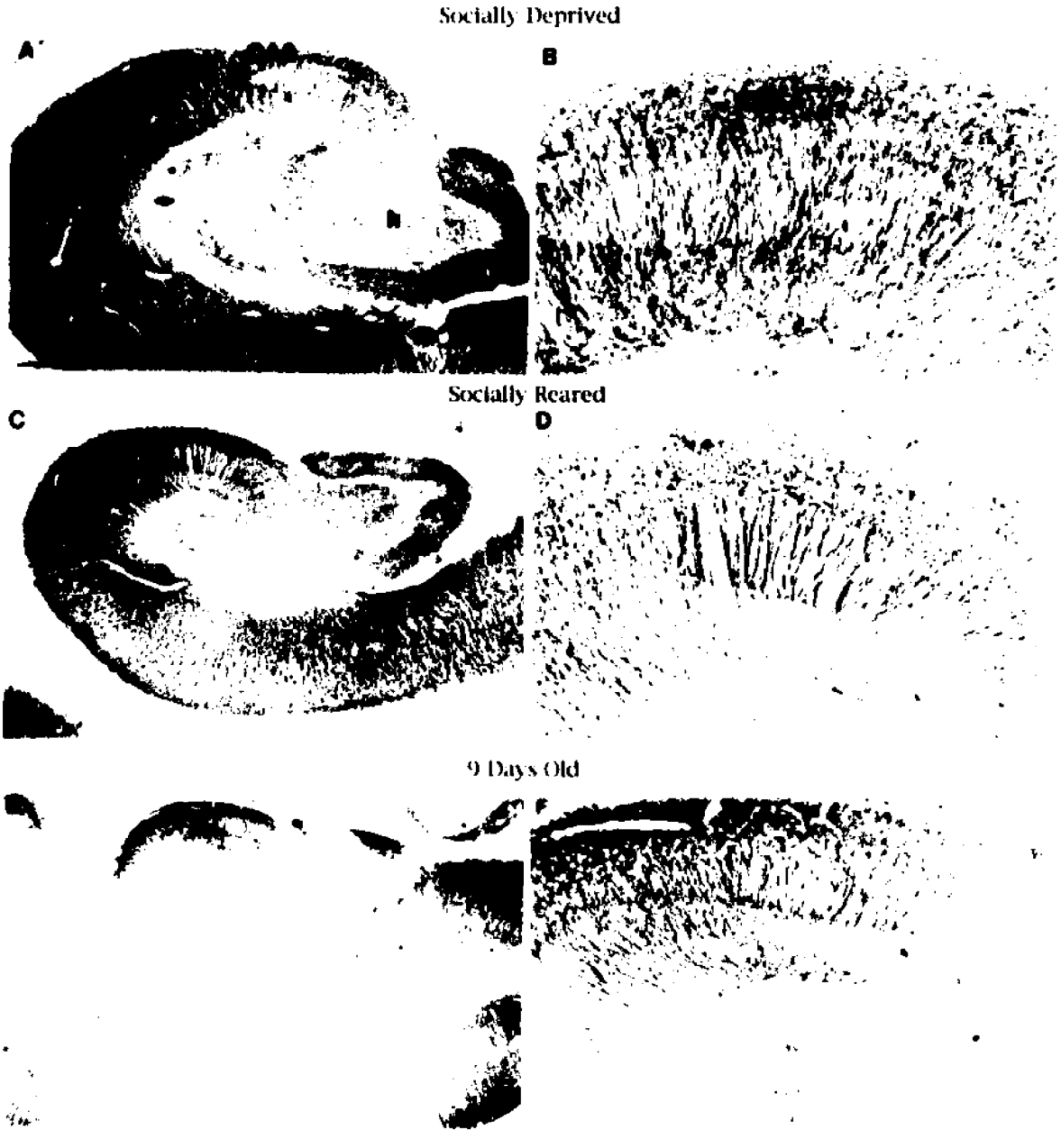
Socially Deprived
A
B
Socially Reared
C
D
9 Days Old

Figure 4.4

DiI-labeled mossy fiber axons in nine day old monkeys which have been immunolabeled for phosphorylated NF proteins. A) DiI-labeled mossy fibers in a 9 day old monkey taken from approximately the same rostro-caudal plane as the placement of DiI crystals in the granule cell layer. Notice how DiI is not seen within the stratum lucidum of CA3 at this level. B) Immunoreactivity for phosphorylated NF proteins labels mossy fiber axons within the stratum lucidum in the section shown in A. C) DiI-labeled mossy fibers in a 9 day old monkey taken from approximately 1 cm caudal to the placement of DiI crystals. Notice that at this level DiI is seen within the stratum lucidum. D) Immunoreactivity for phosphorylated NF proteins within mossy fiber axons are colocalized with DiI within the stratum lucidum. Scale bar = 100 μm

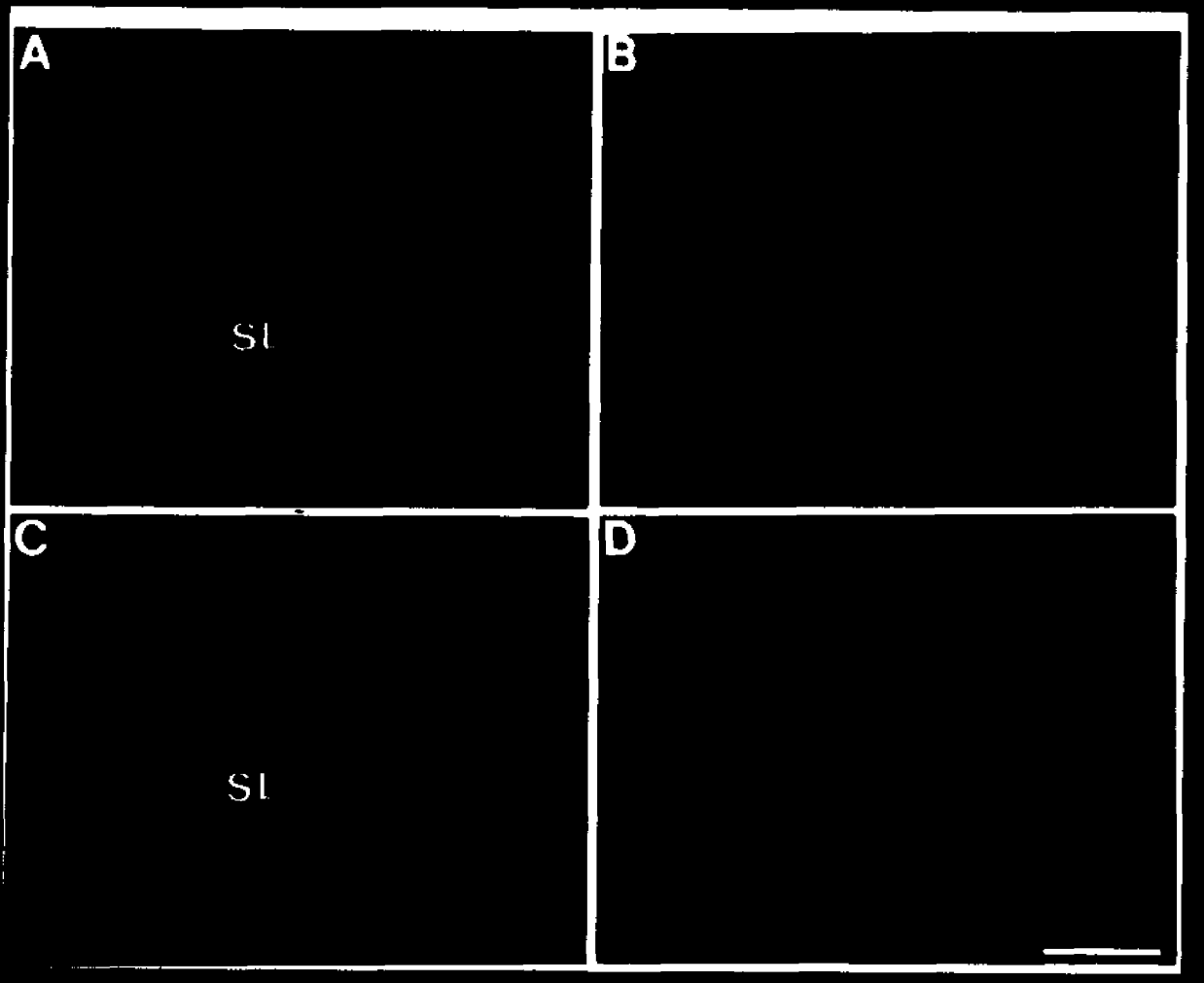
A
SL
B
C
SL
D

Chapter 5

Regional, Cellular, and Ultrastructural Distribution of the Excitatory Amino Acid Receptor Subunit NMDAR1 in Monkey Hippocampus [5]

Abstract

The regional, cellular and subcellular distributions of the N-methyl-D-aspartate (NMDA) receptor subunit, NMDAR1, were investigated in monkey hippocampus using a monoclonal antibody directed against a fusion protein corresponding to amino acids 660-811 of NMDAR1. The data indicate that a high density of neurons in each subfield of the hippocampus contain NMDAR1 protein, although the intensity and distribution of immunoreactivity varied across regions, strata and cellular compartments. In stratum lucidum of CA3, mossy fiber axons were immunoreactive for NMDAR1, which may correspond to previously hypothesized presynaptic receptors. NMDAR1-labeled postsynaptic profiles were present in stratum radiatum of CA3, but were largely absent from stratum lucidum. Such intraneuronal segregation of GluR subunits or classes may be spatially correlated with afferent systems that exhibit laminar segregation and terminate in different portions of the postsynaptic dendritic tree. For example, in CA3 pyramidal cells, NMDA receptors are postsynaptic in distal apical dendrites (stratum radiatum) where NMDA-dependent long term potentiation in rats is mediated by associational/commissural afferents, and absent from proximal apical dendrites (stratum lucidum) where NMDA-independent LTP is mediated by the mossy fiber input.

---

[5] This chapter appears in *The Proceedings of the National Academy of Sciences* (1994) **91** pp 564-568, and is reprinted here with the express permission of *The Proceedings of the National Academy of Sciences*.

Introduction

Excitatory neurotransmission in the central nervous system is thought to be largely mediated by the excitatory amino acids glutamate and aspartate through their effects at pre- and postsynaptic receptors (Fagg and Foster, 1983). The molecular, physiological and structural characteristics of various EAA receptors have been recently reviewed elsewhere (Heinemann and Hollmann, 1994; Nakanishi, 1992; Seeburg, 1993), and therefore will not be comprehensively described in this report [6].

The function and distribution of putative postsynaptic NMDA receptors has been investigated in numerous physiological, pharmacological and *in situ* hybridization studies (Cotman et al., 1987; Nakanishi, 1992). However, presynaptic NMDA receptors have also been proposed to exist (Cotman et al., 1986). Although, several immunohistochemical studies have recently been published on the distribution of non-NMDA receptor subunit proteins, (Good et al., 1993; Huntley et al., 1993; Martin et al., 1993; Petralia and Wenthold, 1992; Rogers et al., 1991; Vickers et al., 1993), the cellular and synaptic distribution of the NMDA subunit proteins has yet to be characterized in detail. Such data will be crucial to the development of a precise anatomical framework for the role of NMDA receptors in synaptic transmission, LTP, and the synaptic interactions between NMDA and non-NMDA receptor classes.

LTP, a potential early step in the cellular mechanism for learning (Bliss and Lømo, 1973), has been induced in various subfields of the hippocampus in rats, including CA1 via stimulation of Schaffer collaterals;

[6] Please see chapter 6 for further elaboration on the molecular biology of glutamate receptors.

CA3 via mossy fiber and associational/commissural fiber stimulation; and in dentate gyrus granule cells following stimulation of the perforant path (Collingridge and Bliss, 1987). Furthermore, the induction of LTP in each of these regions has been shown to be dependent on the activation of NMDA and/or non-NMDA receptors. Specifically, LTP in both CA1 (Harris et al., 1984) and the dentate molecular layer (Errington et al., 1987) is NMDA-dependent, while LTP in CA3 varies between lamina, such that LTP in the stratum radiatum via associational/commissural fiber stimulation is NMDA-dependent, while LTP in the stratum lucidum secondary to mossy fiber stimulation is not (Cotman et al., 1986; Katsuki et al., 1991; Zalutsky and Nicoll, 1990). Furthermore, LTP at synapses involving associational/commissural fibers display cooperativity with mossy fiber stimulation, but mossy fiber synapses do not display cooperativity with associational/commissural stimulation (Chattarji et al., 1989). These regional and laminar differences in the physiologic properties of LTP and the ability of various NMDA/non-NMDA antagonists to disrupt the induction of LTP suggest that different complements of receptor subtypes may be present and/or functional in different cell groups and circuits within the hippocampus (Katsuki et al., 1991). The present study examines the distribution of NMDAR1 protein in the monkey hippocampus and tests the hypothesis that the synaptic distribution of NMDA receptors, as revealed by the presence of NMDAR1, will correspond to the physiological properties of synaptic interactions associated with a given hippocampal field or circuit. In addition, the synaptic distribution of NMDA receptors is likely to be related to the pattern of differential vulnerability to excitotoxicity apparent in the hippocampus in various pathologic conditions, and in particular to the alterations described in chapter 3 following social deprivation.

Methods and Materials

Animals

The hippocampal formation from the brains of twelve monkeys were examined in this study including three monkeys at three months of age, three monkeys at six months of age, and six adult monkeys. All protocols were conducted within NIH guidelines for animal research and were approved by the Institutional Animal Care and Use Committee (IACUC).

Tissue Preparation

Animals were deeply anesthetized with ketamine hydrochloride (15-25 mg/kg i.m.) and pentobarbital sodium (10-20 mg/kg i.p.) and perfused transcardially with cold 1% paraformaldehyde in PBS for approximately 1 minute and then with cold 4% paraformaldehyde in PBS for an additional 8-9 minutes. The brains were removed, cut into approximately 5 mm tissue-blocks and placed in cold 4% paraformaldehyde in PBS for 6 hours. Blocks were then placed directly into PBS and sectioned in a plane perpendicular to the superior temporal sulcus at 50-80 μm using a vibratome (Ted Pella Inc., Irvine, CA).

Immunocytochemistry

The monoclonal antibody 54.1 is an γ-type immunoglobulin (IgG) which was generated according to standard procedures (Jahn et al., 1985; Köhler and Milstein, 1975), using a fusion protein encoding glutathione-S-transferase (GST) in frame with NMDAR1 residues 660-811, representing the putative intracellular loop between transmembrane regions III and IV; residue numbers as in Moriyoshi et al. (Moriyoshi et al., 1991) and

recognizes NMDAR1. This antibody has been previously characterized biochemically with immunoblots as well as immunohistochemically in transiently transfected cells and primate hippocampus and neocortex (table 2.1) (Huntley et al., 1994; Siegel et al., 1994) [7]. Tissue sections were incubated with anti-NMDAR1 antibody for 48 hours followed by the avidin-biotin-peroxidase method using Vectastain ABC kit (Vector Laboratories, Burlingame, CA) followed by treatment with 0.05% 3,3-diaminobenzidine tetrahydrochloride (DAB) with 0.003% hydrogen peroxide. Additional sections which were labeled with anti-NMDAR1 (mAb 54.1) were further processed for electron microscopy. Following DAB, these sections were treated with 0.5% osmium tetroxide in 7% sucrose, embedded in resin (Araldite, Electron Microscopy Services, Fort Washington, PA), and sectioned at 3 μm on an ultramicrotome (Ultracut E, Reichert-Jung, Germany). These sections were then re-imbedded and thin sectioned for electron microscopy.

Analysis

Tissue sections were examined on an Axiophot microscope (Zeiss, Germany) for conventional bright field analyses. Ultrastructural analyses were performed on a Hitachi 7000 electron microscope (Hitachi, Japan).

Results

Characterization of anti-NMDAR1 mAb 54.1

The monoclonal antibody 54.1 has been previously characterized biochemically by western blot analysis and immunohistochemically in

[7] Please see appendix for characterization data regarding this antibody.

transiently transfected mammalian cells (Siegel et al., 1994) (see appendix 1 fig. A.1). The specificity of this antibody is also demonstrated in the present study through immunohistochemical blocking experiments. Specific immunolabeling of tissue sections was abolished by preadsorption of mAb 54.1 with a histadine-conjugated fusion protein containing the same region of the NMDAR1 used in the GST-fusion protein against which mAb 54.1 was generated. However, labeling was unaffected by pre-incubation with GST (data not shown).

Regional pattern of NMDAR1-Immunoreactivity

Within the hippocampus, mAb 54.1 labeled neuronal cell bodies and dendrites in all fields of Ammon's horn, as well as the subiculum and dentate gyrus. However, there were subtle differences in the pattern and intensity of immunoreactivity which distinguished each zone (fig. 5.1). Pyramidal cells within the CA1 region were intensely NMDAR1-immunoreactive (ir) (fig. 5.1 A). Cell bodies as well as apical dendrites were clearly visible in the strata pyramidale and radiatum. More distal apical dendritic segments were also intensely labeled within the stratum moleculare. Proximal basal dendrites in continuity with cell somata were intensely labeled, as were fine processes within the neuropil of the strata pyramidale and oriens. Within the prosubiculum and subiculum, pyramidal cell somata as well as apical and basal dendrites were intensely labeled similar to those in CA1. Cell somata within the dentate granule cell layer were NMDAR1-ir. Additionally, granule cell dendrites were labeled throughout the entire extent of the molecular layer (fig. 5.1 B). The mossy fiber projection, which is composed of granule cell axons, was also labeled within the dentate hilus and stratum lucidum of CA3 (fig. 5.1 C). Hilar polymorphic cells displayed intense

immunoreactivity within their somata and dendrites. In CA3, the labeling of somata in stratum pyramidale, as well as basal and distal apical dendrites was similar in intensity to that of corresponding structures in CA1. In contrast, proximal apical dendrites in stratum lucidum contained small regions of more intense immunoreactivity interspersed with regions of less intense immunoreactivity as compared to the more homogeneous labeling pattern characteristic of proximal apical dendrites in other hippocampal regions (fig. 5.1). Various non-pyramidal cells and neuroglial cells were also labeled with mAb 54.1 throughout Ammon's horn and the subiculum. Small multipolar cells and larger bipolar cells in the stratum oriens as well as small cells in the alveus which had the morphologic characteristics of glial cells were also NMDAR1-ir.

Ultrastructural localization of NMDAR1

NMDAR1 immunoreactivity at the ultrastructural level was localized to somatic, dendritic and axonal profiles (fig. 5.2). Within the dentate molecular layer and CA1 region, immunoreactivity for NMDAR1 was localized primarily to asymmetric postsynaptic densities (PSDs) on dendritic spines (fig. 5.2 A, B). However, within the CA3 region the primary localization of NMDAR1 immunoreactivity varied among strata. Pyramidal cell bodies within the stratum pyramidale were labeled in their perikaryal region. Immunolabeling within the stratum lucidum was localized to axons, with adjacent dendrites within the same field either labeled or unlabeled. Approximately 10 % of axons in each section analyzed were strongly immunoreactive, with the remainder faintly to non-immunoreactive. Darkly labeled axons were often found in groups of 2-5 with accumulations of immunoreactivity along a limited portion of their membranes (fig. 5.2 C).

Mossy fiber terminals also occasionally contained NMDAR1 immunoreactivity associated with discrete membrane regions (fig. 5.2 D, F). Although the unique synaptic complexes characteristic of CA3 stratum lucidum involving multiple thorny excrescences embedded within large mossy fiber terminals (Frotscher, 1991) were clearly apparent in this material, PSDs on thorny excrescences were almost exclusively unlabeled (fig. 5.2 D). However, within the stratum radiatum, asymmetric PSDs on dendritic spines were commonly NMDAR1-ir. Accumulations of immunoreactivity were seen in both the spine head and neck directly below immunolabeled PSDs (fig. 5.2 E). Immunolabeled axonal profiles similar to those seen in the stratum lucidum were not visible in the stratum radiatum.

Discussion

The current study has described regional, laminar, cellular and intracellular patterns of localization for the NMDAR1 receptor subunit protein within the hippocampal formation of cynomolgus monkeys. Each subdivision of the hippocampal formation displayed patterns of localization for NMDAR1 with both shared and distinguishing characteristics. With the exception of CA3 pyramidal cells, labeled neurons in all hippocampal fields exhibited homogenous dense labeling throughout the full extent of their soma and dendrites. However, apical dendrites of CA3 pyramidal cells within the stratum lucidum were characterized by segments with relatively faint labeling interspersed with more intensely labeled segments. Additionally, the mossy fibers were faintly NMDAR1-ir at the light level, with an appearance similar to that for other immunohistochemical preparations which label this projection, such as NF proteins and the calcium-binding protein calbindin (Seress et al., 1991; Siegel et al., 1993).

Ultrastructurally, approximately 10% of the mossy fiber axons were seen to be intensely NMDAR1-ir within stratum lucidum, which may account for the homogenous zones of immunoreactivity apparent at the light microscopic level between pyramidal cell dendrites in this region. These immunohistochemical data for the NMDAR1 protein are consistent with previously described patterns for *in situ* hybridization (Nakanishi, 1992) and ligand binding studies in rat (Monaghan and Cotman, 1985), particularly with respect to relatively low levels of NMDA receptor binding in stratum lucidum of CA3 relative to other hippocampal areas. Furthermore, since it is currently thought that NMDA receptor complexes require the NMDAR1 subunit to function (Nakanishi, 1992), it is likely that mAb 54.1 labels all NMDA receptors.

Physiological experiments in rat hippocampal slice preparations have demonstrated that synaptic transmission between the mossy fibers and CA3 pyramidal cells is almost entirely blocked by non-NMDA antagonists, and that the NMDA mediated component is negligible (Katsuki et al., 1991). Furthermore, LTP mediated by the mossy fiber input to the stratum lucidum in CA3 has been shown to be NMDA-independent in rats (Cotman et al., 1986; Katsuki et al., 1991; Zalutsky and Nicoll, 1990). The relative absence of postsynaptic NMDA receptors in monkey stratum lucidum in the present study is consistent with the observed NMDA-independent synaptic transmission and LTP (fig. 5.3), and suggests that primates may exhibit an NMDA-independent form of LTP similar to that previously described for the mossy fiber system in rats. This pattern is in striking contrast to the pattern for GluR5-7 (kainate subunits) which are well represented at synapses between mossy fiber terminals and thorny excrescences of CA3 pyramidal

cells in monkey (Good et al., 1993). Furthermore, distal dendritic segments of CA3 pyramidal cells in monkeys do contain postsynaptic NMDAR1 immunoreactivity on spines, and LTP mediated by inputs to this portion of the dendritic tree is NMDA-dependent in rats (Katsuki et al., 1991; Zalutsky and Nicoll, 1990). Additionally, recent data indicate that the ultrastructural distribution of the NMDAR1 subunit in CA3 with respect to the mossy fiber system may be similar in rats and monkeys (Petralia and Wenthold, 1993; Siegel et al., 1993; Siegel et al. 1994) Thus, in addition to the implications for differential vulnerability (see below), these data predict that models of LTP developed in rodents may apply to the primate hippocampus. However, subtle differences in connectivity exist between rodent and primate hippocampus such that basal dendrites of CA3 pyramidal cells receive mossy fiber inputs in primates but not rodents (Seress, 1992), which may result in different patterns of LTP to this portion of the dendritic tree.

Data in the current study also suggest that GluR subunits and classes may be segregated within dendritic processes such that different excitatory afferents to the same neuron might be mediated preferentially through different classes of GluRs, even though all three classes are present within the same postsynaptic neuron. The combination of laminar segregation of inputs, such as the mossy fibers to the stratum lucidum and the associational/commissural fiber input to the stratum radiatum, with intradendritic segregation of GluR subunits, confers upon the system a high capacity for specificity in the postsynaptic coding of excitatory inputs. Furthermore, this segregation of inputs and receptor subunits may underlie the ability of associational/commissural fiber synapses to exhibit associative changes with mossy fiber stimulation, while mossy fiber synapses do not

exhibit such associative changes with associational/commissural fiber inputs. Such postsynaptic specificity is further enhanced by the localization of NMDAR1-labeled PSDs to spines in hippocampus, while NMDAR1-labeled PSDs in neocortex (Huntley et al., 1993) as well as GluR5-7-labeled PSDs in hippocampus (Good et al., 1993) and neocortex (Huntley et al., 1993) are found on spines and shafts. Although the apparent lack of NMDAR1-ir PSDs on dendritic shafts in this study implies the absence of NMDA receptors on aspiny neurons in the hippocampus, further interpretation of this finding requires quantitative double label ultrastructural analyses to determine more precisely the degrees of segregation and colocalization of all GluR families. Additionally, the interpretation of specific labeling on dendritic shaft PSDs is somewhat complicated by the possibility that immunoreactive DAB product may spread beyond sights of antibody binding, thus obscuring postsynaptic densities which might otherwise be apparent.

In addition to their role in neurotransmission, NMDA receptors have been linked to excitotoxicity, which has been implicated as an underlying basis for the cellular damage which occurs in a wide range of pathologic conditions including traumatic events as well as a host of disease processes (Choi, 1988; Rothman and Olney, 1987). Furthermore, discrete portions of the hippocampal formation are major loci of damage in ischemia and epileptic seizure. Cellular pathology in ischemic injury is particularly severe in the CA1 region, and can be dramatically decreased by specific NMDA antagonists (Rothman and Olney, 1987). Conversely, CA3 cells are among the most vulnerable to seizure-induced cellular pathologic changes (Choi, 1988), but are relatively resistant to damage resulting from ischemic insult.

These differential patterns of vulnerability may be related in part to the EAA receptor subunit content and subcellular compartmentalization within various cell groups. Specifically, the relative resistance to degeneration of CA3 neurons in certain conditions may be linked to the apparent lack of postsynaptic NMDA receptors in the stratum lucidum, the site of termination of the mossy fiber system. Therefore, in addition to determining the complement of GluR subunits found within a given neuron, information regarding the relationship between known afferents and the synaptic distribution of specific subunits will be essential in understanding the role of these subunits in neurotransmission, cellular mechanisms of learning and memory, and differential vulnerability.

Figure 5.1

Pattern of immunoreactivity for NMDAR1 in monkey hippocampal regions CA1 (A), dentate gyrus (B) and CA3 (C). (A) CA1 Pyramidal cell somata in stratum pyramidale and dendrites in all layers are well labeled. (B) dentate granule cell somata and dendrites (arrows) are clearly labeled within the granule cell layer and throughout the molecular layer. (C) CA3 Pyramidal cell somata and basal dendrites can be seen in strata pyramidale and oriens. Apical dendrites within stratum lucidum contain regions of more intense immunoreactivity (arrows) interspersed between faintly labeled areas. Dark zones between segments of groups of dendrites contain primarily mossy fiber axons (asterisk). Abbreviations: GCL - granule cell layer, SL - stratum lucidum, SM - stratum moleculare, SO - stratum oriens, SP - stratum pyramidale, SR - stratum radiatum. Scale bars in A, C = 100 μm; B = 50 μm.


A
SM
SM
SO

Figure 5.2

Ultrastructural localization of NMDAR1 immunoreactivity in the hippocampus. (A) Examples of an immunolabeled postsynaptic density and spine, as well as an adjacent unlabeled postsynaptic density and dendritic profile in the molecular layer of the dentate gyrus. (B) Immunolabeled postsynaptic density and spine on a labeled dendritic shaft, as well as an unlabeled dendritic profile and postsynaptic density in stratum radiatum of CA1. (C) Cluster of immunolabeled mossy fiber axons among unlabeled axons in stratum lucidum of CA3. (D) Multiple unlabeled postsynaptic densities (arrows) on a single unlabeled thorny excrescence and an unlabeled postsynaptic density on a dendritic protuberance emerging from an unlabeled dendritic shaft in the stratum lucidum of CA3. Such unlabeled profiles were virtually always seen adjacent to NMDAR1-ir axons in the same field, and were often on the same thin section as immunolabeled PSDs in the stratum radiatum. (E) Immunolabeled postsynaptic density on a labeled dendritic spine in the stratum radiatum of the CA3. (F) Multiple examples of unlabeled thorny excrescences within a mossy fiber terminal adjacent to a labeled dendrite. Open arrow head indicates a region of immunoreactivity within a mossy fiber terminal, possibly representing presynaptic receptors. Abbreviations and symbols: d - dendrite, la - labeled axon, ls - labeled spine, mt - mossy fiber terminal, t - terminal, te - thorny excrescence, ua - unlabeled axon. Asterisk - unlabeled dendritic profile. Scale bar = 500 nm.

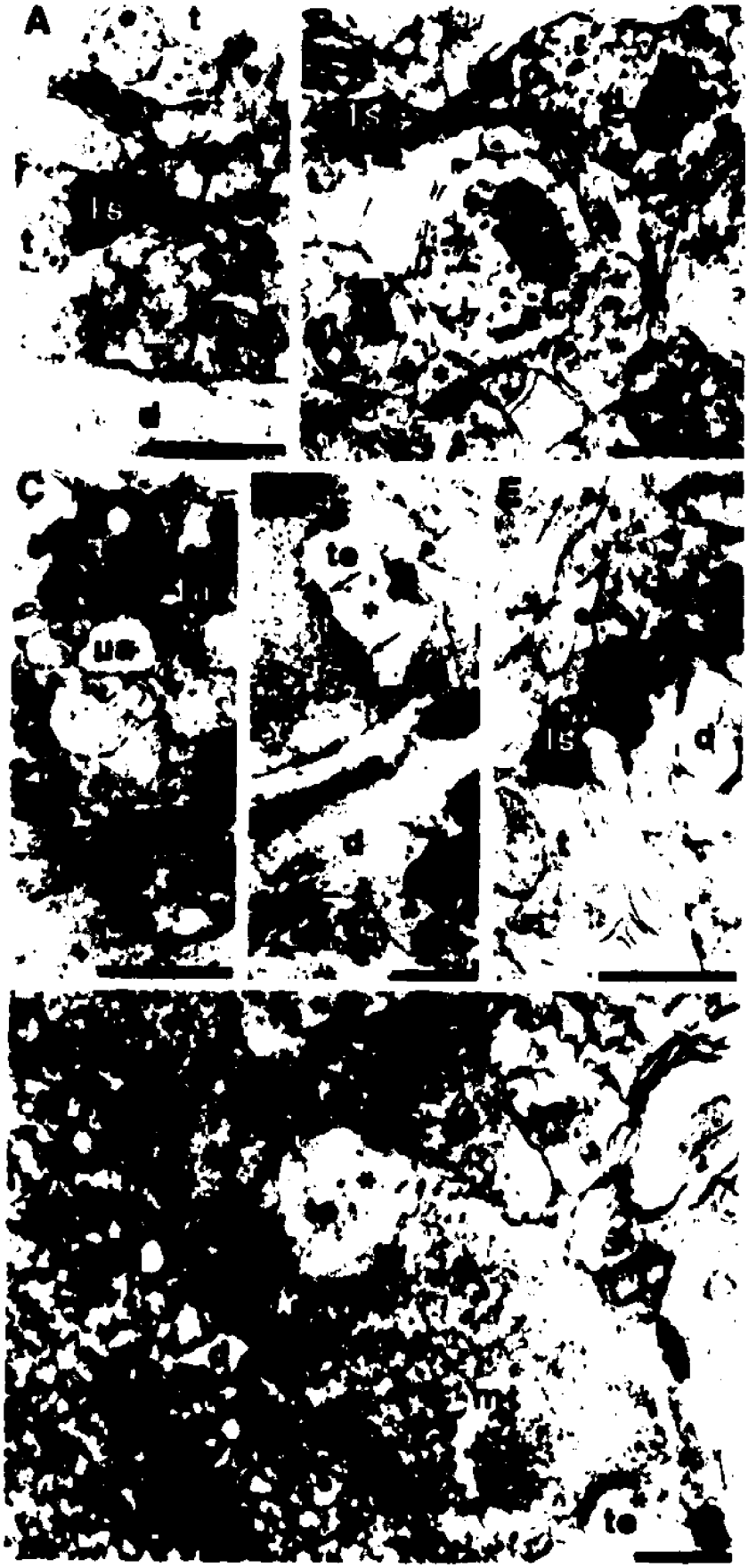
A
t
ls
B
ls
C
ub
to
d
E
ls
d
to

Figure 5.3

Schematic representation of CA3 pyramidal cell with laminar organization of afferent fibers, ultrastructural localization of NMDAR1 and forms of LTP exhibited. See (Cotman et al., 1986; Katsuki et al., 1991; Zalutsky and Nicoll, 1990) regarding forms of LTP demonstrated in CA3 and presynaptic NMDA receptors in stratum lucidum. Abbreviations: A/C - associational/commissural fibers, MF - mossy fibers, SL - stratum lucidum, SM stratum moleculare, SO - stratum oriens, SP - stratum pyramidale, SR - stratum radiatum.

Figure 5.3

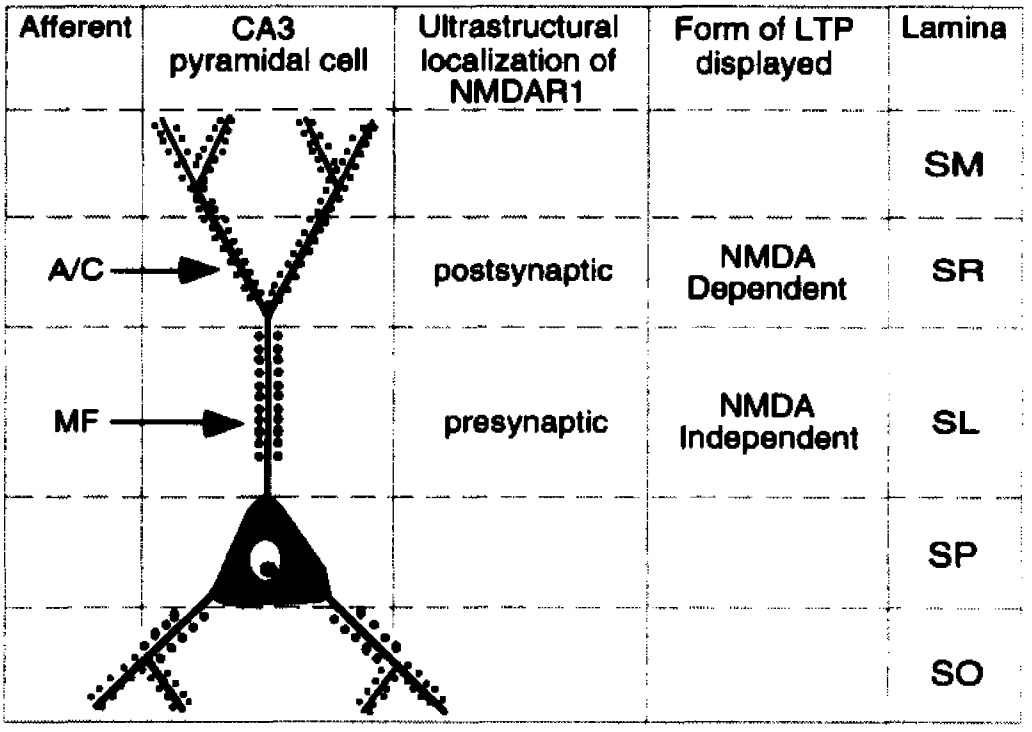
Afferent
CA3 pyramidal cell
Ultrastructural localization of NMDAR1
Form of LTP displayed
Lamina
SM
A/C
postsynaptic
NMDA Dependent
SR
MF
presynaptic
NMDA Independent
SL
SP
SO

Chapter 6

Distribution of the Excitatory Amino Acid Receptor Subunit GluR2 in Monkey Hippocampus and Colocalization with Subunits GluR5-7 and NMDAR1

Abstract

The EAA receptor subunit GluR2 has been previously demonstrated to be a key determinant of many of the physiologic properties of heteromeric AMPA/kainate selective receptors (Seeburg, 1993). These properties include the ability of a channel to allow Ca^{2+} flux and therefore to mediate Ca^{2+}-dependent cellular processes, possibly including excitotoxic injury. Within the current study, the regional, cellular and subcellular distribution patterns of the EAA receptor subunit GluR2 were investigated in monkey hippocampus with the use of the monoclonal antibody 3A11, which is directed against the putative extracellular N-terminal domain of the GluR2 protein, and is the only GluR2 specific antibody to date. Immunocytochemically, 3A11 labeled pyramidal cell somata and dendrites in each field of the hippocampus as well as granule cells and polymorphic hilar cells in the dentate gyrus. Additionally, small cells with the morphologic characteristics of astroglia were immunolabeled for GluR2 within the alveus and fimbria. Ultrastructurally, immunoreactivity was localized to postsynaptic densities on dendritic spines and shafts, as well as within the somatodendritic cytoplasm. Additionally, a subset of dentate granule cell axons within the mossy fiber projection contained immunoreactivity for GluR2. Furthermore, double label immunohistochemical experiments using subunit specific antibodies for

GluR2, GluR5-7 and NMDAR1 demonstrated that virtually all neurons in each subfield of the hippocampus contain subunits from the AMPA/kainate, kainate and NMDA receptor families.

Introduction

The unique response properties of individual neuronal classes are likely to be related to their compliment of EAA receptor subunits. The particular physiologic response properties of the individual AMPA/kainate class ionotropic EAA receptor subunits has been previously determined through transient transfections of GluR1, 2, 3, or 4. Such experiments have shown that heteromeric non-NMDA receptor channels containing the subunit GluR2 are Ca^{2+} impermeable, while those containing only GluRs 1 and/or 3 allow Ca^{2+} flux (Pellegrini-Giampietro et al., 1992). Thus, the presence or absence of GluR2 within an AMPA/kainate receptor dictates whether or not that channel will be capable of mediating Ca^{2+} dependent intracellular processes. Additionally, channels containing 1, 3 or 4 display both inward and outward rectification, while those containing GluR2 display only outward rectification (Verdoorn et al., 1991). Finally, GluR2 gene expression has been shown to be reduced to a greater extent than either GluR1 or 3 following global ischemia in rats, which may contribute to increased Ca^{2+} influx and subsequent excitotoxic injury (Pellegrini-Giampietro et al., 1992). Developmentally, GluR2 mRNA has been shown to be at nearly adult levels at birth in rats, while mRNAs for GluRs 1 and 3 showed more prominent developmental fluctuations characterized by high levels during the first two postnatal weeks relative to adult levels (Pellegrini-Giampietro et al., 1991). Such fluctuations in the relative amount of each of the AMPA/kainate receptor subunits may allow for the markedly different responses to injury exhibited by juvenile and adult animals (Duffy et al., 1975). Therefore, as GluR2 appears to be highly regulated both developmentally and in response to injury, possibly allowing neurons to

adapt their physiologic response properties, it will be of great interest to determine the normal regional, cellular and subcellular locations of this subunit throughout the nervous system.

Several immunocytochemical studies have recently been published on the localization of NMDA and non-NMDA EAA receptor subunit proteins in the mammalian central nervous system (Good et al., 1993; Huntley et al., 1993; Huntley et al., 1994; Martin et al., 1993; Petralia and Wenthold, 1992; Vickers et al., 1993; Siegel et al., 1994). These studies have demonstrated that EAA receptor subunits are distributed among many brain areas and are localized to a variety of neuronal and non-neuronal cell types. Studies of the hippocampus have demonstrated NMDA and non-NMDA receptor subunits are present at a subset of postsynaptic densities and diffusely present within the somatodendritic cytoplasm (Good et al., 1993; Martin et al., 1993; Petralia and Wenthold, 1992). Additionally, NMDA receptor subunits have also been reported to be found in dentate granule cell axons in the mossy fiber projection to CA3 (Siegel et al., 1994). Although the distribution of the AMPA/kainate selective subunits GluR2/3 has been described with the use of polyclonal antisera in rat brain (Martin et al., 1993; Petralia and Wenthold, 1992), the current report constitutes the first description of the distribution of the GluR2 subunit in monkey hippocampus employing an antibody which is selective for GluR2. Furthermore, through the use of double label immunohistochemistry for AMPA/kainate, kainate and NMDA receptor subunits, the current study examines the EAA receptor subunit composition within specific cell types and/or lamina in the monkey hippocampus. These distribution patterns may correlate with known circuits in the hippocampus and underlie the individual response profiles of different

hippocampal cell groups to a variety of physiological, pharmacological and toxicological conditions.

Methods and Materials

Animals

The hippocampal formation from the brains of twelve monkeys were examined in this study including three monkeys at three months of age, three monkeys at six months of age, and six adult monkeys. All protocols were conducted within NIH guidelines for animal research and were approved by the Institutional Animal Care and Use Committee (IACUC).

Tissue Preparation

Animals were deeply anesthetized with ketamine hydrochloride (15-25 mg/kg i.m.) and pentobarbital sodium (10-20 mg/kg i.p.) and perfused transcardially with cold 1% paraformaldehyde in PBS for approximately 1 minute and then with cold 4% paraformaldehyde in PBS for an additional 8-9 minutes. The brains were removed, cut into approximately 5 mm tissue-blocks and placed in cold 4% paraformaldehyde in PBS for 6 hours. Additional material was prepared with fixation that included 0.25-1% glutaraldehyde as well as 4% paraformaldehyde. Blocks were then placed directly into PBS and sectioned in a plane perpendicular to the superior temporal sulcus at 50-80 μm using a vibratome (Ted Pella Inc., Irvine, CA). Tissue sections were then processed for either single or double labeling immunohistochemistry using the subunit specific EAA receptor antibodies described below.

Immunocytochemistry

Immunohistochemistry was performed with the use of three monoclonal antibodies which are specific for members of the AMPA/kainate, kainate and NMDA receptor families, respectively. The monoclonal antibody 3A11 is an IgG which selective for the EAA receptor subunit GluR2 (table 2.1). The specificity of this antibody has been demonstrated biochemically by western blot analysis (Puchalski et al., Submitted) and radioimmunoassay (RIA) (Siegel et al., in preparation) (see appendix 2 for data regarding RIA) as well as immunohistochemically with preadsorption of specific labeling with GluR2 specific fusion protein. Preadsorption of the anti-GluR2 monoclonal antibody 3A11 was performed with fusion proteins encoding the N-terminal portion of GluR2 as well as GluRs 1, 3 and 5, the ß4 subunit of the nicotinic acetylcholine receptor (ß4) and TrpE alone. Primary antibody was incubated overnight at 4°C with each of the fusion proteins listed above. Following centrifugation, supernatant was extracted and incubated with fresh fusion proteins for one hour. Preadsorbed primary antibody was then cleared by centrifugation and was used for immunohistochemistry as described above.

The mAb 4F5 is a μ type immunoglobulin (IgM) which was raised against a fusion protein corresponding to the putative extracellular N-terminal domain of GluR5, and recognizes GluR subunits 5-7 (table 2.1) (Huntley et al., 1993). This antibody has been previously characterized biochemically with immunoblots, and immunohistochemically in transfected cells, as well as primate neocortex and hippocampus (Good et al., 1993; Huntley et al., 1993; Vickers et al., 1993).

Sections for single label immunocytochemistry were incubated with anti-GluR2 antibody for 48 hours followed by the avidin-biotin-peroxidase method using Vectastain ABC kit (Vector Laboratories, Burlingame, CA) followed by treatment with 0.05% DAB with 0.003% hydrogen peroxide. Additional sections which were labeled with the anti-GluR2 mAb 3A11 were further processed for electron microscopy. Following DAB, these sections were treated with 0.5% osmium tetroxide in 7% sucrose, dehydrated, embedded in resin (Araldite, Electron Microscopy Services, Fort Washington, PA), and sectioned at 3 μm on an ultramicrotome (Ultracut E, Reichert-Jung, Germany). These sections were then re-imbedded in resin and thin sectioned for electron microscopy.

Double label immunohistochemistry for GluR2 with GluR5-7 and NMDAR1 with GluR5-7 were performed by incubating tissue sections with mABs 4F5 (anti-GluR5-7) and either 54.1 (anti-NMDAR1) or 3A11 (anti-GluR2) for 24-48 hours. Following three washes in PBS, sections were incubated for 2 hours in FITC-conjugated goat anti-mouse IgM μ chain specific antisera (Vector Laboratories, Burlingame, CA) and biotinylated horse anti-mouse IgG γ chain specific antisera (Vector Laboratories, Burlingame, CA). Following three additional washes in PBS, sections were incubated with Texas Red-conjugated avidin (Vector Laboratories, Burlingame, CA). As an immunohistochemical control for this procedure, additional sections were incubated with mABs 54.1 or 3A11 followed by FITC-conjugated goat anti-mouse IgM μ chain specific antisera or mAb 4F5 followed by biotinylated horse anti-mouse IgG γ chain specific antisera and Texas Red-conjugated avidin. Neither of these conditions resulted in the visualization of the appropriate primary antibody by an inappropriate

secondary antibody. As both mABs 3A11 and 54.1 are IgG type antibodies, this combination could not be directly examined with these immunofluorescent procedures.

Analysis

Both DAB- and Texas Red/FITC-labeled tissue sections were examined on an Axiophot microscope (Zeiss, Germany) for conventional bright field and fluorescence light microscopic analyses. Double labeled fluorescence material was also analyzed on a confocal laser scanning microscope (Zeiss, Germany). Ultrastructural analyses were performed on a Hitachi 7000 electron microscope (Hitachi, Japan).

Results

Characterization of mAb 3A11

The monoclonal antibody 3A11 has been previously demonstrated to be selective for the EAA receptor subunit GluR2 by western blot analysis (Puchalski et al., Submitted) and radioimmunoassay (Siegel et al., in preparation). The specificity of this antibody is also demonstrated immunohistochemically through blocking experiments in the current report. Specific labeling in monkey hippocampus was abolished following preadsorption with a fusion protein containing a N-terminal portion of GluR2, but was unaffected by incubation with fusion proteins encoding homologous portions of GluR1, GluR3, GluR5, ß4 or TrpE alone.

Pattern of GluR2 immunoreactivity

The monoclonal antibody 3A11 labeled neuronal elements within each of the major hippocampal fields. Dentate gyrus granule cell somata and proximal dendrites within the granule cell layer, as well as dendrites throughout the molecular layer were intensely labeled including extremely fine distal dendritic processes which terminated at the hippocampal fissure (fig. 6.1 C). The intensity of immunoreactivity was equivalent between the inner and outer portions of the dentate molecular layer. Hilar neurons were intensely GluR2-ir within their somatodendritic compartment (fig. 6.4 D). Cell somata and proximal dendrites were well labeled throughout their cytoplasm, as were both proximal dendrites and extremely fine, presumably distal dendritic processes within the neuropil. Both the somata and basal dendrites of CA3 pyramidal cells in the stratum pyramidale and stratum oriens, as well as the apical dendrites extending through the stratum lucidum, stratum radiatum and stratum moleculare displayed immunoreactivity for GluR2 (fig. 6.2 F). Within the stratum lucidum, inter-dendritic spaces occupied by axons and terminals of the mossy fiber projection displayed a diffuse pattern of immunoreactivity similar to that seen with antibodies to other proteins which label the mossy fiber projection such as the calcium binding protein calbindin (Seress et al., 1991). Furthermore, GluR2-immunoreactivity in the mossy fiber projection could be seen within the dentate hilus as it coursed from the dentate granule cells to the CA3 region. In both CA1 (fig. 6.1 A) and the subiculum, pyramidal cell somata, as well as large caliber apical and basal dendrites, were intensely GluR2-immunoreactive (GluR2-ir). Strata radiatum and moleculare were characterized by increasingly fine caliber immunoreactive

processes terminating at the hippocampal fissure. The neuropil within stratum pyramidale throughout Ammon's horn had a reticular appearance, presumably representing immunolabeling of extremely fine caliber distal dendritic processes. Non-pyramidal fusiform cells in stratum oriens were lightly labeled for GluR2 with immunoreactivity visible in their somata and proximal dendrites. Small cells with the morphologic characteristics of fibrous astrocytes in the alveus and fimbria were also labeled for GluR2 throughout Ammon's horn and the subiculum (fig. 6.1 B).

Patterns of immunoreactivity for GluR5-7 and NMDAR1

The patterns of immunoreactivity for GluR5-7 (Good et al., 1993) and NMDAR1 (Siegel et al., 1994) within the hippocampal formation have been described previously and therefore will be described here only briefly. Dentate granule cells were labeled in their somatodendritic compartment for both GluR5-7 and NMDAR1 with a pattern similar to that described for GluR2. Hilar polymorphic cells were intensely immunoreactive with antibodies directed against both receptor categories, as were pyramidal cells in all subdivisions of Ammon's horn and the subiculum. Similarly, non-pyramidal cells in the stratum oriens and neuroglial cells in the alveus and fimbria were also labeled for GluR5-7 as well as NMDAR1.

Colocalization of GluR2 and GluR5-7

Double label immunofluorescence employing mABs directed against GluR2 and GluR5-7 resulted in a pattern of colocalization throughout the hippocampus in which virtually all cells in the hippocampus which were labeled with one mAb were also labeled with the other (fig. 6.2). Subtle differences were however evident between the patterns of immunoreactivity

for mAbs 3A11 (anti-GluR2) and 4F5 (anti-GluR5-7). For example, mAb 3A11 displayed a pattern of slight nuclear labeling that was not evident with mAb 4F5. Pyramidal cells in both CA1 (fig. 6.2 A, B) and the subiculum were immunoreactive for both antibodies in virtually every somatic and dendritic segment examined, as were polymorphic hilar neurons (fig. 6.4 D-F). Dentate granule cells displayed colocalization of GluR2 and GluR5-7 within their somata and throughout the entire extent of their dendrites (fig. 6.2 C, D). Similarly, CA3 pyramidal cell bodies as well as both apical and basal dendrites were labeled in virtually all cases with both antibodies (fig. 2 E, F). Inter-dendritic spaces in stratum lucidum of CA3 occupied by mossy fiber axons displayed a low level of immunoreactivity for both receptor subtypes.

Colocalization of GluR5-7 and NMDAR1

Immunohistochemistry utilizing mAbs directed against GluR5-7 (mAb 4F5) and NMDAR1 (mAb 54.1) resulted in a cellular pattern of colocalization which was similar to that seen for GluR5-7 and GluR2. Virtually all somatic and dendritic profiles within each of the subfields were labeled with both of these antibodies, resulting in immunoreactive patterns which were very similar on both conventional (fig. 6.3) and confocal laser scanning (fig. 6.4) images. Dentate granule cells displayed colocalization of these receptor subtypes within their somata and throughout their dendritic arbor (fig. 3 A, B). Similarly, pyramidal cells in CA1 (fig. 3 C, D), the subiculum and the hilus (fig. 6.4 A-C) were double labeled for GluR5-7 and NMDAR1 in virtually every somatic and dendritic segment examined. CA3 pyramidal cell bodies and dendrites also displayed colocalization of GluR5-7 and NMDAR1, although apical dendrites in the stratum lucidum were more

intensely labeled for GluR5-7 than NMDAR1 (fig. 3 E, F). Mossy fibers within inter-dendritic spaces in stratum lucidum were faintly labeled for NMDAR1 and to a far lesser extent for GluR5-7. As stated in the methods section, μ- and γ- chain specific secondary antibodies used in these double-label immunohistochemical procedures did not cross react with the inappropriate primary antibody, suggesting that such a high degree of colocalization between each of the combinations tested reflects a ubiquitous cellular distribution of AMPA, kainate and NMDA receptors within the hippocampus.

Ultrastructural localization of GluR2

Immunoreactivity for GluR2 at the ultrastructural level was localized to asymmetric postsynaptic densities, as well as diffusely within somatodendritic cytoplasm (fig. 6.5). GluR2-ir postsynaptic densities in the dentate molecular layer were present on profiles consistent with both dendritic spines and shafts (fig. 6.5 C, D). Postsynaptic densities were considered to be specifically labeled when the postsynaptic specialization had a thickened, dark appearance and the underlying dendritoplasm contained floculant opaque material, corresponding to DAB-peroxidase deposits. Such labeled postsynaptic densities were found on both spines and shafts within strata radiatum and moleculare of both CA1 (fig. 6.5 A, B) and CA3 (fig. 6.5 F). Within the stratum lucidum of CA3, labeled postsynaptic densities were seen on thorny excrescences embedded within mossy fiber terminals, as well as asymmetric synapses on dendritic shafts. Unlabeled asymmetric postsynaptic densities on spines and shafts were apparent throughout all regions of the hippocampus in close proximity to labeled profiles. Specifically, multiple thorny excrescences within a single mossy

fiber terminal often consisted of both labeled and unlabeled profiles (fig. 6.5 F). Myelinated axonal profiles were generally not immunoreactive throughout all regions of the hippocampus. However, mossy fiber axons within the stratum lucidum occasionally contained immunoreactivity. Immunoreactivity within such unmyelinated axonal profiles was seen as labeled puncta in the axonal cytoplasm and often more intensely along membranes (fig. 6.5 E). Immunoreactive axons within this projection were occasionally seen in groups, with increased immunoreactivity at membranes between labeled axons.

Discussion

The current study has described regional, cellular and ultrastructural immunocytochemical patterns of localization for the ionotropic EAA receptor subunit GluR2 within the hippocampus. Additionally, double label immunohistochemistry using antibodies which are selective for GluR2, GluR5-7 and NMDAR1 was used to describe patterns of colocalization for members of the AMPA/kainate, kainate and NMDA receptor categories. At the light microscopic level, dentate granule cells and hilar polymorphic cells, as well as hippocampal pyramidal cells in all regions of Ammon's horn and the subiculum were intensely GluR2-ir throughout their entire somato-dendritic extent. Small cells with the appearance of fibrous astrocytes within the alveus and fimbria were also immunoreactive for GluR2, which is consistent with recent reports of the presence of AMPA-selective GluR subunits in primary astroglial cultures from rat brain (Condorelli et al., 1993). Ultrastructurally, GluR2 immunoreactivity was seen within the somatodendritic cytoplasm and at postsynaptic densities in all regions of the hippocampus and dentate molecular layer and within a limited number of

mossy fiber axons in stratum lucidum of CA3. While numerous asymmetric post synaptic densities were unlabeled as well, the ubiquitous presence of GluR2 throughout the various regions and lamina of the hippocampus suggest that this subunit is potentially situated to participate in excitatory neuro-transmission at a subset of synapses within all major extrinsic and intrinsic glutamatergic hippocampal circuits. Furthermore, GluR2 has been shown to play a crucial role in determining many of the physiological properties of heteromeric AMPA receptors. For example, AMPA/kainate selective receptors which contain GluR2 are impermeable to Ca^{2+}, while those which do not contain this subunit allow Ca^{2+} flux. Data presented in the current report suggest that there is a major subset of AMPA/kainate receptors in each of the major excitatory pathways of hippocampal circuitry that contain GluR2 and therefore do not flux Ca^{2+} under normal conditions. However, previously reported *in situ* hybridization data suggest that there is a selective down regulation of GluR2 mRNA following ischemic injury in rats (Pellegrini-Giampietro et al., 1992). It will therefore be of great interest in the future to use GluR2 selective antibodies to examine the regulation of GluR2 protein following ischemic episodes.

Colocalization of EAA Receptor Subunits

Physiological studies have previously demonstrated that individual neurons exhibit response properties typical of both NMDA and non-NMDA receptors in amphibian cell cultures and within specific regions of the mammalian nervous system such as the CA1 region of the hippocampus, spinal cord and neocortex (MacDermott and Dale, 1987). However, until the advent of subunit-specific antibodies, it was not possible to generate precise anatomic data regarding which complement of subunits from the three

ionotropic receptor categories are present within given cell classes, individual neurons or neuronal compartments in vivo. The present data indicate that virtually all of the GluR5-7-ir neurons in the monkey hippocampus are also immunoreactive for both GluR2 and NMDAR1. Similarly, a high degree of colocalization of GluR1-3 and GluR5-7 in monkey neocortex has been previously reported (Vickers et al., 1993). Since recent reports indicate that members of the AMPA/kainate, kainate and NMDA receptor classes do not combine to form functional channels with each other (Brose et al., 1993), the high degree of colocalization for GluR2 and GluR5-7, as well as GluR5-7 and NMDAR1 described within the current report is likely to reflect the presence of distinct AMPA/kainate, kainate and NMDA receptors in virtually all hippocampal neurons.

Ultrastructural Localization of GluR2

Although all three classes of receptor subunits appear to be highly colocalized at the regional and cellular levels, ultrastructural data indicate that their subcellular distribution may not be equivalent. Although NMDAR1-ir postsynaptic densities in hippocampus appear to be localized primarily to dendritic spines (Siegel et al., 1994), GluR5-7 (Good et al., 1993) as well as GluR2 (current report) are localized to postsynaptic densities on both dendritic spines and shafts. As previously mentioned in chapter 5, the interpretation of specific labeling on dendritic shaft PSDs may be complicated by the possibility that immunoreactive DAB product may spread beyond locations of antibody binding resulting in sights of nonspecific labeling. However, differences between the immunoreactive patterns exhibited by antibodies directed against NMDAR1 (chapter 5) and GluR2 (current chapter) suggest that at least some component of the

apparent segregation of GluR subtypes is real. For example, GluR2 (current report) and GluR5-7 (Good et al., 1993) are localized to postsynaptic densities on thorny excrescences within the stratum lucidum of CA3, while NMDAR1 has been recently shown to be virtually absent from such dendritic specializations (fig. 6.6) (Siegel et al., 1994). Conversely, all three receptor subtypes have been shown to be localized to postsynaptic densities on distal dendritic segments within the strata radiatum/moleculare (Good et al., 1993, current report; Siegel et al., 1994). Such a subcellular distribution of NMDA and non-NMDA receptor subunits on CA3 pyramidal cells is consistent with previously demonstrated physiologic data indicating that the excitatory mossy fiber input to CA3 is almost exclusively mediated by non-NMDA receptors, while the associational/commissural input to the stratum radiatum is mediated by both NMDA and non-NMDA receptors (Cotman et al., 1986; Katsuki et al., 1991; Zalutsky and Nicoll, 1990).

Comparison with Ligand Binding Data

Although ligand binding studies lack the cellular and subcellular resolution of immunocytochemical techniques as demonstrated for GluR2 in the current report, pharmacologic agents have been shown to display differential patterns of binding to different regions of the hippocampus. AMPA binding in rats has been demonstrated to be high in CA1 and the dentate gyrus relative to CA3, where the extent of binding of these agents is comparable to neocortex (Insel et al., 1990). Although AMPA binding in vivo is likely to reflect the composition and distribution of native heteromeric channels rather than individual subunits, the immunohistochemical distribution of GluR2 in the current report is consistent with binding data since the dentate molecular layer as well as both

the CA1 and CA3 regions of the hippocampus displayed a high intensity of immunolabeling. Similarly, within CA3, ligand binding studies have predicted a segregation of NMDA receptors with low numbers of receptors in the mossy fiber terminal zone (stratum lucidum) (Harris and Cotman, 1986) and higher numbers of receptors in the associational/commissural fiber terminal zone (stratum radiatum) (Monaghan and Cotman, 1985; Monaghan et al., 1983), which is highly consistent with the previously reported ultrastructural localization of the NMDAR1 subunit (Siegel et al., 1994).

In contrast to NMDA and AMPA, kainate binding is greatest in CA3, relative to the dentate gyrus and CA1 (Miller et al., 1990; Werner et al., 1991). However, this pattern is not consistent with the pattern of immunoreactivity for GluR5-7, which was relatively high in CA1 and the dentate molecular layer (Good et al., 1993), (present study). However, regional patterns for kainate binding may reflect the presence of high affinity kainate binding proteins such as KA1 and KA2 (Herb et al., 1992; Werner et al., 1991), which are not recognized by any of the antibodies included in the current study. In addition, since mAb 4F5 recognizes GluR5-7, preferential localization of any single subunit would not be apparent with this antibody.

Comparison with In situ Hybridization Data

Multiple studies using *in situ* hybridization techniques have described regional patterns for the mRNA expression of individual EAA receptor subunits. In the rat hippocampus, GluR1-3 mRNAs are highly expressed in CA1, CA3 and the dentate gyrus relative to other cortical structures (Pellegrini-Giampietro et al., 1991). The intensity of immunoreactivity for

GluR2 was consistent with this pattern, as the majority of neuronal cells in each of these regions were labeled with anti-GluR2 mAb 3A11. Similarly, the ubiquitous distribution of NMDA mRNA within the rat hippocampus (Moriyoshi et al., 1991) is consistent with patterns of immunoreactivity for NMDAR1 in monkey (Siegel et al., 1994). Among the kainate binding subunits, GluR5 mRNA is not highly expressed in any regions of the hippocampus in adult rat (Bettler et al., 1990), while GluR6 mRNA is most abundant in dentate granule cells and CA3 cells (Egebjerg et al., 1991) and GluR7 is expressed primarily in the dentate granule cells (Bettler et al., 1992). Although mAb 4F5 labels cells in CA3 and the dentate gyrus, as would be expected from the corresponding mRNA expression patterns, the pattern of GluR5-7 immunoreactivity in CA1 is inconsistent with *in situ* hybridization data. The apparent mismatch in CA1 between immunoreactivity for GluR5-7 proteins and the low signal intensity in *in situ* hybridization experiments for individual receptor subunits, may be due to the presence of particularly low levels of the individual mRNAs, further amplified by the fact that mAb 4F5 recognizes three proteins, which may be individually present in relatively small amounts. Alternatively, this mismatch may be due to differences in the stability and turnover of receptor subunit proteins and their corresponding mRNAs. Finally, differences between the immunoreactivity for EAA receptor subunit proteins in monkeys and either mRNA or ligand binding data in rats, may reflect species differences in EAA receptor distribution.

Differential vulnerability of hippocampal neurons

The current study has demonstrated that the AMPA/kainate subunit GluR2 is located at asymmetric postsynaptic densities within each major

subdivision of the hippocampus. Furthermore, this study has demonstrated that at least some subset of the kainate binding subunits GluR5-7 are highly colocalized with GluR2, as well as NMDAR1 throughout the hippocampus. The unique response properties of individual neuronal classes within the hippocampus are likely to be related to their complement of EAA receptor subunits. Similarly, neurons within each subdivision of the hippocampus exhibit characteristic patterns of differential vulnerability to a host of deleterious processes. For example, discrete portions of the hippocampal formation are major loci of damage in ischemia, kainate toxicity and epileptic seizure. Cellular pathology in ischemic injury is particularly severe in the CA1 region, and can be dramatically decreased by specific NMDA antagonists (Rothman and Olney, 1987). Conversely, CA3 cells are among the most vulnerable to seizure-induced cellular pathologic changes (Choi, 1988) and kainate mediated damage (Nadler et al., 1981), but are relatively resistant to damage resulting from ischemic insult. Although the ubiquitous cellular patterns demonstrated within the current study for members of the AMPA/kainate, kainate and NMDA receptor families suggest that the mere presence of a particular EAA receptor subunit or subtype within a particular neuronal class is insufficient to explain patterns of differential vulnerability, such patterns may be in part determined by the types of EAA receptors which mediate excitatory neurotransmission within specific intrinsic and extrinsic hippocampal circuits.

Figure 6.1

Light microscopic distribution of GluR2 containing immunolabeled cells within CA1 (A), the fimbria (B) and dentate gyrus (C). (A) CA1 Pyramidal cell somata in stratum pyramidale and dendrites in all layers are well labeled. (B) Small immunolabeled cells with the appearance of fibrous astrocytes (arrow) were visible within the fimbria. (C) dentate granule cell somata and dendrites are clearly labeled within the granule cell layer and throughout the molecular layer. Abbreviations: ALV - alveus, GCL - granule cell layer, H - hilus, SM - stratum moleculare, SO - stratum oriens, SP - stratum pyramidale, SR - stratum radiatum. Scale bar = 100 μm in A; 65 μm in B; and 40 μm in C.


A
B
SR
C
SP
SO
GCL
ALV

Figure 6.2

Pairs of photographs showing double label immunohistochemistry for FITC-labeled GluR5-7 (A, C, E) and Texas red-labeled GluR2 (B, D, F) in monkey hippocampus. Virtually all cells which label with either antibody also colocalized the other. (A, B) CA1 pyramidal cells, (C, D) dentate granule cells, (E, F) CA3 pyramidal cells. Notice the presence of GluR2, as well as GluR5-7 immunoreactivity throughout all layers. Arrows - examples of double labeled cells. Scale bars = 100 μm in A, B, E; F; 50 μm in C, D.

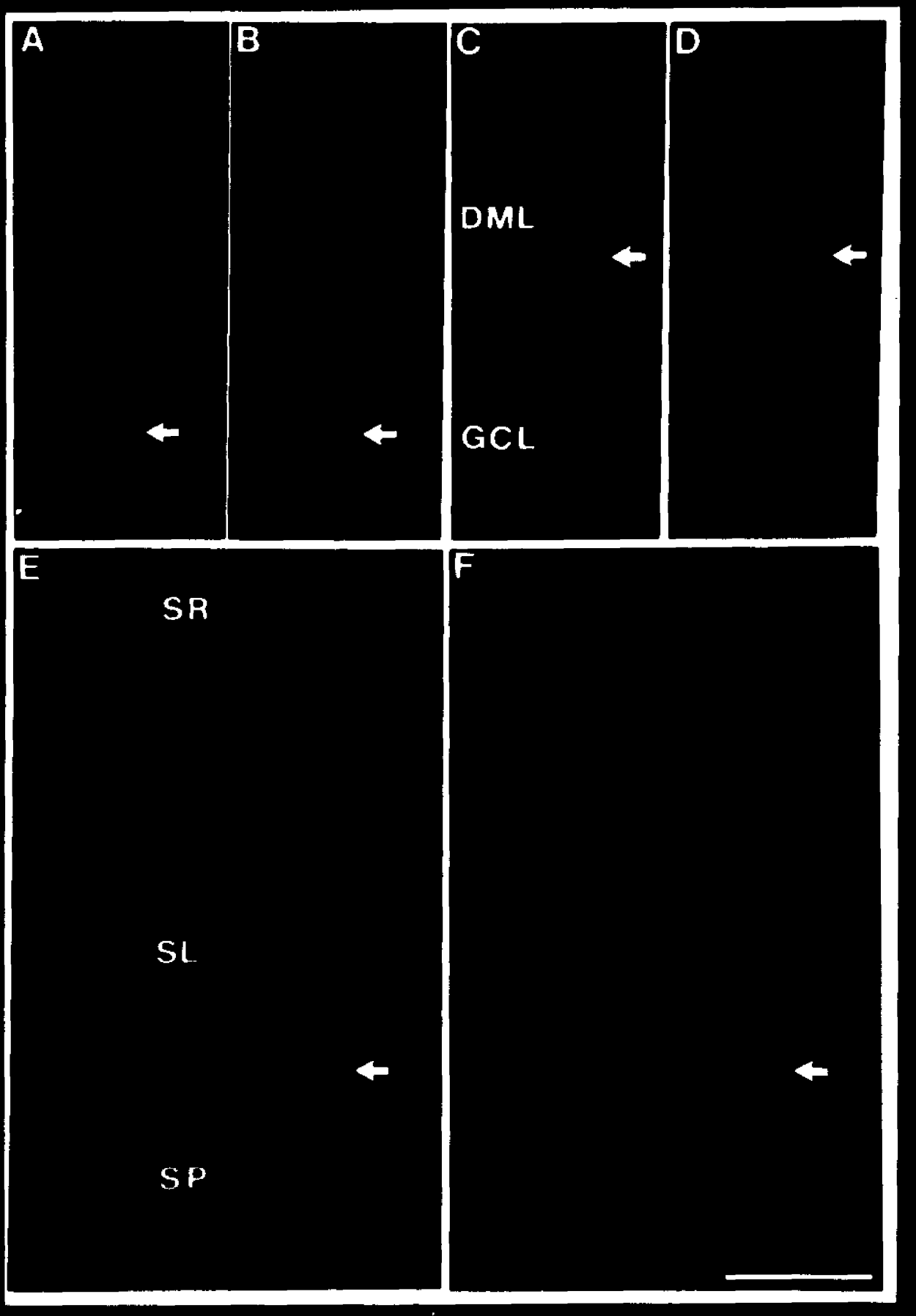
A
B
C
DML
GCL
D
E
SR
SL
SP
F

Figure 6.3

Pairs of photographs showing double label immunohistochemistry for FITC-labeled GluR5-7 (A, C, E) and Texas red-labeled NMDAR1 (B, D, F) in monkey hippocampus. Virtually all cells which label with either antibody also colocalized the other. (A, B) dentate granule cells, (C, D) CA1 pyramidal cells, (E, F) CA3 stratum lucidum. Arrows - examples of double labeled cells. Scale bars = 50 μm.

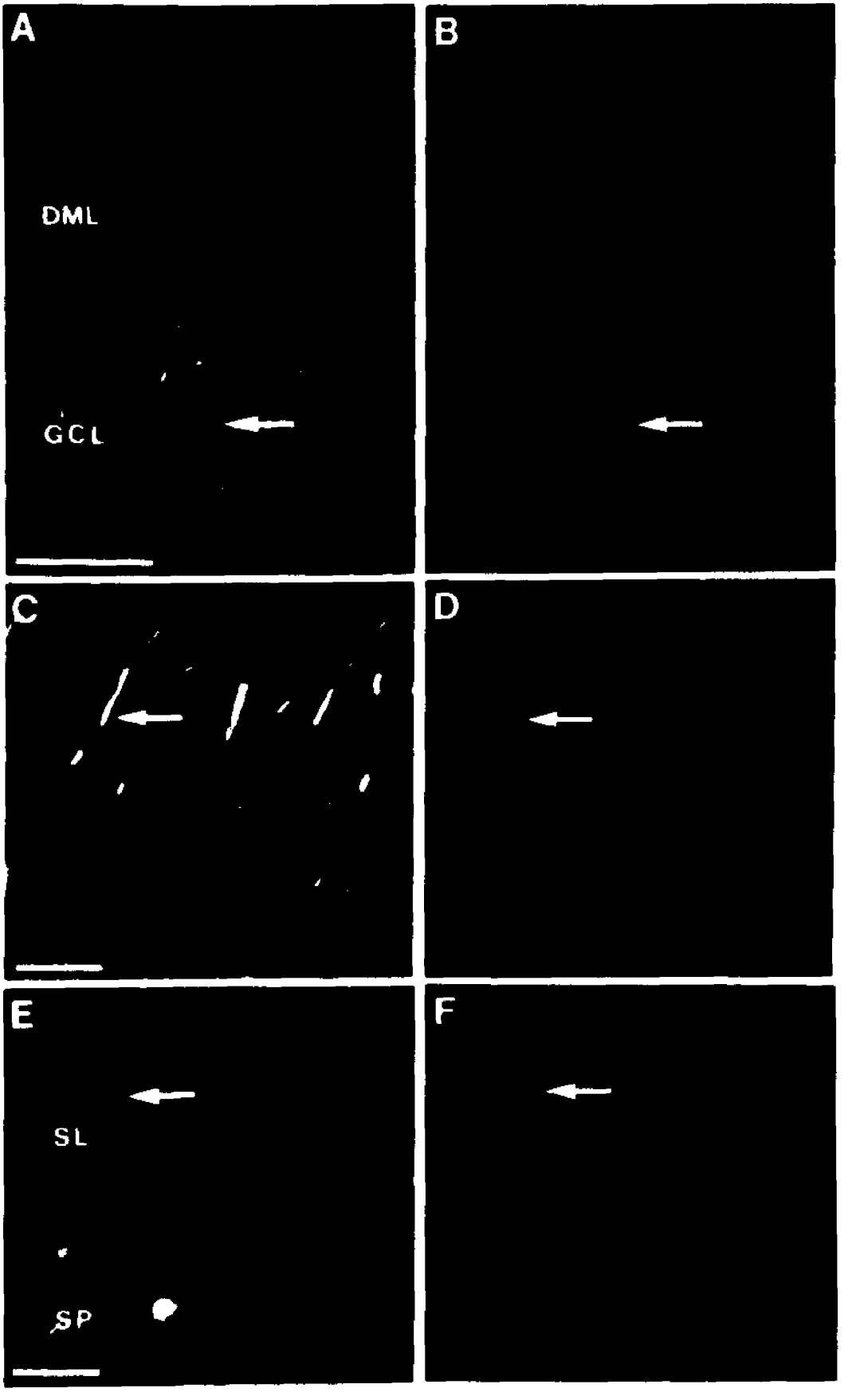
A
DML
GCL
B
C
D
E
SL
SP
F

Figure 6.4

Pairs of pseudo-colored confocal images of double labeled hilar polymorphic cells. (A) Texas red-labeled NMDAR1 in red. (B) FITC-labeled GluR5-7 in green. (C) Overlaid combination of A and B shows points of colocalization of GluR5-7 and NMDAR1 in yellow. (D) Texas red-labeled GluR2 in red. (E) FITC-labeled GluR5-7 in green. (F) Overlaid combination of D and E shows points of colocalization of GluR5-7 and GluR2 in yellow. Notice, in C and F, virtually 100% of immunolabeled elements display colocalization of GluR5-7 with NMDAR1 and GluR5-7 with GluR2, respectively. Orange perinuclear dots in C and F are accumulations of lipofuscin. Scale bar = 50 μm.

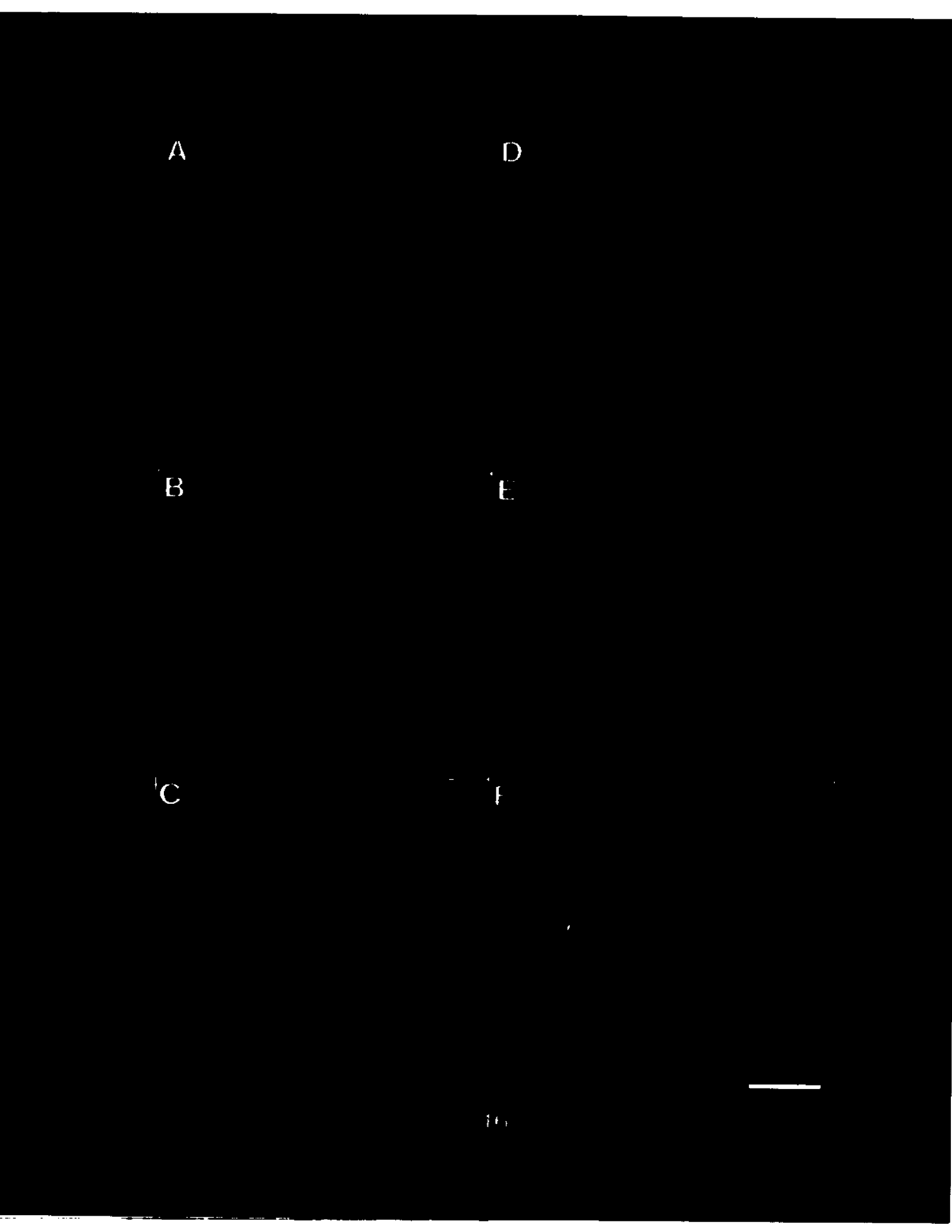
A
D
B
E
C
F

Figure 6.5

Ultrastructural localization of GluR2 immunoreactivity in the hippocampus. (A, B) Examples of GluR2-ir postsynaptic densities in CA1 on a labeled dendritic shaft (A) and spine (B). (C, D) Within the dentate molecular layer, immunolabeled postsynaptic densities were present on both labeled dendritic shafts (C) and spines (D). (E, F) Immunoreactivity within the stratum lucidum of CA3 was found in both axonal (E) and dendritic (F) profiles. Mossy fiber terminals in CA3 often contained examples of immunolabeled and unlabeled thorny excrescences. (B) Abbreviations and symbols: arrows - labeled post synaptic density, arrow heads - labeled mossy fiber axons, a - axon, ld - labeled dendrite, ls - labeled spine, mt - mossy fiber terminal, t - terminal, te thorny excrescence. Asterisk - unlabeled dendritic profile. Scale bar = 1.0 μm in A, B, D, E and 1.5 μm in C.

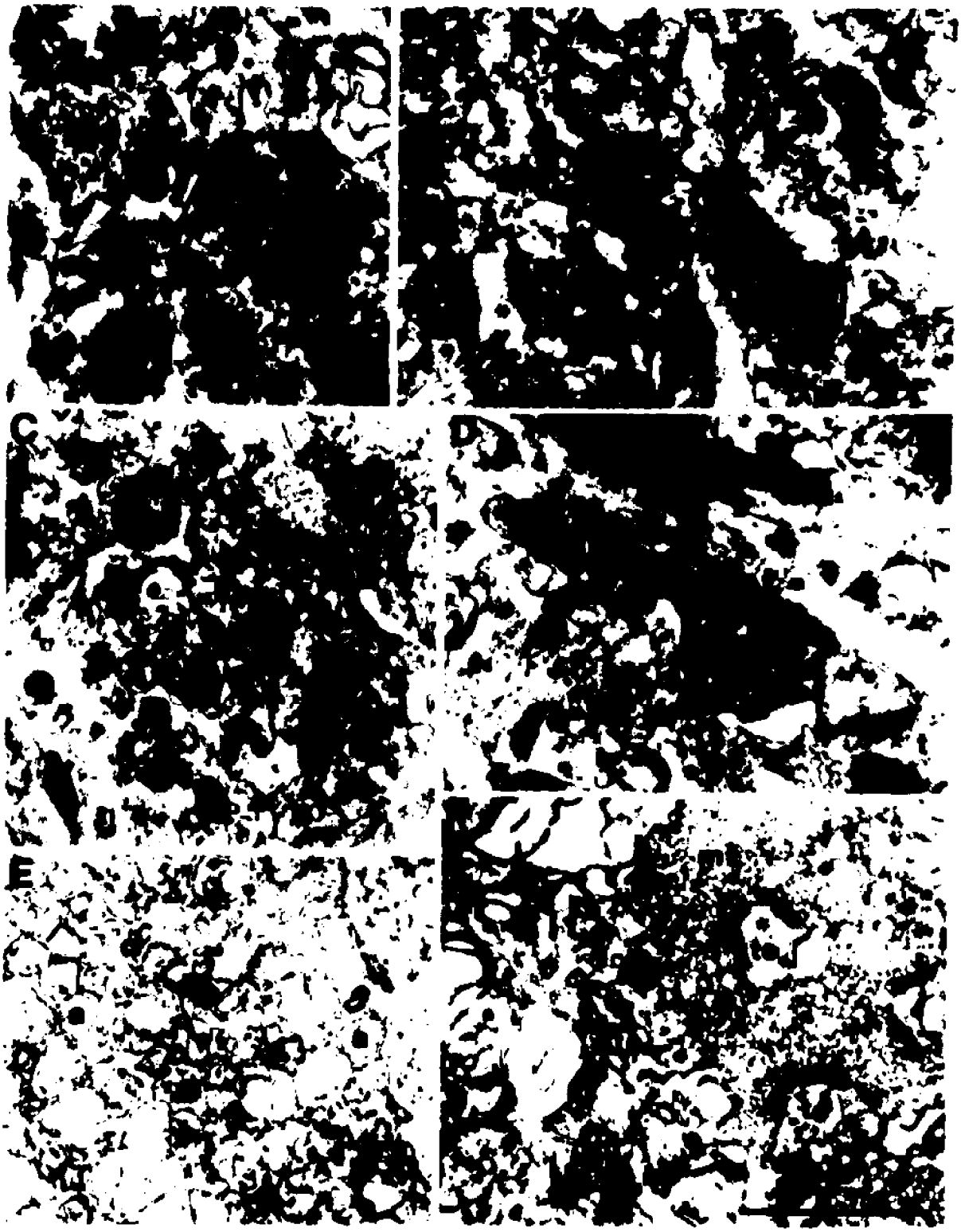
C
D
E

Figure 6.6

Schematic representation of CA3 pyramidal cell with laminar organization of afferent fibers (Frotscher et al., 1988), ultrastructural localization of EAA receptor subunits and forms of LTP exhibited. References regarding ultrastructural data of the EAA receptor subunits are; GluR2 (present report), NMDAR1 (Siegel et al., 1994), and GluR5-7 (Good et al., 1993). See (Cotman et al., 1986; Katsuki et al., 1991; Zalutsky and Nicoll, 1990) regarding forms of LTP demonstrated in CA3 and physiologic evidence for presynaptic NMDA receptors in stratum lucidum. Abbreviations: A/C - associational/commissural fibers, MF - mossy fibers, SL - stratum lucidum, SM stratum moleculare, SO - stratum oriens, SP - stratum pyramidale, SR - stratum radiatum.

Figure 6.6

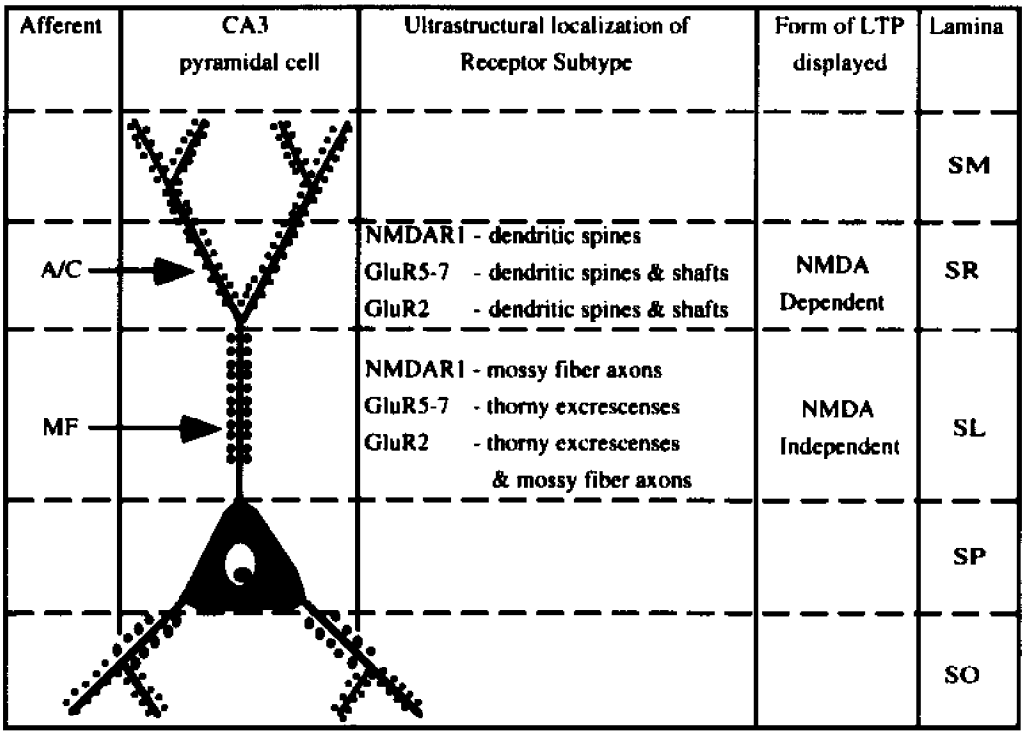
Afferent
CA3 pyramidal cell
Ultrastructural localization of Receptor Subtype
Form of LTP displayed
Lamina
SM
A/C
NMDAR1 - dendritic spines
GluR5-7 - dendritic spines & shafts
GluR2 - dendritic spines & shafts
NMDA Dependent
SR
MF
NMDAR1 - mossy fiber axons
GluR5-7 - thorny excrescenses
GluR2 - thorny excrescenses & mossy fiber axons
NMDA Independent
SL
SP
SO

Chapter 7

Conclusions

Social Deprivation

The first component of this thesis sought to identify neuroanatomic substrates for the behavioral abnormalities observed in monkeys which were raised in social deprivation, while the second described the distribution patterns for three classes of ionotropic EAA receptor subunits in monkey hippocampus, with the goal of relating immunohistochemical patterns to differential vulnerability observed in hippocampal neurons. Specifically, the first component demonstrated that early social deprivation results in an increased amount of somatic NF protein in the dentate gyrus granule cells relative to both age matched socially reared and newborn rhesus monkeys. Additionally, the mossy fiber axons from the dentate granule cells display abnormal phosphorylated NF protein and calbindin immunoreactivity in two of the four socially deprived monkeys relative to both age matched socially reared and newborn monkeys. Furthermore, there appears to be a disruption in the normal pattern of dendritic organization within the stratum lucidum of the two socially deprived monkeys which displayed abnormalities within the mossy fiber projection. These demonstrated changes may reflect a neuropathologic change rather than a delayed developmental process, as new born animals had immunoreactive profiles which closely matched 18 month old socially reared animals and differed from 18 month old socially deprived monkeys. The phenotypic difference observed in dentate gyrus granule cells and CA3 pyramidal cells between differentially reared monkeys supports the notion that specific brain regions or biochemical systems which subserve

complex behaviors may undergo long-term modifications induced by environmental conditions. Furthermore, the data suggest that constitutive structural proteins may be at least as plastic with regard to environmental manipulations as the more traditionally viewed indices of neuronal plasticity, such as neurotransmitter dynamics, cell number and the establishment of connectivity. The observed modifications may serve as an anatomical substrate for the behavioral abnormalities apparent in socially deprived animals.

Neuronal Degeneration and Differential Vulnerability

Although no objective criteria are available for the degree of behavioral abnormalities in socially deprived animals, subjective evaluation of the four socially deprived monkeys indicates that the behavior of the two animals with axonal alterations was the most severely affected. It is therefore possible that neuropathologic changes might be most pronounced in these two animals. Previous reports have attempted to compile a composite picture of the progression of events which occur during specific forms of neuronal degeneration. One such study examined the progressive changes in hippocampal CA1 pyramidal cells during age- and Alzheimer's disease-related degeneration (Vickers et al., 1992). This study proposed that degenerating neurons may go through an initial phase of increased immunoreactivity for nonphosphorylated NF protein within the somatodendritic compartment prior to neurofibrillary tangle formation and eventual loss. Similarly, the data suggest that increased immunoreactivity for nonphosphorylated NF proteins may also represent a relatively early neuropathologic change in dentate granule cells, which may precede alterations in the axonal output of these cells.

The current report suggests that alterations in the axonal projection from one cell population, granule cells, may lead to alterations in the dendritic organization of their target cell population, CA3 pyramidal cells. Within the hippocampal formation, such a relationship has been previously demonstrated for the mossy fiber circuit, where early ablation of the axonal projection in rats led to the absence of the normal postsynaptic element, thorny excrescences, on CA3 pyramidal cell dendrites (Represa et al., 1991). One potential mechanism for the influence of an axonal pathway on its target is through the action of a diffusible growth factor (Leslie, 1993). Alternatively, an axonal projection might exert such an effect on its target via activity dependent alterations in the normal synaptic organization between the two populations (Schmidt, 1985; Stell and Riesen, 1987). It is also possible that the increased level of nonphosphorylated NF proteins in dentate granule cells is mediated through glutamatergic neurotransmission. Previous reports have linked both NMDA and non-NMDA agonists with the regulation of NF protein phosphorylation and degradation (Gardner et al., 1990; Haglid et al., 1991; Wang et al., 1992). For example, kainate administration in the hippocampi of live rats led to the dephosphorylation of high molecular weight NF protein (Wang et al., 1992). While dephosphorylation of NF proteins in and of itself has not been linked to neurodegeneration, alterations in NF proteins has been observed within vulnerable neuronal populations in a host of degenerative disease processes, including Huntington's disease (Cudkowicz and Kowall, 1990), Parkinson's disease (Goldman et al., 1983), amyotrophic lateral sclerosis (Manetto et al., 1989), and Alzheimer's disease (Hof and Morrison, 1990; Morrison et al., 1987; Vickers and Morrison, 1992). Furthermore, neurodegenerative changes in each of these diseases has been linked to glutamate mediated

excitotoxicity (Choi, 1988; Rothman and Olney, 1987). Similarly, NMDA mediated excitotoxicity has been proposed as a mechanism for stress induced neurodegenerative changes within the hippocampus (Armanini et al., 1990).

Distribution of Excitatory Amino Acid Receptor Subtypes

Physiological studies have demonstrated that individual neurons exhibit response properties typical of both NMDA and non-NMDA receptors (MacDermott and Dale, 1987). The present data indicate that virtually all of the GluR5-7-ir neurons are also immunoreactive for both NMDAR1 and GluR2, indicating that all three classes of ionotropic GluRs are represented in neurons of each subdivision of the hippocampus. Similarly, a high degree of colocalization of GluR1-3 and GluR5-7 in monkey neocortex has been previously reported (Vickers et al., 1993). However, ultrastructural data indicate that while all three classes might be represented in a given neuron, their subcellular distribution is not uniform or equivalent. Although a comprehensive quantitative analysis has not been completed, preliminary evidence suggests that NMDAR1-ir postsynaptic densities in hippocampus are localized specifically to dendritic spines, while GluR2 was localized to both dendritic spines and shafts. Similarly, it has recently been reported that GluR5-7 are also localized to both dendritic spines and shafts in hippocampus (Good et al., 1993) and neocortex (Huntley et al., 1993). Furthermore, NMDAR1 was localized to mossy fiber axons and terminals within the stratum lucidum of CA3, while GluR2 was localized postsynaptically on thorny excrescences.

The relative absence of postsynaptic NMDA receptors in monkey stratum lucidum indicates that primates may exhibit an NMDA-independent form of LTP similar to that previously described for the mossy fiber system in rats. Similarly, more distal dendritic segments of CA3 pyramidal cells in monkeys do contain postsynaptic NMDAR1 immunoreactivity on spines, and LTP mediated by inputs to this portion of the dendritic tree is NMDA-dependent in rats. Thus, in addition to the implications for differential vulnerability, these data demonstrate that models of LTP developed in rodents may apply to the primate hippocampus. However, subtle differences in connectivity exist between rodent and primate hippocampus such that basal dendrites of CA3 pyramidal cells receive mossy fiber inputs in primates but not rodents (Frotscher et al., 1988), which may result in different patterns of LTP to this portion of the dendritic tree. Furthermore, GluR subunits and classes may be segregated within dendritic processes such that different excitatory afferents to the same neuron might be mediated preferentially through different classes of GluRs, even though all three classes are present within the same postsynaptic neuron. These data have important implications for the organization of converging excitatory inputs to a laminated structure such as the hippocampus or neocortex (Huntley et al., 1993; Vickers et al., 1993). The combination of laminar segregation of inputs, such as the mossy fibers to the stratum lucidum and the associational/commissural fiber input to the stratum radiatum, with intradendritic segregation of GluR subunits, confers upon the system a high capacity for specificity in the postsynaptic coding of excitatory inputs. Furthermore, this segregation of inputs and receptor subunits may underlie the ability of associational/commissural fiber synapses to exhibit associative changes with mossy fiber stimulation, while mossy fiber synapses do not

exhibit such associative changes with associational/commissural fiber inputs. Such postsynaptic specificity is further enhanced by the strong preference of NMDAR1 for spines in hippocampus, while GluR2 and GluR5-7 (Good et al., 1993) are found on spines and shafts in hippocampus as well as in neocortex (Huntley et al., 1993). While the preference of NMDA receptors for spines is likely to have profound implications regarding the roles of both spines and NMDA receptors in the mechanisms of learning and memory, further interpretation of this finding requires quantitative double label ultrastructural analyses to determine more precisely the degrees of segregation and colocalization of all GluR families in respect to receptor localization on individual spines and shafts.

Excitotoxicity

Excitotoxicity has been implicated as an underlying basis for the cellular damage which occurs in a wide range of pathologic conditions including traumatic events as well as a host of disease processes (Choi, 1988; Rothman and Olney, 1987). Furthermore, discrete portions of the hippocampal formation are major loci of damage in ischemia, epileptic seizure and Alzheimer's disease. Cellular pathology in ischemic injury is particularly severe in the CA1 region, and can be dramatically decreased by specific NMDA antagonists (Rothman and Olney, 1987). Similarly, the neuropathologic changes which occur in Alzheimer's disease are particularly severe in the subiculum and CA1 regions. Conversely, CA3 cells are among the most vulnerable to kainate damage (Nadler et al., 1981) and seizure-induced cellular pathologic changes (Choi, 1988), but are relatively resistant to damage resulting from ischemic insult or the neurodegenerative process in Alzheimer's disease. These differential patterns of vulnerability may be

related in part to the EAA receptor subunit content and subcellular compartmentalization within various cell groups. Specifically, all three classes of ionotropic EAA receptors are heavily represented in CA1 neurons, which may confer vulnerability to both NMDA and non-NMDA mediated excitotoxicity. The relative resistance to degeneration of CA3 neurons in certain conditions may be linked not only to the relatively low representation of all three classes of EAA ionotropic receptors as compared to CA1, but in particular, to the apparent lack of postsynaptic NMDA receptors in the stratum lucidum, the site of termination of the mossy fiber system.

Within the hippocampus, there is regional specialization with respect to both physiologic and pathologic conditions, which may be related to the composition of EAA receptor subunits present in various cell groups, as well as the subcellular/laminar segregation of these subunits with respect to specific afferents. Studies within this thesis have demonstrated that although members of the three ionotropic EAA receptor subgroups are largely colocalized throughout the hippocampus, they can be segregated intraneuronally and display differing patterns of subcellular localization within a particular cell class. This intraneuronal segregation may permit various GluR subunits and classes to play different roles with respect to identified afferent systems that exhibit laminar segregation and terminate in different portions of the postsynaptic dendritic tree.

Future Investigations

Based on the series of experiments included in this thesis, several predictions and recommendations can be made regarding future investigations of the effects of environmental manipulations on specific

neuronal populations in the primate brain. Data presented in chapters 3 and 4 indicate that social deprivation may lead to neuropathologic changes in dentate granule cells, and eventually to the disruption of the mossy fiber projection. Previous investigations have suggested that the formation of specialized dendritic spines called thorny excrescences found on CA3 pyramidal cells in the stratum lucidum form in direct response to the presence of mossy fiber terminals, and do not exist if the ingrowth of this projection is disrupted (Represa et al., 1991). Therefore, one might expect to see a decrease in the number of thorny excrescences on CA3 pyramidal cells of animals which experience social deprivation. Data presented within chapters 5 and 6 suggest that there is normally an intraneuronal segregation of EAA receptors such that synapses between mossy fiber terminal and CA3 pyramidal cell thorny excrescences contain only non-NMDA receptors, while synapses at more distal portions of the dendritic tree contain both NMDA and non-NMDA receptors. Therefore, we would expect to see a disruption of this pattern of receptor subtype segregation in socially deprived animals. Such an alteration would be expected to have profound effects on the physiologic properties of this circuit, and ultimately on neurotransmission in the hippocampus. Accordingly, we recommend that future investigations into the effects of rearing condition on the development and maturation of the primate brain include a detailed evaluation of the morphology of CA3 pyramidal cells, with particular emphasis on the degree to which thorny excrescences develop. Furthermore, such a study should determine the degree of intraneuronal segregation of EAA receptor subtypes in CA3 with respect to normal patterns described in this thesis.

Appendix 1

The methods and results contained within this section are from (Siegel et al., 1994), and were performed primarily by Dr. Nils Brose and colleagues in the laboratory of Dr. Stephen Heinemann. Blocking experiments for monoclonal antibody 54.1 were performed by S. Siegel with the assistance of N. Brose.

Generation of Monoclonal Antibodies Against NMDAR1.

Monoclonal antibodies directed against the NMDAR1 subunit were generated according to standard procedures (Jahn et al., 1985; Köhler and Milstein, 1975), using a fusion protein encoding glutathione-S-transferase (GST) in frame with NMDAR1 residues 660-811, representing the intracellular loop between transmembrane regions III and IV; residue numbers as in Moriyoshi *et al.* (1991).

Gel Electrophoresis and Immunoblotting.

Western blot detection of NMDAR1 was performed on rat synaptic plasma membranes, monkey hippocampus and NMDAR1-transfected human embryonic kidney (HEK) 293 cells. Equal amounts of protein (20 μg per lane) were separated by SDS-PAGE according to the method of Laemmli (Laemmli, 1970), blotted onto nitrocellulose membranes as described by Towbin et al. (Towbin et al., 1979) with minor modifications (Rogers et al., 1991), and probed with anti-NMDAR1 mAb 54.1. Immunodetection of proteins was performed using anti-NMDAR1 mAb 54.1 and horseradish peroxidase-conjugated goat anti-mouse IgG (Bio-Rad, Richmond CA). Proteins were visualized by enhanced chemoluminescence (ECL,

Amersham, Arlington Heights, IL) according to the manufacturers specifications.

Expression and Immunodetection of NMDAR1 in HEK Cell Line 293.

A full length NMDAR1 insert, subcloned into a eukaryotic expression vector that had been modified from pBluescript to include the pcDNAI multiple cloning site and human CMV promoter and enhancer, was obtained from J. Sullivan and G. Sharma (Salk Institute, San Diego, CA). For calcium phosphate-mediated transfection (Graham and van der Eb, 1973; Sambrook et al., 1989), 20 μg of DNA were added to a 100 mm culture dish with 293 cells that were approximately 70% confluent. Cells were harvested after 48 hours into SDS-PAGE sample buffer.

For immunocytochemistry, transfected cells were cultured on polylysine-coated coverslips. Cells were fixed with 4% paraformaldehyde for 30 minutes and prepared for immunohistochemistry as previously described (Huntley et al., 1993). Cells were then incubated for 30 hours at 4° C with anti-NMDAR1 monoclonal antibody 54.1 diluted 1:500 in 3% goat serum in phosphate buffered saline (PBS), washed and incubated for one hour at room temperature with biotinylated goat anti-mouse IgG (Vector Laboratories, Burlingame, CA) diluted 1:50 in 3% goat serum in PBS. Samples were then washed, incubated in Vector Elite ABC reagent (Vector Laboratories, Burlingame, CA), and visualized with 3,3'-diaminobenzidine.

Preadsorption of Antibodies Against NMDAR1.

Primary antiserum was passed over a column comprised of Reacti-Gel GF-2000 (glycine/lysine blocked) (Pierce, Rockford, IL) which was

conjugated to a peptide (NIII) containing amino acids 660-811 of NMDAR1 and 6 histadine residues. Following an additional 48 hours of preadsorption with a molar excess of soluble NIII at room temperature, tissue sections were incubated with anti-NMDAR1 antibody for one hour and processed for immunohistochemistry as described below. Additional sections were processed simultaneously as positive controls using anti-NMDAR1 antibody which was passed over a blank column or by preadsorption with a molar excess of GST.

Antibody Characterization

The specificity of mAb 54.1 was examined in the current study by both western blotting and immunocytochemical techniques. Western blot analyses of monkey hippocampus, rat synaptic plasma membranes (SPMs) and human embryonic kidney 293 cells (HEK 293) which were transfected with cDNA encoding full length NMDAR1 resulted in the labeling of one major band with a molecular weight of approximately 116 kDa (fig. A.1 A), which is consistent with previous reports using polyclonal antibodies or photoaffinity labeling (Chazot et al., 1992; Sonders et al., 1990). Although a single band was labeled in homogenized extracts from monkey hippocampus, an additional band of approximately 75 kDa and a doublet of approximately 100 kD were also labeled on rat SPMs and/or NMDAR1 transfected HEK 293 cells. These bands presumably represent breakdown products of the NMDAR1 protein, since no bands were labeled in HEK 293 cells which were not transfected with NMDAR1. Immunocytochemistry using mAb 54.1 specifically labeled paraformaldehyde fixed NMDAR1 transfected HEK 293 cells, but did not label wild type HEK 293 cells (fig. A.1 B, C).

Figure A.1

(A) Western blot detection of NMDAR1 in rat synaptic plasma membranes, monkey hippocampus and transiently transfected HEK 293 cells. Lane 1 - rat synaptic plasma membranes; lane 2 - monkey hippocampus; lane 3 - human embryonic kidney 293 cells transfected with NMDAR1; lane 4 - human embryonic kidney 293 cells transfected with NMDAR2A as a control. (B and C) Immunocytochemical detection of NMDAR1 transfected 293 cells. Human embryonic kidney cells transfected with NMDAR1 (B) and untransfected 293 cells (C) were stained with anti-NMDAR1 monoclonal antibody 54.1 as described in materials and methods. Arrows in B indicate examples of NMDAR1-ir cells. Scale bar in B and C = 50 μm.

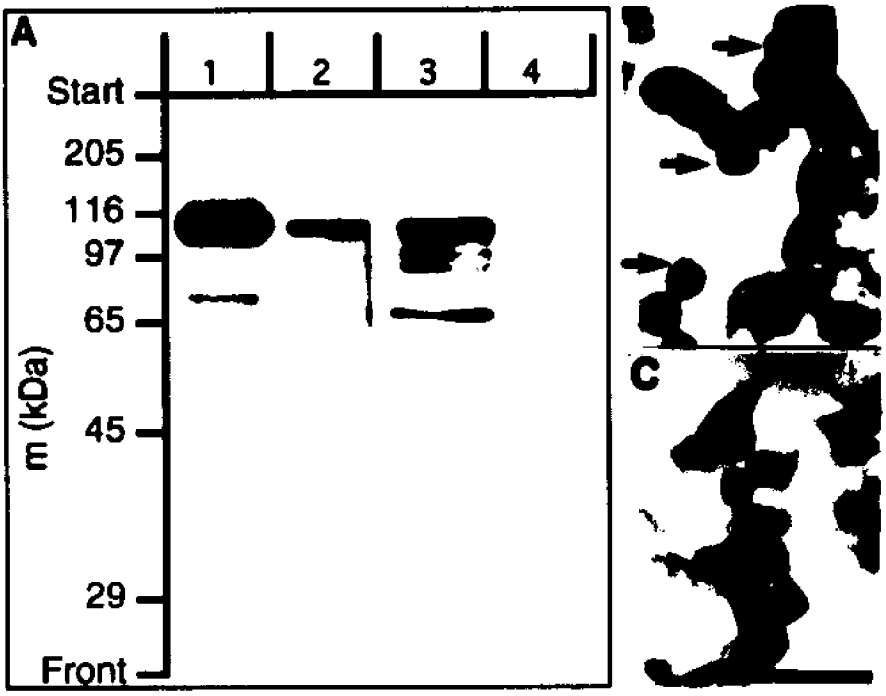
A
1
2
3
4
Start
205
116
97
65
45
29
Front
m (kDa)
B
C

Appendix 2

The methods and results in this section will appear in (Siegel et al., in preparation) and represent the work of Dr. Scott Rogers and Dr. Thomas Moran.

Generation and Characterization of Anti-GluR2 mAb 3A11

The monoclonal antibody 3A11 is a mouse γ type immunoglobulin (IgG) of the subclass IgG2a, which was generated according to procedures described previously in (Huntley et al., 1993) against a fusion protein encoding the putative extracellular N-terminal domain of GluR2. The TrpE bacterial overexpression system (Dieckmann and Tzagoloff, 1985) was used to obtain GluR2 antigen for antibody production as previously described (Rogers et al., 1991). Briefly, a Bgl II-Sma 1 fragment of the GluR2 cDNA containing nucleotides 170-430, (Boulter et al., 1990) was shuttle cloned into the Bam H1-Hind 2 sites of vector pUC18. This fragment was then removed using Sma1 and Hind 3 for subcloning into the pATH2 expression vector at the same restriction enzyme sites. Protein from GluR1 (long construct), GluR3, and GluR5 were the same as previously described (Rogers et al., 1991). Antigen production, enrichment, and purification by SDS-PAGE fractionation was done exactly as described previously (Rogers et al., 1991).

Soluble fusion proteins were prepared by dissolving enriched antigen into freshly prepared 8 M urea (10 ml per gram of protein) at room temperature for 1 hr. The solution was clarified by centrifugation and the supernatant diluted 1:10 by the slow addition of a solution consisting of 50

mM KCl and 50 mM NaCl (pH 10.5). After an additional hour of stirring at room temperature, the solution was brought to pH 8 with 1 N HCl and repeatedly dialyzed against 10 mM NaCl in 10 mM sodium phosphate buffer (pH 7.2) at 40 C. The concentration of soluble protein was then measured by the method of Lowry (Lowry et al., 1951).

Monoclonal antibodies were produced by immunizing 6-8 week old BALB/c mice with polyacrylamide gel strips emulsified in Complete Freund's Adjuvant in the foot pads and intraperitoneally. The animals were boosted after 3 weeks with gel strips emulsified in Incomplete Freund's Adjuvant. Boosts were repeated two additional times at monthly intervals. Serum antibody titers were checked by RIA (described below) and the animal with the highest titer was selected for fusion. Ten million SP2/0 BALB/c myeloma cells were mixed with 100 x 106 spleen cells and fused by the dropwise addition of PEG 4000 using a standard technique. Colonies were visible 12 days later and supernatants were removed and analyzed for the presence of specific antibodies by radioimmunoassay (see below).

Radioimmunoassay

The mAb 3A11 is further characterized in the current study by RIA. RIA was performed by coating 96 well flexible plates (Falcon Microtest III) with 5 µg/ml of fusion proteins encoding GluR1, GluR2, GluR3, ß4 or TrpE alone as a control overnight at 4° C. The plates were then blocked with 1% bovine serum albumin (BSA) in 0.1 molar phosphate buffered saline (PBS) for 30 minutes at room temperature after which undiluted hybridoma supernatants (50µl) were added to triplicate wells. Following a 90 minute incubation at room temperature, 50 µl (50,000 counts per minute) of I-125

labeled goat anti mouse IgG (heavy chain specific) was added to each well. After an additional 90 minute incubation at room temperature, plates were washed, cut up and placed in a gamma counter.

Characterization of mAb 3A11

In addition to the blocking experiment described above in the methods section, the specificity of monoclonal antibody 3A11 was tested by RIA. RIA for the anti-GluR2 mAb 3A11 resulted in binding to the GluR2 specific fusion protein, while not to fusion proteins encoding homologous portions of GluR1, 3, or the two control peptides encoding β4 or TrpE (fig. A.2 1).

Figure A.2

Radioimmunoassay results for the monoclonal antibody 3A11. Individual wells were coated with 5 µg/ml of fusion proteins encoding GluR1, GluR2, GluR3, ß4 or TrpE alone. Wells were then labeled with I^{125} labeled goat anti mouse IgG, washed and counted in a gamma counter. Specific binding of mAb 3A11 was only found to GluR2. Two additional monoclonal antibodies were used as controls to demonstrate the presence of the additional fusion proteins. Monoclonal antibody 2D8 recognizes the EAA receptor subunits GluR1-3, while mAb 3D8 recognizes TrpE.

Figure A.2

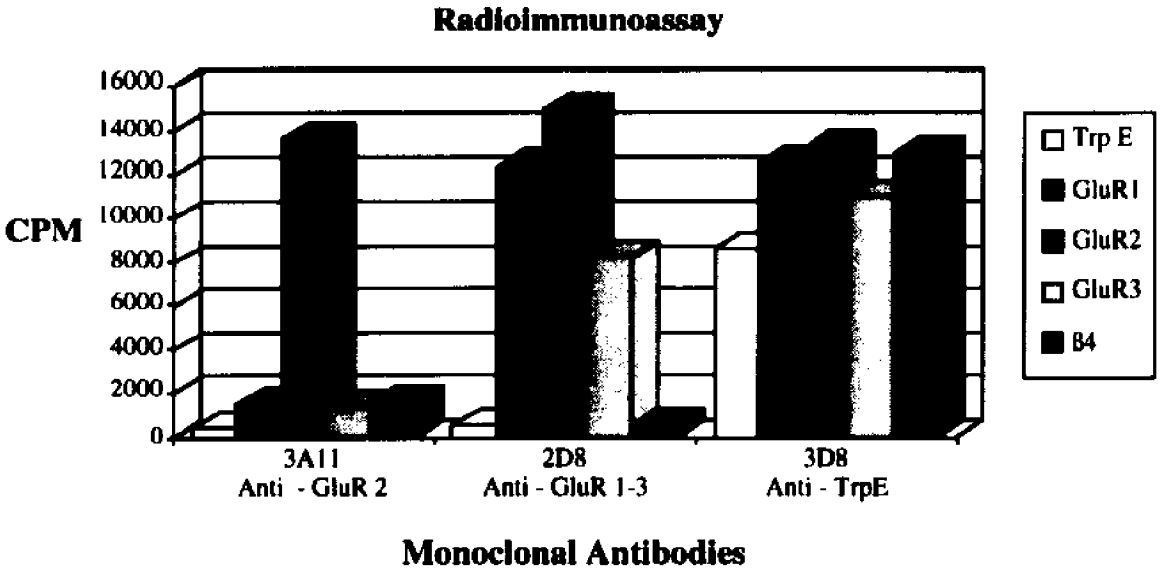
Radioimmunoassay
CPM
16000
14000
12000
10000
8000
6000
4000
2000
0
3A11
Anti - GluR 2
2D8
Anti - GluR 1-3
3D8
Anti - TrpE
Monoclonal Antibodies
Trp E
GluR1
GluR2
GluR3
B4

Bibliography

Amaral DG and Dent JA, (1981) Development of mossy fibers of the dentate gyrus: I. A light and electron microscopic study of the mossy fibers and their expansions. J Comp Neurol 195:51-86.

Anderson CO and Mason WA, (1978) Competitive social strategies in groups of deprived and experienced rhesus monkeys. Dev Psychobiol 11:289-299.

Araujo DM, Lapchak PA, Meaney MJ, Collier B and Quirion R, (1990) Effects of aging on nicotinic and muscarinic autoreceptor function in the rat brain: Relationship to presynaptic cholinergic markers and binding sites. J Neurosci 10:3069-3078.

Armanini MP, Hutchins C, Stein BA and Sapolsky RM, (1990) Glucocorticoid endangerment of hippocampal neurons is NMDA-receptor dependent. Brain Res 532:7-12.

Barnes JM and Henley JM, (1992) Molecular characteristics of excitatory amino acid receptors. Prog Neurobiol 39:113-133.

Beauchamp AJ and Gluck JP, (1988) Associative processes in differentially reared monkeys (*Macaca mulatta*): Sensory preconditioning. Dev Psychobiol 21:355-364.

Beauchamp AJ, Gluck JP, Fouty EH and Lewis MH, (1990) Associative processes in differentially reared monkeys (*Macaca mulatta*): Blocking. Dev Psychobiol 24:175-189.

Beitner-Johnson D, Guitar G and Nestler EJ, (1992) Neurofilament proteins and the mesolimbic dopamine system: Common regulation by chronic morphine and chronic cocaine in the rat ventral tegmental area. J Neuroscience 12:2165-2176.

Bettler B, Boulter J, Hermans-Borgmeyer I, O'Shea-Greenfiels, Deneris ES, C. M, Borgmeyer U, Hollmann M and Heinemann S, (1990) Cloning of a novel glutamate receptor subunit, GluR5: Expression in the nervous system during development. Neuron 5:583-595.

Bettler B, Egebjerg J, Sharma G, Pecht G, Hermans-Borgmeyer I, Moll C, Stevens C and Heinemann S, (1992) Cloning of a putative glutamate receptor: a low affinity kainate-binding subunit. Neuron 8:257-265.

Bignami A, Grossi M and Dahl D, (1985) Transient expression of neurofilament protein without filament formation in Purkinje cells development. Int J Dev Neurosci 3:365-377.

Bliss T and Lømo T, (1973) Long-lasting potentiation of synaptic transmission in the dentate area of the anesthetized rabbit following stimulation of the perforant path. J Physiol 232:331-356.

Boulter J, Hollman M, O'Shea-Greenfield A, Hartley M, Deneris E, Maron C and Heinemann S, (1990) Molecular cloning and functional expression of glutamate receptor subunit genes. Science 249:1033-1037.

Brizzee KR, Ordy JM and Bartus RT, (1980) Localization of cellular changes within multimodal sensory regions in aged monkey brain:

Possible implications for age-related cognitive loss. Neurobiol Aging 1:45-52.

Brose N, Gasic GP, Rogers S, Moran T, Morrison JH, Jahn R and Heinemann SF, (1993) Immunoaffinity purification of glutamate receptors of the non-NMDA and NMDA type. Soc Neurosci Abstract 19:1356.

Burnstock G, Mirsky R and Belai A, (1988) Reversal of nerve damage in streptozotocin-diabetic rats by acute application of insulin *in vitro*. Clin Sci 75:629-35.

Cambray DMA and Burgoyne RD, (1986) Transient expression of neurofilament-like (RT97) immunoreactivity in cerebellar granule cells. Brain Res 393:282-286.

Campbell MJ, Hof PR and Morrison JH, (1991) A subpopulation of primate corticocortical neurons is distinguished by somatodendritic distribution of neurofilament protein. Brain Res 539:133-136.

Campbell MJ and Morrison JH, (1989) Monoclonal antibody to neurofilament protein (SMI32) labels a subpopulation of neurons in the human and monkey neocortex. J Comp Neurol 282:191-205.

Celio MR, (1989) Calcium binding proteins in the brain. Arch Ital Anat Embriol 94:227-236.

Celio MR, (1990) Calbindin D-28k and parvalbumin in the rat nervous system. Neuroscience 35:375-475.

Chattarji S, Stanton PK and Sejnowski TJ, (1989) Commissural synapses, but not mossy fiber synapses, in hippocampal field CA3 exhibit associative long-term potentiation and depression. Brain Res 495:145-150.

Chazot PL, Cik M and Stephenson FA, (1992) Immunological detection of the NMDAR1 glutamate receptor subunit expressed in human embryonic kidney 293 cells and in rat brain. J Neurochem 59:1176-1178.

Choi DW, (1988) Glutamate neurotoxicity and diseases of the nervous system. Neuron 1:623-634.

Collingridge GL and Bliss TVP, (1987) NMDA receptors - their role in long term potentiation. TiNS 10:288-293.

Condorelli DF, Dell'Albani P, Corsaro M, Barresi V and Giuffrida Stella AM, (1993) AMPA--selective glutamate receptor subunits in astroglial cultures. J Neuro Res 36:344-356.

Cotman CW, Flatman JA, Ganong AH and Perkins MN, (1986) Effects of excitatory amino acid antagonists on evoked and spontaneous excitatory potentials in guinea-pig hippocampus. J Physiol 378:403-415.

Cotman CW, Monaghan DT, Ottersen OP and Storm-Mathisen J, (1987) Anatomical organization of excitatory amino acid receptors and their pathways. TiNS 10:273-280.

Cudkowicz M and Kowall NW, (1990) Degeneration of pyramidal projection neurons in Huntington's disease cortex. Ann Neurol 27:200-204.

DeFelipe J and Jones EG, (1992) High-resolution light and electron microscopic immunocytochemistry of colocalized GABA and calbindin D-28k in somata and double bouquet cell axons on monkey somatosensory cortex. Eur J Neurosci 4:46-60.

Dieckmann CL and Tzagoloff A, (1985) Assembly of the mitochondrial membrane system. J Biol Chem 260:1513-1520.

Dotti CG, Sullivan CA and Banker GA, (1988) The establishment of polarity by hippocampal neurons in culture. J Neurosci 8:1454-1468.

Duffy TE, Kohle SJ and Vannucci RC, (1975) Carbohydrate and energy metabolism in perinatal rat brain: relation to survival in anoxia. J Neurochem 24:271-6.

Eckenhoff MF and Rakic P, (1988) Nature and fate of proliferative cells in the hippocampal dentate gyrus during the life span of the rhesus monkey. J Neurosci 8:2729-2747.

Egebjerg J, Bettler B, Hermans-Borgmeyer I and Heinemann SF, (1991) Cloning of a cDNA for a glutamate receptor subunit activated by kainate but not AMPA. Nature 351:745-748.

Enderlin S, Norman AW and Celio MR, (1987) Ontogeny of the calcium binding protein calbindin D-28k in the rat nervous system. Anat Embryol 177:15-28.

Errington Ml, Lynch MA and Bliss TVP, (1987) Long-term potentiation in the dentate gyrus: induction and increased glutamate release are blocked by D(-)aminophosphonovalerate. Neuroscience 20:279-284.

Fagg GE and Foster AC, (1983) Amino acid neurotransmitters and their pathways in the central nervous system. Neuroscience 9:701-719.

Floeter MK and Greenough WT, (1979) Cerebellar plasticity: Modification of Purkinje cell structure by differential rearing in monkeys. Science 206:227-229.

Frotscher M, (1991) Target cell specificity of synaptic connections in the hippocampus. Hippocampus 1:123-130.

Frotscher M, Kraft J and Zorn U, (1988) Fine structure of identified neurons in the primate hippocampus: A combined Golgi/EM study in the baboon. J Comp Neurol 275:254-70.

Frotscher M, Kugler P, Misgeld U and Zilles K, (1988) Neurotransmission in the hippocampus. Adv Anat Embryol Cell Biol 111:1-103.

Gaarskjaer FB, (1981) The hippocampal mossy fiber system of the rat studied with retrograde tracer techniques. Correlation between topographic organization and neurogenetic gradients. J Comp Neurol 203:717-735.

Gaarskjaer FB, (1986) The organization and development of the hippocampal mossy fiber system. Brain Res Rev 11:335-357.

Gaiarsa JL, Beaudoin M and Ben-Ari Y, (1992) Effect of neonatal degranulation on the morphological development of rat CA3

pyramidal neurons: Inductive role of mossy fibers on the formation of thorny excrescences. J Comp Neurol 321:612-625.

Gardner VO, Caiozzo VJ, Munden SK and Bridges RJ, (1990) Excitotoxins can produce protein degradation in the spinal cord. Spine 15:858-63.

Ginsberg SD, Hof PR, McKinney WT and Morrison JH, (1993) Quantitative analysis of tuberoinfundibular tyrosine hydroxylase-immunoreactive neurons and corticotropin-releasing factor-immunoreactive neurons in monkeys raised with differential rearing conditions. Exp Neurol 120:59-105.

Ginsberg SD, Hof PR, Young WG, Kraemer GW, McKinney WT and Morrison JH, (1991) Quantitative analysis of transmitter identified systems in the monkey paraventricular nucleus: Effects of differential rearing conditions. Soc Neurosci Abstr 17:895.

Ginsberg SD, Hof PR, Young WG and Morrison JH, (1993) Noradrenergic innervation of the hypothalamus of rhesus monkeys: Distribution of dopamine-ß-hydroxylase-immunoreactive fibers and a quantitative analysis of varicosities in the paraventricular nucleus. J Comp Neurol 327:597-611.

Ginsberg SD, Siegel SJ, Hof PR, Young WG, Kraemer G, McKinney WT and Morrison JH, (1992) Effects of social isolation on specific neuronal populations in the primate hypothalamus and hippocampus. Biol Psychiatry 31:196A.

Goldman JE, Yen S-H, Chiu F-C and Peress NS, (1983) Lewy bodies of Parkinson's disease contain neurofilament antigens. Science 221:1082-1084.

Good PF, Huntley GW, Rogers SW, Heinemann SH and Morrison JH, (1993) The distribution of kainate receptor subunits GluR5/6/7 in primate hippocampus. Brain Res 624:347-353.

Good PF, Rogers SW, Heinemann SH and Morrison JH, (1993) Ultrastructural localization of kainate class glutamate receptor subunits GluR5/6/7 in monkey hippocampus and entorhinal cortex. Soc Neurosci Abstract 19:473.

Gould E, Woolley CS and McEwen B, (1991) Adrenal steroids regulate postnatal development of the rat dentate gyrus: I effects of glucocorticoids on cell death. J Comp Neurol 313:479-485.

Gould E, Woolley CS and McEwen BS, (1990) Short-term glucocorticoid manipulations affect neuronal morphology and survival in the adult dentate gyrus. Neuroscience 37:367-375.

Graham FL and van der Eb AJ, (1973) A new technique for the assay of infectivity of human adenovirus 5 DNA. Virology 52:456-467.

Griffin GA and Harlow HF, (1966) Effects of three months of total social deprivation on social adjustment and learning in the rhesus monkey. Child Dev 37:533-547.

Haglid KG, Wang S, Hamberger A, Lehmann A and Moller CJ, (1991) Neuronal and glial marker proteins in the evaluation of the protective action of MK 801. J Neurochem 56:1957-61.

Harlow HF, Harlow MK and Suomi SJ, (1971) From thought to therapy: Lessons from a primate laboratory. Am Sci 59:538-549.

Harris EW and Cotman CW, (1986) Long-term potentiation of guinea pig mossy fiber responses in not blocked by N- methyl-D-aspartate antagonists. Neurosci Lett 70:132-137.

Harris EW, Ganong AH and Cotman CW, (1984) Long-term potentiation in hippocampus involves N- methyl-D-aspartate receptors. Brain Res 323:132-137.

Heinemann SF and Hollmann M, (1994) Cloned Glutamate Receptors. Ann Rev Neurosci 17:31-108.

Hendrickson AE, Van-Brederode JF, Mulligan KA and Celio MR, (1991) Development of the calcium-binding protein parvalbumin and calbindin in monkey striate cortex. J Comp Neurol 307:626-646.

Hendry SHC and Jones EG, (1983) The organization of pyramidal and non-pyramidal cell dendrites in relation to thalamic afferent terminations in the monkey somatic sensory cortex. J Neurocytol 12:277-298.

Hendry SHC, Jones EG, Emson PC, Lawson DEM, Heizmann CW and Streit P, (1989) Two classes of cortical GABA neurons defined by differential calcium binding protein immunoreactivity. Exp Brain Res 76:467-472.

Herb A, Burnashev N, Werner P, Sackman B, Wisden W and Seeburg PH, (1992) The KA-2 subunit of excitatory amino acid receptors shows widespread expression in brain and forms ion channels with distantly related subunits. Neuron 8:775-785.

Hirst E, Asante J and Price J, (1991) Clustering of dendrites in the cerebral cortex begins in the embryonic cortical plate. J Neurocytol 20:431-438.

Hof PR and Morrison JH, (1990) Quantitative analysis of a vulnerable subset of pyramidal neurons in Alzheimer's disease: II. Primary and secondary visual cortex. J Comp Neurol 301:55-64.

Hoffman PN, Griffin JW and Price DL, (1984) Control of axonal caliber by neurofilament transport. J Cell Biol 99:705-714.

Hollman M, Hartley M and Heinemann SF, (1991) Ca^{2+} permeability of KA-AMPA-gated glutamate receptor channels depends on subunit composition. Science 252:851-853.

Houamed KM, Kuijper JL, Gilbert TL, Haldman BA, O'Hara PJ, Mulihill ER, Almers W and Hagen FS, (1991) Cloning, expression and gene structure of a G protein-coupled glutamate receptor from rat brain. Science 252:1318-1321.

Hubel D and Wiesel T, (1970) The period of susceptibility to the physiological effects of unilateral eye closure in kittens. J Physiol 206:419-436.

Huntley GW and Jones EG, (1990) Cajal-Retzius neurons in developing monkey neocortex show immunoreactivity for calcium binding proteins. J Neurocytol 19:200-212.

Huntley GW, Rogers SW, Heinemann SH, Moran T, Janssen W, Archin N, Vickers JC and Morrison JH, (1993) Selective distribution of kainate receptor subunit immunoreactivity in monkey neocortex revealed by a monoclonal antibody against glutamate receptor subunits GluR5/6. J Neuroscience 13:2965-2981.

Huntley GW, Vickers JC, Brose N, Janssen W, Archin N, Gasic GP, Jahn R, Heinemann SH and Morrison JH, (1993) NMDA receptors in monkey cerebral cortex: Distribution of NMDAR1 subunit mRNAs and organization and synaptic localization NMDAR1 subunit proteins. Soc Neurosci Abstr 19:472.

Huntley GW, Vickers JC, Janssen W, Brose N, Heinemann SH and Morrison JH, (1994) Distribution and synaptic localization of immunocytochemically identified NMDA receptor subunit proteins in sensory-motor and visual corticies of monkey and human. J Neurosci in press.

Insel TR, Miller LP and Gelhard RE, (1990) The ontogeny of excitatory amino acid receptors in rat forebrain-I. N-methyl-D-aspartate and quisqualate receptors. Neuroscience 35:31-43.

Jahn R, Schiebler W, Ouimet C and Greengard P, (1985) A 38,000-dalton membrane protein (p38) present in synaptic vesicles. Proc Natl Acad Sci USA 82:4137-4141.

Katsuki H, Kaneko S, Tajima A and Satoh M, (1991) Separate mechanisms of long-term potentiation in two input systems to CA3 pyramidal neurons of rat hippocampal slices as revealed by the whole-cell patch-clamp technique. Neurosci Res 12:393-402.

Keinänen K, Wisden W, Sommer B, Werner P, Herb A, Verdoorn TA, Sackmann B and Seeburg PH, (1990) A family of AMPA-selective glutamate receptors. Science 249:556-560.

Köhler G and Milstein C, (1975) Continuous cultures of fused cells secreting antibody of predefined specificity. Nature 256:495-497.

Kraemer GW, (1992) A psychobiological theory of attachment. Behav Brain Sci 15:493-541.

Laemmli UK, (1970) Cleavage of structural proteins during the assembly of the head of bacteriophage T4. Nature 227:680-685.

Lee VM-Y, Otvos L, Carden MJ, Hollosi M, Dietzschold B and Lazzarini RA, (1988) Identification of the major multiphosphorylation site in mammalian neurofilaments. Proc Natl Acad Sci USA 85:1998-2002.

Leslie FM (1993) Neurotransmitters as neurotrophic factors. In: Neurotrophic factors (Loughlin SE and Fallon JH, eds), pp 565-598. San Diego: Academic Press.

Lewis MH, Gluck JP, Beauchamp AJ, Keresztury MF and Mailman RB, (1990) Long-term neurobiological effects of early social isolation in *Macaca mulatta*: Changes in dopamine receptor function following apomorphine challenge. Brain Res 513:67-73.

Lowry O, Rosenbrough N, Farr A and Randall R, (1951) Protein measurement with folin phenol reagent. J Biol Chem 193:265-275.

MacDermott AB and Dale N, (1987) Receptors, ion channels and synaptic potentials underlying the integrative actions of excitatory amino acids. TiNS 10:280-284.

Manetto U, Sternberger NH, Perr G, Sternberger LA and Gambetti P, (1989) Phosphorylation of neurofilaments is altered in amyotrophic lateral sclerosis. J Neuropath Exp Neurol 47:642-653.

Marc C, Clavel MC and Rabie A, (1986) Non-phosphorylated and phosphorylated neurofilaments in the cerebellum of the rat: An immunocytochemical study using monoclonal antibodies. Development in normal and thyroid-deficient animals. Brain Res 391:249-60.

Martin LJ, Blackstone CD, Levey AI, Huganir RL and Price DL, (1993) AMPA receptor subunits are differentially distributed in rat brains. Neuroscience 53:327-358.

Martin LJ, Blackstone CD, Levey AI, Huganir RL and Price DL, (1993) The striatal mosaic in primates: striosomes and matrix are differentially enriched in ionotropic glutamate receptor subunits. J Neuroscience 13:782-792.

Martin LJ, Spicer DM, Lewis MH, Gluck JP and Cork LC, (1991) Social deprivation of infant rhesus monkeys alters the chemoarchitecture of the brain: I. subcortical regions. J Neurosci 11:3344-3358.

McDonald JW and Johnston MV, (1990) Physiological and pathophysiological roles of excitatory amino acids during central nervous system development. Brain Res Rev 15:41-70.

Meaney MJ and Aitken DH, (1985) The effects of early postnatal handling on hippocampal glucocorticoid receptor concentrations: Temporal parameters. Brain Res 354:301-304.

Meaney MJ, Aitken DH, Bodnoff SR, Iny LJ, Tatarewicz JE and Sapolsky RM, (1985) Early postnatal handling alters glucocorticoid receptor concentrations in selected brain regions. Behav Neurosci 99:765-770.

Meaney MJ, Aitken DH, vanBerkel C, Bhatnagar S and Sapolsky RM, (1988) Effect of neonatal handling on age-related impairments associated with the hippocampus. Science 239:766.

Meunier M, Bachevalier J, Mishkin M and Murray EA, (1993) Effects on visual recognition of combined and separate ablations of the entorhinal and perirhinal cortex in rhesus monkeys. J Neurosci 13:5418-5432.

Miller LP, Johnson AE, Gelhard RE and Insel TR, (1990) The ontogeny of excitatory amino acid receptors in the rat forebrain-II. Kainic acid receptors. Neuroscience 35:45-51.

Monaghan DT and Cotman CW, (1985) Distribution of NMDA-sensitive, L-^{3}H-glutamate binding sites in rat brain as determined by quantitative autoradiography. J Neurosci 5:2909-2919.

Monaghan DT, Holets VR, Toy DW and Cotman CW, (1983) Anatomical distributions of four pharmacologically distinct L-^{3}H-glutamate binding sites. Nature 306:176-179.

Moriyoshi K, Masu M, Ishii T, Shigemoto R, Mizuno N and Nakanishi S, (1991) Molecular cloning and characterization of the rat NMDA receptor. Nature 354:31-37.

Morrison JH, Hof PR, Janssen W, Bassett JL, Foote SL, Kraemer GW and McKinney WT, (1990) Quantitative neuroanatomic analysis of cerebral cortex in rhesus monkeys from different rearing conditions. Soc Neurosci Abstr 16:789.

Morrison JH, Lewis DA, Campbell MJ, Huntley GW, Benson DL and Bouras C, (1987) A monoclonal antibody to non-phosphorylated neurofilament protein marks the vulnerable cortical neurons in Alzheimer's disease. Brain Res 416:331-336.

Nadler JV, Evenson DA and Cuthbertson GJ, (1981) Comparative toxicity of kainic acid and other acidic amino acids toward rat hippocampal neurons. Neuroscience 6:2505-2517.

Nakanishi S, (1992) Molecular diversity of glutamate receptors and implications for brain function. Science 258:597-603.

Nixon RA and Sihag RK, (1991) Neurofilament phosphorylation: A new look at regulation and function. TiNS 14:501-506.

Parkinson JK, Murray EA and Mishkin M, (1988) A selective mnemonic role for the hippocampus in monkeys: Memory for the location of objects. J Neurosci 8:4159-4167.

Pellegrini-Giampietro DE, Bennett MVL and Zukin RS, (1991) Differential expression of three glutamate receptor genes in developing rat brain: An *in situ* hybridization study. Proc Natl Acad Sci USA 88:4157-4161.

Pellegrini-Giampietro DE, Zukin RS, Bennett MVL, Cho S and Pulsinelli WA, (1992) Switch in glutamate receptor gene expression in CA1 subfield of hippocampus following global ischemia in rats. Proc Natl Acad Sci USA 89:10499-10503.

Petralia RS and Wenthold RJ, (1992) Light and Electron immunocytochemical localization of AMPA-selective glutamate receptors in the rat brain. J Comp Neurol 318:329-354.

Petralia RS and Wenthold RJ, (1993) Light and Electron microscopic distribution of the NMDA receptor subunit NMDAR1, in rat using a selective antipeptide antibody. Soc Neurosci Abstr 19:473.

Puchalski RB, Louis J-C, Traynelis S, Brose N, Egebjerg J, Wenthold R, Rogers S, Kukekov V, O'Leary L, Lin F, Sharma G, Moran T, Morrison JH, Stevens C and Heinemann SF, (Submitted) Structurally and functionally distinct native glutamate receptor channels expressed by glial progenitor-oligodendrocyte cell line. Neuron

Rami A, Brehier A, Thomasset M and Rabie A, (1987) Cholecalcin (28-kDa calcium-binding protein) in the rat hippocampus: Development in

normal animals and in altered thyroid states. An immunocytochemical study. Dev Biol 124:228-238.

Represa AF, Dessi F, Beaudoin M and Ben Ari Y, (1991) Effects of neonatal gamma-ray irradiation on rat hippocampus. I. Postnatal maturation of hippocampal cells. Neuroscience 42:137-150.

Riederer BM, (1990) Some aspects of neuronal cytoskeleton in development. Eur J Morphol 28:347-378.

Rogers SW, Hughes TE, Hollmann M, Gasic GP, Deneris ES and Heinemann S, (1991) The characterization and localization of the glutamate receptor subunit GluR1 in the rat brain. J Neurosci 11:2713-2724.

Rosene DL and Van Hoesen GW (1987) The hippocampal formation of the primate brain: A review of some comparative aspects of cytoarchitecture and connections. In: Cerebral Cortex (Jones EG and Peters A, eds), pp 345-456. New York: Plenum Press.

Rothman SM and Olney JW, (1987) Excitotoxicity and the NMDA receptor. TiNS 10:299-302.

Sapolsky RM, Stein-Behrens BA and Armanini MP, (1991) Long-term adrenalectomy causes loss of dentate gyrus and pyramidal neurons in the adult hippocampus. Exp Neurol 114:246-249.

Sapolsky RM, Uno H, Rebert CS and Finch CE, (1990) Hippocampal damage associated with prolonged glucocorticoid exposure in primates. J Neurosci 10:2897-2902.

Sapolsky RM, Zola-Morgan S and Squire LR, (1991) Inhibition of glucocorticoid secretion by the hippocampal formation in the primate. J Neurosci 11:3695-3704.

Schmidt JT, (1985) Activity-dependent synaptic stabilization in development and learning: how similar the mechanisms? Cellular and Molecular Neurobiol 5:1-3.

Seeburg PH, (1993) The molecular biology of mammalian glutamate receptor channels. TiNS 16:359-365.

Seress L, (1992) Morphological variability and developmental aspects of monkey and human granule cells: Differences between the rodent and primate dentate gyrus. Epilepsy Res Suppl 7:3-28.

Seress L, Gulyas AI and Freund TF, (1991) Parvalbumin- and Calbindin D28k- immunoreactive neurons in the hippocampal formation of the macaque monkey. J Comp Neurol 313:162-177.

Seress L, Gulyas AI and Freund TF, (1992) Pyramidal neurons are immunoreactive for calbindin D28k in the CA1 subfield of the human hippocampus. Neurosci Lett 138:257-260.

Seress L and Mrzljak L, (1992) Postnatal development of the mossy cells in the human dentate gyrus: A light microscopic Golgi study. Hippocampus 2:127-142.

Serfling R and Schuster T, (1983) Light-microscopic investigations on the problem of a dendritic bundling in the rat hippocampus. J Hirnforsch 24:241-52.

Shaw G, Winialski D and Reier P, (1988) The effect of axotomy and deafferentation on phosphorylation dependent antigenicity of neurofilaments in rat superior cervical ganglion neurons. Brain Res 460:227-234.

Shepherd GM (1983) Development. In: Neurobiology eds), pp 164-183. New York: Oxford University Press.

Siegel SJ, Brose N, Janssen WG, Gasic GP, Jahn R, Heinemann SF and Morrison JH, (1994) Regional, Cellular, and Ultrastructural Distribution of the Glutamate Receptor Subunit NMDAR1 in Monkey Hippocampus. Proc Natl Acad Sci USA 91:564-568.

Siegel SJ, Ginsberg SD, Hof PR, Foote SL, Young WG, Kraemer GW, McKinney WT and Morrison JH, (1993) Effects of Social Deprivation in Prepubescent Rhesus Monkeys: Immunohistochemical Analysis of the Neurofilament Protein Triplet in the Hippocampal Formation. Brain Res 619:299-305.

Siegel SJ, Hof PR, Kraemer G, McKinney WT and Morrison JH, (1992) Effects of postnatal mossy fiber development on CA3 Apical dendrites in differentially reared monkeys. Soc Neurosci Abstr 18:34.

Siegel SJ, Janssen WG, Brose N, Rogers SW, Moran T, Gasic GP, Jahn R, Heinemann SF and Morrison JH, (1993) Immunocytochemical distribution of NMDA and non-NMDA ionotropic excitatory amino acid (eea) receptors in monkey hippocampus. Soc Neurosci Abstr 19:926.

Siegel SJ, Janssen WG, Rogers SW, Moran T and Heinemann SF, (in preparation) Distribution of the Glutamate Receptor Subunit GluR2 in Monkey Hippocampus and Colocalization with Subunits GluR5-7 and NMDAR1.

Sloviter RS, Valiquette G, Abrams GM, Ronk EC, Sollas AL, Paul LA and Neubort S, (1989) Selective loss of hippocampal granule cells in the mature rat brain after adrenalectomy. Science 243:535-538.

Sommer B and Seeburg PH, (1992) Glutamate receptor channels: Novel properties and new clones. TiPS 13:291-296.

Sonders MS, Barmettler P, Lee JA, Kitahara Y, Keans JFW and Weber E, (1990) A novel photoaffinity ligand for the phencyclidine site of the N-methyl-D-aspartate receptor labels a Mr 120,000 polypeptide. J Biol Chem 12:6776-6781.

Stanfield BB and Cowan MM (1988) The development of the hippocampal region. In: Cerebral Cortex (Peters A and Jones EG, eds), pp 91-131. New York: Plenum Press.

Stell M and Riesen A, (1987) Effects of early environments on monkey cortex neuroanatomical changes following somatomotor experience: Effects on layer III pyramidal cells in monkey cortex. Behavioral Neurosci 101:341-346.

Sternberger LA and Sternberger NH, (1983) Monoclonal antibodies distinguish phosphorylated and nonphosphorylated forms of neurofilaments *in situ*. Proc Natl Acad Sci USA 80:6126-6130.

Struble RG and Riesen AH, (1978) Changes in cortical dendritic branching subsequent to partial social isolation in stumptailed monkeys. Dev Psychobiol 11:479-486.

Towbin H, Staehelin T and Gordon J, (1979) Electrophoretic transfer of proteins from polyacrylamide gels to nitrocellulose sheets: procedure and some applications. Proc Natl Acad USA 76:4350-4354.

Tucker RP, (1990) The role of microtubule-associated proteins in brain morphogenesis: A review. Brain Res Rev 15:101-120.

Uno H, Glugge G, Thieme C, Johren O and Fuchs E, (1991) Degeneration of the hippocampal pyramidal neurons in the socially stressed tree shrew. Soc Neurosci Abstr 17:129.

Uno H, Lohmiller L, Thieme C, Kemnitz JW, Engle MJ, Roecker EB and Farrell PM, (1990) Brain damage induced by prenatal exposure to dexamethasone in fetal rhesus macaques. I. Hippocampus. Dev Brain Res 53:157-67.

Uno H, Tarara R, Else JG, Suleman MA and Sapolsky RM, (1989) Hippocampal damage associated with prolonged and fatal stress in primates. J Neurosci 9:1705-1711.

Verdoorn TA, Burnashev N, Monyer H, Seeberg PH and Sackmann B, (1991) Structural Determinants of Ion Flow Through Recombinant Glutamate Receptor Channels. Science 252:1715-1718.

Vickers JC, Chiu FC and Costa M, (1992) Selective distribution of the 66-kDa neuronal intermediate filament protein in the sensory and autonomic nervous system of the guinea-pig. Brain Res 585:205-211.

Vickers JC and Costa M, (1992) The neurofilament triplet is present in distinct subpopulations of neurons in the central nervous system of the guinea pig. Neuroscience 49:73-100.

Vickers JC, Delacoute A and Morrison JH, (1992) Progressive transformation of the cytoskeleton associated with normal aging and Alzheimer's disease. Brain Res 594:273-278.

Vickers JC, Huntley GW, Edwards AM, Moran T, Rogers SW, Heinemann SH and Morrison JH, (1993) Quantitative localization of AMPA/kainate and kainate glutamate receptor subunit immunoreactivity in neurochemically identified subpopulations of neurons in the prefrontal cortex of the macaque monkey. J Neuroscience 13:2982-2992.

Vickers JC and Morrison JH, (1992) Aberrant neurofilament protein immunoreactivity in hippocampal pyramidal neurons in Alzheimer's disease. J Neuropathol Exp Neurol 51:319.

Vickers JC, Vitadello M, Parysek LM and Costa M, (1991) Complementary immunohistochemical distribution of the neurofilament triplet and novel intermediate filament proteins in the autonomic and sensory nervous system of the guinea pig. Neuroscience 4:259-270.

Walker LC, Kitt CA, Struble RG, Wagster MV, Price DL and Cork LC, (1988) The neural basis of memory decline in aged monkeys. Neurobiol Agirg 9:657-666.

Wang S, Hamberger A, Ding M and Haglid KG, (1992) In vivo Activation of kainate receptors induces dephosphorylation of the heavy neurofilament subunit. J Neurochem 1975-.

Wang S, Lees GJ, Rosengren LE, Karlsson JE, Hamberger A and Haglid KG, (1992) Proteolysis of filament proteins in glial and neuronal cells after in vivo stimulation of hippocampal NMDA receptors. Neurochem Res 17:1005-9.

Watanabe Y, Gould E and McEwen BS, (1992) Stress induces atrophy of apical dendrites of hippocampal CA3 pyramidal neurons. Brain Res 588:341-345.

Werner P, Voigt M, Keinänen K, Wisden W and Seeburg PH, (1991) Cloning of a putative high-affinity kainate receptor expressed predominantly in hippocampal CA3 cells. Nature 351:742-744.

Zalutsky RA and Nicoll RA, (1990) Comparison of two forms of long-term potentiation in single hippocampal neurons [published erratum appears in Science 1991 Feb. 22;251(4996):856]. Science 248:1619-24.

Zola-Morgan SM and Squire LR, (1990) The primate hippocampal formation: Evidence for a time-limited role in memory storage. Science 250:288-290.